AD-A046 762 UNIVERSITY COLL OF WALES ABERYSTWYTH DEPT OF PHYSICS F/G 20/14
ATS-6 OBSERVATIONS OF IONOSPHERIC/PROTONOSPHERIC ELECTRON CONTE--ETC(U)
FEB 77 L KERSLEY, H KAJEB-HOSSEINIEH AFOSR-72-2267

UNCLASSIFIED AFGL-TR-77-0107 NL

1 OF 2
AD
A046 762

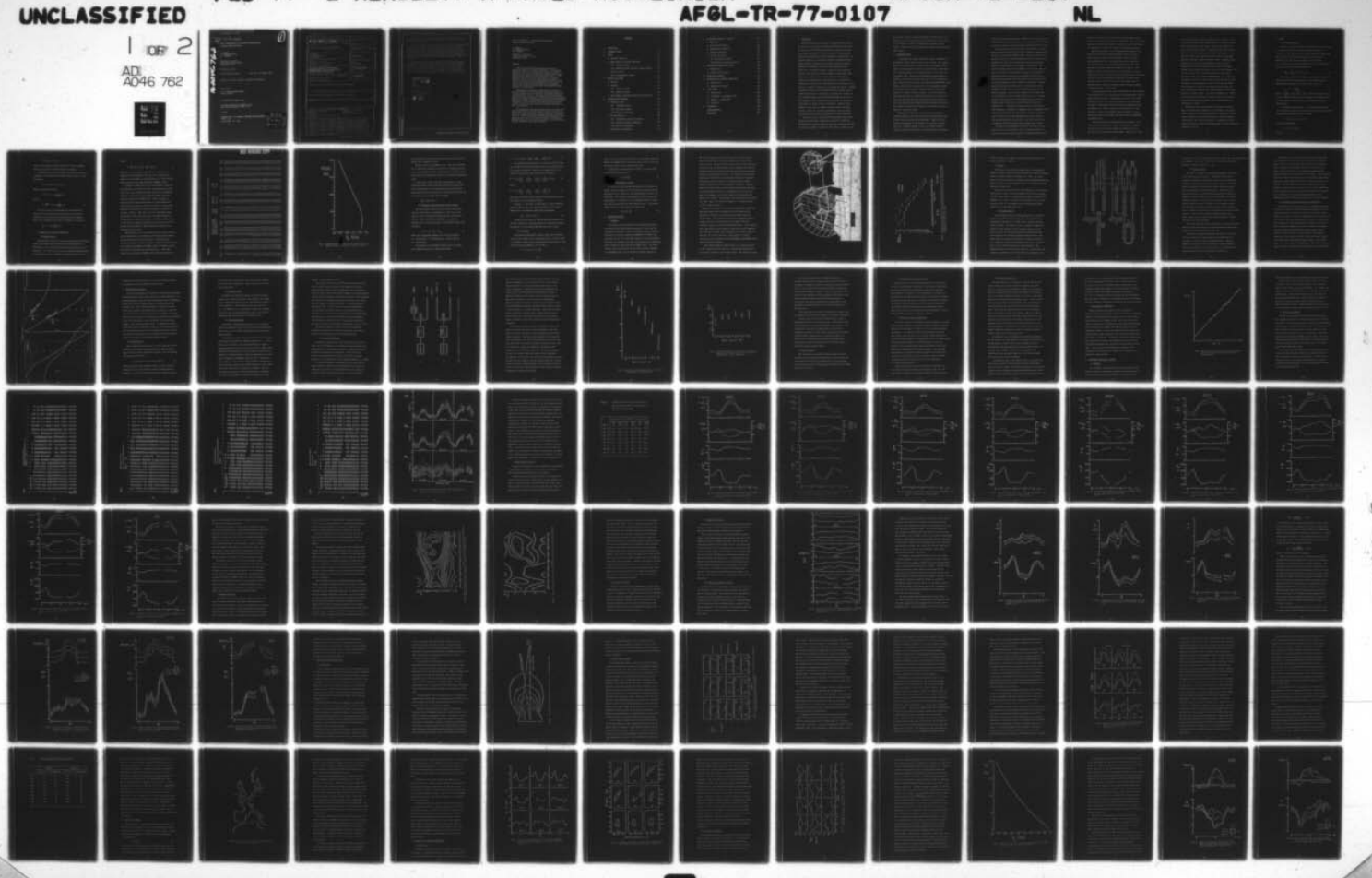

Grant AFOSR - 72 - 2267

ATS-6 OBSERVATIONS OF IONOSPHERIC/PROTONOSPHERIC ELECTRON CONTENT AND FLUX

L. KERSLEY
H. HAJEB-HOSSEINIEH
K.J. EDWARDS

Department of Physics
University College of Wales
Aberystwyth, U.K.

28 February, 1977

Final Scientific Report 1 July 1975 - 31 December 1976

Approved for public release; distribution unlimited

Sponsored by

U.K. SCIENCE RESEARCH COUNCIL
Grant: SG/R/052

with additional support from

AIR FORCE GEOPHYSICAL LABORATORY (LIR)
Bedford, Massachusetts, 01730, U.S.A.

through

EUROPEAN OFFICE OF AEROSPACE RESEARCH AND DEVELOPMENT
London, U.K.

Grant AFOSR - 72 - 2267

Unclassified

SECURITY CLASSIFICATION OF THIS PAGE (When Data Entered)

REPORT DOCUMENTATION PAGE

1. REPORT NUMBER: AFGL-TR-77-0107	2. GOVT ACCESSION NO.
3. RECIPIENT'S CATALOG NUMBER	
4. TITLE (and Subtitle): ATS-6 OBSERVATIONS OF IONOSPHERIC/ PROTONOSPHERIC ELECTRON CONTENT AND FLUX	5. TYPE OF REPORT & PERIOD COVERED: Final Scientific Report 1 July 1975 - 31 December 1976
	6. PERFORMING ORG. REPORT NUMBER
7. AUTHOR(s): L. KERSLEY, H.HAJEB-HOSSEINIEH, K.J. EDWARDS	8. CONTRACT OR GRANT NUMBER(s): AFOSR-72-2267
9. PERFORMING ORGANIZATION NAME AND ADDRESS: DEPARTMENT OF PHYSICS, UNIVERSITY COLLEGE OF WALES, ABERYSTWYTH, WALES, U.K.	10. PROGRAM ELEMENT, PROJECT, TASK AREA & WORK UNIT NUMBERS: 62101F, 4643-01-05
11. CONTROLLING OFFICE NAME AND ADDRESS: Air Force Geophysics Laboratory, Hanscom AFB, Massachusetts 01731, Monitor/John P. Mullen/PHP	12. REPORT DATE: 28 February 1977
	13. NUMBER OF PAGES: 118
14. MONITORING AGENCY NAME & ADDRESS (if different from Controlling Office): EUROPEAN OFFICE OF AEROSPACE RESEARCH AND DEVELOPMENT, 223/231 MARYLEBONE ROAD, LONDON, N.W.1., U.K.	15. SECURITY CLASS. (of this report): Unclassified
	15a. DECLASSIFICATION/DOWNGRADING SCHEDULE

16. DISTRIBUTION STATEMENT (of this Report)

Approved for public release; distribution unlimited

17. DISTRIBUTION STATEMENT (of the abstract entered in Block 20, if different from Report)

Approved for public release; distribution unlimited

18. SUPPLEMENTARY NOTES

19. KEY WORDS (Continue on reverse side if necessary and identify by block number)

Ionospheric group delay
Total electron content
F2-region
Protonosphere
Ionospheric/protonospheric interaction
Plasma flux
Conjugate point effects
Slab thickness
Geomagnetic storm effects

20. ABSTRACT (Continue on reverse side if necessary and identify by block number)

The ATS-6 radio beacon experiment carried out at Aberystwyth (52.42°N, 4.05°W) is described. A preliminary analysis of the data is described concentrating on hourly values of total electron content (N_m), Faraday content (N_F), protonospheric content (N_p) and layer shape F-factor. The monthly median behaviour of the parameters is discussed together with the effects of observational and analysis error on the accuracy of the protonospheric content values. The correction for layer height changes

DD FORM 1 JAN 73 1473 EDITION OF 1 NOV 65 IS OBSOLETE

SECURITY CLASSIFICATION OF THIS PAGE (When Data Entered)

has been found to be of much less importance for European stations observing during Phase II ATS-6 operations than for measurements made in America during Phase I.

The dynamic interchange of plasma betwen ionosphere and protonosphere has been studied by estimating hourly values of average integrated net fluxes from the temporal gradient of protonospheric content. The protonospheric flux data have been interpreted qualitatively in terms of diffusive interaction between ionosphere and protonosphere in both local and conjugate hemispheres. Added confirmation is obtained by consideration of contrasting protonospheric data from an American sector station which can also be related to ionospheric behaviour in the two hemispheres.

The Aberystwyth observations indicate that the inner flux tubes intersected by the slant path are filled in a matter of hours almost every day and the average behaviour of N_p reflects a diurnal partial draining but complete refilling of tubes up to $L \sim 4$. Case studies show that following a geomagnetic storm depletion some 7 days are required to saturate these tubes, but approximately 14 quiet days are necessary to reach absolute dynamic equilibrium along the slant path.

ATS-6 OBSERVATIONS OF IONOSPHERIC/PROTONOSPHERIC ELECTRON CONTENT AND FLUX

L. KERSLEY
H. HAJEB-HOSSEINIEH
K.J. EDWARDS

Department of Physics
University College of Wales
Aberystwyth, U.K.

Abstract

The ATS-6 radio beacon experiment carried out at Aberystwyth (52.42°N, 4.05°W) is described. A preliminary analysis of the data is described concentrating on hourly values of total electron content (N_T), Faraday content (N_F), protonospheric content (N_p) and layer shape F-factor. The monthly median behaviour of the parameters is discussed together with the effects of observational and analysis errors on the accuracy of the protonospheric content values. The correction for layer height changes has been found to be of much less importance for European stations observing during Phase II ATS-6 operations than for measurements made in America during Phase I.

The dynamic interchange of plasma between ionosphere and protonosphere has been studied by estimating hourly values of average integrated net fluxes from the temporal gradient of protonospheric content. The protonospheric flux data have been interpreted qualitatively in terms of diffusive interaction between ionosphere and protonosphere in both local and conjugate hemispheres. Added confirmation is obtained by consideration of contrasting protonospheric data from an American sector station which can also be related to ionospheric behaviour in the two hemispheres.

The Aberystwyth observations indicate that the inner flux tubes intersected by the slant path are filled in a matter of hours almost every day and the average behaviour of N_p reflects a diurnal partial draining but complete refilling of tubes up to $L \sim 4$. Case studies show that following a geomagnetic storm depletion some 7 days are required to saturate these tubes, but approximately 14 quiet days are necessary to reach absolute dynamic equilibrium along the slant path.

CONTENTS

1. INTRODUCTION

The ATS-6 satellite was launched into geostationary orbit in May 1974 and was stationed at longitude 94°W until mid-1975 when it was moved to 35°E becoming available to observers in Europe. Among other experiments the satellite carried a multifrequency radio beacon designed for several ionospheric investigations. Of specific interest to the present study were transmissions which enabled absolute measurements to be made of electron content, a parameter of importance in assessing the ionospheric delay correction in very high frequency communication and navigation systems. Two types of measurement possible with the ATS-6 radio beacon are of concern here. In the first the total electron content (N_T) between satellite and ground can be determined by comparison of the phase of a 1MHz modulation on a VHF carrier with that of an identical modulation on a coherent VHF carrier. Secondly, a weighted estimate of the ionospheric electron content, the so-called Faraday electron content (N_F), restricted to a measure of the integrated plasma below some arbitrary height at the top of the ionosphere, can be obtained from the rotation of the polarisation plane of the VHF carrier transmission. Absolute determination of the total and Faraday electron contents to a high accuracy enables the so-called protonospheric electron content (N_p) along the slant path to be determined from the difference.

The present work is concerned with preliminary results from ATS-6 observations made at Aberystwyth (52.42°N, 4.05°W) from November 1975 to July 1976 when the satellite was situated at 35°E. As particular emphasis is placed in this report on aspects of the

protonospheric electron content measurement the description of the experiment and the results obtained are preceded by a short review of the literature relevant to plasmaspheric processes and the dynamic coupling between the ionospheric F2-region and the overlying protonosphere.

2. LITERATURE REVIEW

In discussing the complex interaction between ionosphere and protonosphere several factors should be kept in mind. For example, the plasma is constrained to diffuse along the geomagnetic field lines, the configuration of which on a global scale is complicated and in practice subject to ill-defined changes in both space and time (HESS, 1968). Secondly, the ionosphere and protonosphere or exosphere are dominated by different ions O^+ and H^+ respectively with a diffusive barrier between them (HANSON and ORTENBERGER, 1961). Thirdly, the effective vertical motion of the ionospheric plasma is controlled by thermospheric winds and electric fields whose patterns on a global scale are complex. It is thus perhaps not surprising that despite considerable interest in the problem for some time relatively few direct measurements have been made of the relationship between ionosphere and protonosphere and reports have tended to concentrate on individual events with the data too sparse for statistical study.

Observations of whistlers were used in early studies to estimate geomagnetic flux tube content and the associated plasma fluxes between ionosphere and protonosphere. PARK (1970) used whistler measurements of tube content, for a period of several days after a moderate magnetic storm, and from the temporal changes estimated the magnitude of the upwards flux of electrons

from the ionosphere during daytime. CHAPPELL et al. (1971) obtained confirmation of this flux rate from in situ measurements of H^+ density by means of a light ion mass spectrometer aboard the OGO-5 satellite.

An early attempt to obtain continuous measurements of protonospheric electron content along the line of sight to a geostationary satellite was reported by ALMEIDA (1970). Using transmissions from the ATS-3 satellite the Faraday content and the total content were estimated, the latter by the differential phase path technique, allowing the protonospheric contribution to be obtained. The results, discussed more fully by ALMEIDA (1973 and 74), show that while in principle the protonospheric content can be measured, apparently anomalous results are on occasions obtained with N_p minimising during daytime when the upwards flux of electrons from the sunlit ionosphere would be expected to be greatest. Similar diurnal variations were obtained from a restricted data set by KLOBUCHAR and KIDD (1972), for ATS-3 observations again in the Western Hemisphere. These workers suggest that the anomaly may be an observational effect arising from the choice of a constant height for the estimate of the so-called $\overline{M}$-factor used in the Faraday content estimation, a point discussed more fully by ALMEIDA (1974). Semi-empirical model studies by SMITH (1970) and independently by KERSLEY and SAMBROOK (1971) and SAMBROOK (1974), combining geostationary satellite Faraday rotation measurements with incoherent scatter data supplemented by a model, implied that the protonospheric contribution to the total content could be typically about 10% by day rising to perhaps 40% at night.

The idea of the plasmasphere acting as a reservoir for ions which can flow to the ionosphere when the F-region pressure is low and vice-versa has been discussed by BANKS and DOUPNIK (1974).

The plasma transport between ionosphere and protonosphere implies an ion transfer between the conjugate hemispheres. MAYR et al.(1972) using model calculations obtained an estimate of the H^+ flux between the hemispheres to account for aspects of ionospheric behaviour.

Theoretical estimates of the ionospheric/protonospheric flux have also been carried out by solving the continuity equation, using composition data from the incoherent scatter technique (HO and MOORCROFT, 1975). The density and vertical velocity of the different plasma constituents measured by this method have been used to estimate plasma flux (EVANS, 1975 a and b). This method is perhaps the most direct way of estimating the vertical ionisation flux but it suffers from the usual operational limitations to only a few day observations per month, while in addition the transition height from O^+ to H^+ is often much higher than the maximum height at which the incoherent scatter technique produces a reasonable signal to noise ratio.

The multifrequency radio beacon aboard ATS-6 has made available a new technique for the determination of the protonospheric electron content along the path to a geostationary satellite. The overall description of the ATS-6 radio beacon experiment and associated ionospheric observations have been discussed by HARGREAVES (1970) and DAVIES et al. (1972). Estimates of the sensitivity of the technique to different ionospheric and protonospheric electron density distributions were made using model studies by HARGREAVES and HOLMAN (1972).

Some early results of ATS-6 observations at Boulder, U.S.A. were reported by DAVIES et al. (1975 a and b) while a complete set of data for this station covering the period July 1974 to May 1975 has been published by FRITZ (1976). DAVIES et al. (1976)

have linked this data to model calculations, but a feature of the results which passes largely without comment is a diurnal variation of the monthly median protonospheric content which maximises at night during the winter months. SOICHER (1975 and 1976a) reports ATS-6 measurements of protonospheric content for periods of a few days one of which shows enhanced values followed by an extended depletion following a sudden commencement storm. SOICHER (1976b) contrasts the behaviour of protonospheric content for ATS-6 observations in U.S.A, South America and Northern Europe while SOICHER (1976c) presents multi-plots of data for Fort Monmouth, U.S.A for four months in 1975. ATS-6 measurements of N_p have been compared to model simulations by POLETTI-LIUZZI et al. (1976) for two periods in 1976, one a long string of quiet days and the other including two major geomagnetic storms. The diurnal variations of protonospheric content for this American sector station are small and show some evidence for a daytime minimum, a result again passed over without comment. By contrast, HARTMANN et al. (1976), with observations from Europe in a paper primarily concerned with travelling ionospheric disturbances, show a daytime maximum in protonospheric content.

The present report concerns ATS-6 observations from Europe where the monthly median behaviour of the ionospheric and protonospheric contents is discussed and compared to observations from the Western Hemisphere and consideration given to the plasma dynamics contributing to the observed variations. In addition, detailed attention is given to certain individual periods of quiet and enhanced geomagnetic activity.

3. THEORY

a. The Basic Equations

Consider a linearly polarised electromagnetic wave of frequency f, characterised by two circularly polarised components, the ordinary (o) and extraordinary (x) modes, propagating along a small path increment ds in an ionised medium in the presence of a magnetic field. The refractive indices will be given by $\mu_{o,x} = c/f\lambda_{o,x}$ so that the phase changes of the two modes $d\phi_o$ and $d\phi_x$ will be given in the usual notation by

$$d\phi_{o,x} = \frac{2\pi}{\lambda_{o,x}} ds = \frac{\omega}{c} \mu_{o,x} ds \qquad 1.$$

The refractive indices are obtained from the Appleton Hartree equation, which for QL propagation in a collisionless medium, approximations relevant to the present work, reduces to

$$\mu_{o,x} \simeq 1 - \frac{X}{2(1 \pm Y_L)} \qquad 2.$$

where $X = \frac{Ne^2}{\varepsilon_o m\omega^2}$ and $Y_L = \frac{eB_L}{m\omega} = \frac{f_L}{f}$ in the usual notation with N the free electron density, B_L the component of the magnetic field in the propagation direction and f_L the longitudinal electron gyrofrequency.

For propagation along a path s the polarisation rotation of the linearly polarised wave will be given by half the accumulated phase difference between the modes, that is

$$\Omega = \frac{\omega}{2c} \int_s (\mu_o - \mu_x) ds$$

so that by substitution

$$\Omega = \frac{\omega}{c} \int_s XY_L \, ds$$

that is

$$\Omega = \frac{k}{f^2} \int_s N f_L \, ds \qquad 3.$$

where k has a numerical value 4.840×10^{-11} for Ω in degrees, with the frequencies in MHz and distances in metres.

Considering now only the ordinary mode circularly polarised component, its accumulated phase change along the path s will be given by

$$\Phi = \int_s d\phi_o \, ds = \frac{\omega}{c} \int_s \mu_o \, ds$$

which by substitution becomes

$$\Phi = \frac{\omega}{c} \int_s \left(1 - \frac{X}{2(1+Y_L)}\right) ds$$

that is

$$\Phi = \frac{2\pi f}{c} s - k \int_s \frac{N}{(f+f_L)} \, ds \qquad 4.$$

The first term on the right hand side of this equation represents the geometrical phase path while the second term corresponds to the phase delay resulting from the ionosphere. That is the ionospheric phase delay at frequency f is given by

$$\phi_f = - k \int_s \frac{N}{(f+f_L)} \, ds \qquad 5.$$

b. Application to the ATS-6 Experiment

(i) Faraday content

The Aberystwyth receiving system measures the phase difference between the ordinary and extraordinary circular modes of the 140.056MHz carrier allowing the Faraday rotation angle (Ω) to be determined. If a mean value of f_L can be determined representative of conditions along the ionospheric path then Equation 3 can be

written

$$\Omega = \frac{k}{f^2} \bar{f}_L \int_o^h N ds = \frac{k}{f^2} \bar{f}_L N_F \qquad 6.$$

where N_F is the so-called Faraday content. Because of the weighting of the geomagnetic field N_F can be considered as a measure of the ionospheric electron content up to some arbitrary height usually between 2000 and 3000 km (SAMBROOK, 1974).

To estimate a mean value of f_L it is necessary to know how this parameter varies along the path. The computation has been carried out using a spherical harmonic model of the geomagnetic field with coefficients based on CAIN and SWEENEY (1970) but up-dated to epoch 1974 (DAVIES 1975). Table 1 displays an output from the program listing values of several geometrical and geomagnetic parameters relevant to the ATS-6 to Aberystwyth geometry at 50 km vertical intervals through the ionosphere to a height of 2000 km. The values of f_L over this height range are plotted in Fig.1 which shows that the height variation of this parameter is double valued about a maximum at around 200 km, a shape which has important consequences for the accuracy of the Faraday and protonospheric content measurements which will be discussed in detail later.

The parameter f_L is closely related to the so-called M-factor used by many workers in the reduction of Faraday rotation angles to equivalent vertical electron content. A so-called mean ionospheric height of 375 km, at which to evaluate the mean M-factor, was recommended by KERSLEY and TAYLOR (1974) for Faraday rotation measurements using satellites in 1000 km orbit. From semi-empirical model studies TITHERIDGE (1972) found that 420 km was

TABLE 1 GEOPHYSICAL PARAMETERS ALONG THE RAY PATH FROM A GEOSTATIONARY SATELLITE

STATION LATITUDE	52.42	LONGITUDE	-4.05
SATELLITE LATITUDE	0.00	LONGITUDE	35.00
SATELLITE HEIGHT(KM)	35790		
ANTENNA AZIMUTH	134.33	ELEVATION	20.11

HEIGHT KM	RANGE KM	LAT DEG	LONG DEG	AZ DEG	ZENITH DEG	HX GAUSS	HY GAUSS	HZ GAUSS	H GAUSS	FL GAMMA	FL MHZ	DIP DEG	DEC DEG	THETA DEG
0	39543	52.4	-4.0	134.3	69.9	0.179	-0.028	0.445	0.480	28889	0.809	67.9	-0.9	53.0
50	39402	51.6	-2.7	135.4	68.7	0.180	-0.025	0.431	0.468	29230	0.818	67.1	-0.8	51.3
100	39268	50.8	-1.5	136.4	67.6	0.181	-0.023	0.417	0.455	29463	0.825	66.4	-0.7	49.7
150	39139	50.0	-0.3	137.2	66.6	0.181	-0.021	0.405	0.444	29602	0.829	65.7	-0.6	48.1
200	39016	49.3	0.7	138.0	65.6	0.181	-0.019	0.392	0.432	29661	0.831	65.1	-0.6	46.7
250	38897	48.6	1.6	138.7	64.6	0.181	-0.018	0.380	0.421	29649	0.830	64.4	-0.5	45.3
300	38782	47.9	2.5	139.4	63.7	0.181	-0.017	0.368	0.410	29575	0.828	63.7	-0.5	43.9
350	38671	47.3	3.3	140.0	62.9	0.180	-0.016	0.357	0.400	29447	0.825	63.1	-0.4	42.6
400	38563	46.7	4.1	140.5	62.1	0.180	-0.015	0.346	0.390	29272	0.820	62.4	-0.4	41.3
450	38457	46.0	4.8	141.1	61.3	0.179	-0.014	0.335	0.380	29054	0.814	61.8	-0.4	40.1
500	38355	45.5	5.5	141.5	60.5	0.178	-0.013	0.324	0.370	28801	0.806	61.2	-0.3	38.9
550	38254	44.9	6.1	142.0	59.8	0.177	-0.012	0.314	0.361	28516	0.798	60.6	-0.3	37.8
600	38156	44.3	6.7	142.4	59.1	0.176	-0.012	0.305	0.352	28204	0.790	60.0	-0.3	36.7
650	38059	43.8	7.3	142.8	58.4	0.174	-0.011	0.295	0.343	27868	0.780	59.4	-0.3	35.7
700	37965	43.3	7.8	143.2	57.8	0.173	-0.011	0.286	0.334	27511	0.770	58.8	-0.3	34.6
750	37872	42.8	8.4	143.5	57.2	0.171	-0.011	0.277	0.326	27139	0.760	58.2	-0.3	33.7
800	37780	42.3	8.8	143.9	56.5	0.170	-0.010	0.269	0.318	26753	0.749	57.7	-0.3	32.7
850	37690	41.8	9.3	144.2	55.9	0.168	-0.010	0.260	0.310	26359	0.738	57.1	-0.3	31.8
900	37602	41.3	9.8	144.5	55.4	0.166	-0.010	0.252	0.302	25961	0.726	56.6	-0.3	30.9
950	37514	40.9	10.2	144.8	54.8	0.165	-0.009	0.245	0.295	25564	0.715	56.0	-0.3	30.1
1000	37428	40.4	10.6	145.0	54.3	0.163	-0.009	0.237	0.288	25181	0.703	55.5	-0.2	29.3
1050	37343	40.0	11.0	145.3	53.7	0.161	-0.009	0.230	0.281	24823	0.691	55.0	-0.2	28.5
1100	37259	39.6	11.4	145.5	53.2	0.159	-0.009	0.223	0.274	24493	0.679	54.5	-0.2	27.7
1150	37176	39.1	11.8	145.8	52.7	0.157	-0.009	0.216	0.267	24191	0.667	53.9	-0.1	27.0
1200	37094	38.7	12.1	146.0	52.2	0.155	-0.008	0.210	0.261	23919	0.655	53.4	-0.1	26.3
1250	37013	38.3	12.5	146.2	51.7	0.153	-0.008	0.203	0.255	23647	0.643	53.0	-0.1	25.7
1300	36933	37.9	12.8	146.4	51.3	0.151	-0.008	0.197	0.249	23516	0.630	52.5	-0.1	25.1
1350	36853	37.5	13.1	146.6	50.8	0.149	-0.008	0.191	0.243	23083	0.616	52.0	-0.1	24.5
1400	36774	37.2	13.4	146.8	50.3	0.147	-0.008	0.185	0.237	21463	0.607	51.5	-0.1	23.9
1450	36696	36.8	13.7	147.0	49.9	0.145	-0.008	0.180	0.231	21241	0.595	51.1	-0.1	23.4
1500	36619	36.4	14.0	147.2	49.5	0.143	-0.008	0.175	0.226	20923	0.583	50.6	-0.2	22.9
1550	36542	36.1	14.3	147.3	49.0	0.141	-0.008	0.170	0.221	20410	0.572	50.1	-0.2	22.4
1600	36466	35.7	14.6	147.5	48.6	0.139	-0.008	0.165	0.216	20002	0.560	49.7	-0.2	22.0
1650	36391	35.4	14.8	147.6	48.2	0.137	-0.008	0.160	0.211	19601	0.549	49.3	-0.2	21.6
1700	36316	35.1	15.1	147.8	47.8	0.135	-0.008	0.155	0.206	19203	0.538	48.8	-0.2	21.2
1750	36242	34.7	15.4	147.9	47.4	0.133	-0.008	0.151	0.201	18811	0.527	48.4	-0.2	20.9
1800	36168	34.4	15.6	148.1	47.1	0.132	-0.008	0.146	0.197	18425	0.516	48.0	-0.2	20.6
1850	36095	34.1	15.8	148.2	46.7	0.130	-0.007	0.142	0.192	18047	0.505	47.6	-0.2	20.3
1900	36023	33.8	16.1	148.3	46.3	0.128	-0.007	0.138	0.188	17675	0.495	47.1	-0.2	20.1
1950	35950	33.5	16.3	148.5	46.0	0.126	-0.007	0.134	0.184	17309	0.485	46.7	-0.2	19.9
2000	35879	33.2	16.5	148.6	45.6	0.124	-0.007	0.130	0.180	16951	0.475	46.3	-0.2	19.7

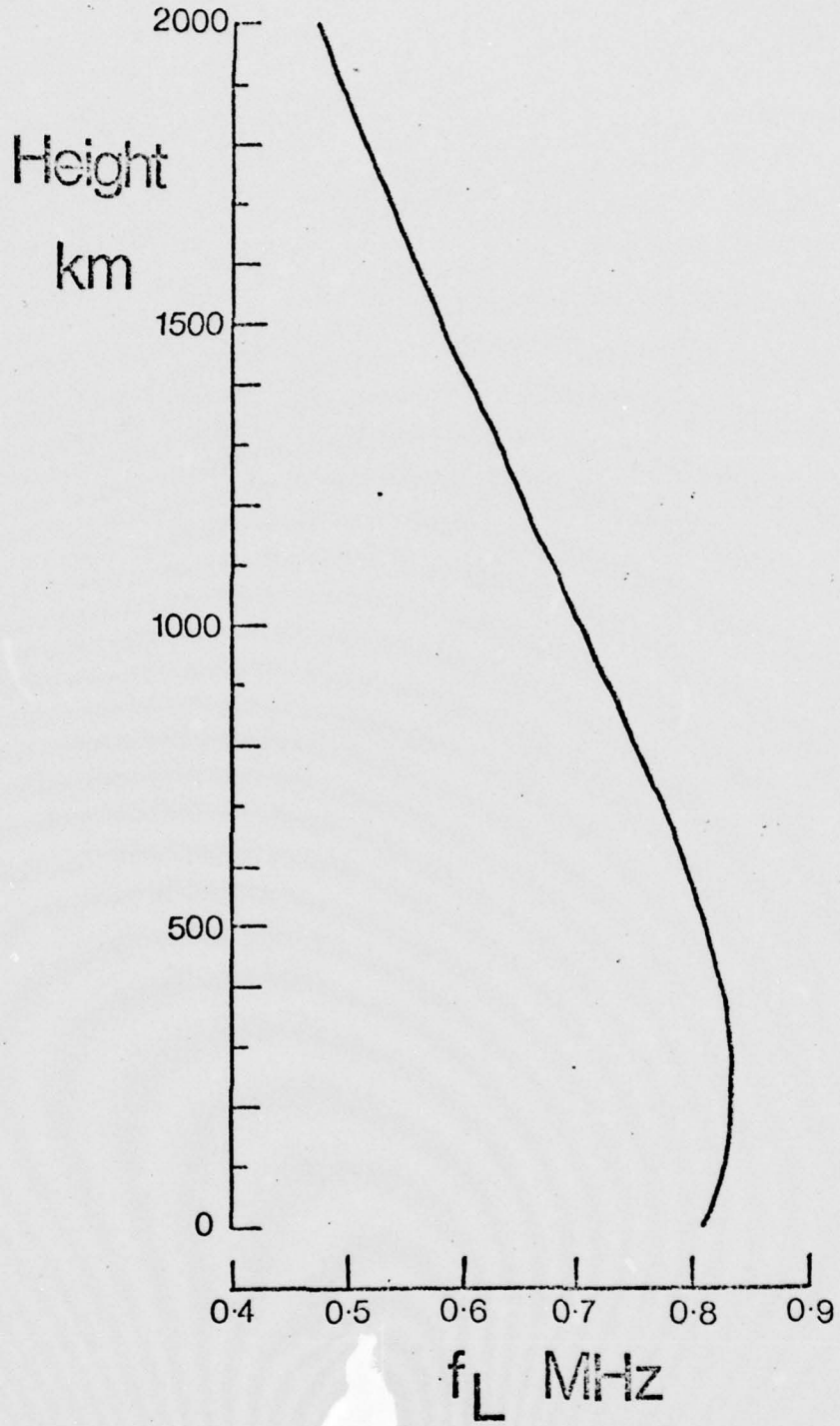

Fig.1. Height variation [illegible] longitudinal gyrofrequency for ATS-6 to Aberyst[illegible]th path to a height of 2000 km.

most appropriate for work with geostationary satellites although ALMEIDA (1973) suggested 350 km.

Several workers (e.g. MENDILLO et al., 1974 and PAPAGIANNIS et al., 1975) have considered the effects of a diurnal variation in the mean ionospheric height on measurements of Faraday content. This point will be considered in detail for the ATS-6 measurements later.

A fixed value of $\overline{f}_L$ = 0.817 MHz corresponding to a mean ionospheric height of 420 km has been used in the present work. Thus, from Equation 6, the relationship between the measured polarisation rotation (in degrees) of the 140.056 MHz carrier and the Faraday electron content (in m^{-2}) becomes

$$N_F = 4.96 \times 10^{14} \Omega \qquad 7.$$

(ii) Modulation phase and total electron content

The other angular parameter measured by the Aberystwyth receiver is the phase of a modulation on a VHF carrier with respect of that of an identical modulation on a coherent UHF carrier. After calibration to eliminate non-ionospheric contributions to the measured phase, the ionospheric phase delay is given by

$$\phi = \phi_2 - \phi_1 - (\phi_4 - \phi_3) \qquad 8.$$

where the corresponding suffixes refer to the frequencies f_1 = 140.056 MHz, f_2 = 141.0564 MHz, f_3 = 360.144 MHz and f_4 = 361.1444 MHz.

From Equation 5 the modulation phase delay for ordinary wave components measured at Aberystwyth becomes

$$\phi = - k \int_s \left[\frac{1}{f_2+f_L} - \frac{1}{f_1+f_L} - \frac{1}{f_4+f_L} + \frac{1}{f_3+f_L} \right] Nds \qquad 9.$$

The longitudinal gyrofrequency is always less than 0.83 MHz for the ATS-6 to Aberystwyth geometry and is thus small compared to the signal frequencies. Hence if an average value $\bar{f}_L$ is chosen for the path the above equation can be written

$$\phi = - k \left[\frac{1}{f_2+\bar{f}_L} - \frac{1}{f_1+\bar{f}_L} - \frac{1}{f_4+\bar{f}_L} + \frac{1}{f_3+\bar{f}_L} \right] \int_s Nds \qquad 10.$$

that is

$$\phi = - k \left[\frac{1}{f_2+\bar{f}_L} - \frac{1}{f_1+\bar{f}_L} - \frac{1}{f_4+\bar{f}_L} + \frac{1}{f_3+\bar{f}_L} \right] N_T \qquad 11.$$

where N_T is the total electron content along the slant path from the satellite to the receiving antennas.

Using $\bar{f}_L$ = 0.817 MHz, corresponding to a mean ionospheric height of 420 km, the total electron content (in m^{-2}) can be obtained from the modulation phase delay (in degrees)

$$N_T = - 4.87 \times 10^{14} \phi \qquad 12.$$

The mean value of f_L up to 2000 km has been estimated to be 0.66 MHz, however the resulting change in the numerical constant in Equation 12 is less than 0.25% when this value is used.

(iii) F-factor

An additional experimental parameter which can be obtained from the ATS-6 angular data is the shape factor or F-factor which is a weighted average electron gyrofrequency along the path. This has been defined by DAVIES et al. (1975a) as

$$F = \int_s N f_L \, ds \; / \int_s Nds \qquad 13.$$

and is closely related to the $\bar{M}$- factor used by SMITH (1970) and KERSLEY and SAMBROOK (1971) which represents conditions along the equivalent vertical rather than the slant path.

By substitution from Equations 3 and 10 F can be related to the measured parameters by

$$F = 0.832 \frac{\Omega}{\phi} \qquad 14.$$

Protonospheric content

It can be seen that absolute measurements of the total and Faraday electron contents will, in principle, allow the electron contribution from $\sim$ 2000 km to the geostationary satellite to be determined. The effective upper boundary for this region, the protonosphere or exosphere, is the plasmapause which is usually well below the geostationary orbit height of L$\sim$6.6. The protonospheric electron content (N_P) can be found from

$$N_P = N_T - N_F \qquad 15.$$

4. RECEIVING EQUIPMENT

a. Antennas

The antenna system constructed at Aberystwyth consisted of two single element short-backfire antennas for the UHF and VHF transmissions from ATS-6. The short-backfire antenna, originally designed for microwave frequencies (EHRENSPECK and STROM, 1971) was chosen for the ATS-6 experiment because of its wide bandwidth, high gain, low sidelobe levels and, very importantly for modulation phase comparisons, small group delay (GRUBB, 1972). The actual antennas constructed followed the optimised designs of HARTMANN and ENGELHARDT (1974) for the 140 MHz and 360 MHz frequencies.

The circular framework for the reflectors was of steel conduit covered with galvanised steel wire weldmesh with a square mesh size of 2.5 cm. The small forward reflector was of sheet aluminium in each case and the crossed dipoles, also aluminium, followed the dimensions specified by Hartmann and Engelhardt and were positioned to give an antenna impedance of 50Ω. The outputs from the crossed dipoles were fed directly to 50Ω miniature balanced to unbalanced transformers and then combined in a quadrative hybrid mounted inside the support tube for the dipoles and reflector. From the hybrid 50Ω coaxial feeds for both circular polarisations were taken to the preamplifiers mounted in a weatherproof steel box at the base of the antennas, only the left hand circular ordinary mode being used at 360 MHz. A photograph of the actual antennas, mounted on a small slope in the satellite azimuth at a viewing elevation of 20^{o} is shown in Plate 1.

Approximate estimates of the antenna beamwidths can be made from Fig.2 which shows relative changes in received signal levels averaged over 24 hours as the satellite was moved through the antenna beams. The satellite was started on a westwards drift on 2 August 1974 with a second manoeuvre on 4 August 1974 with consequent changes in viewing azimuth and elevation. Fig.2 indicates that, neglecting the small change in elevation, the half beamwidth for a 3dB drop in signal level corresponds to an azimuth change of less than 15^{o} for both antennas, a result which is in broad agreement with the estimates quoted by HARTMANN and ENGELHARDT (1974) for short-backfire antennas.

This antenna beamwidth suggests that for a viewing elevation of 20^{o} a ground reflected component of appreciable magnitude may be present to interfere with the direct wave. The effects of ground

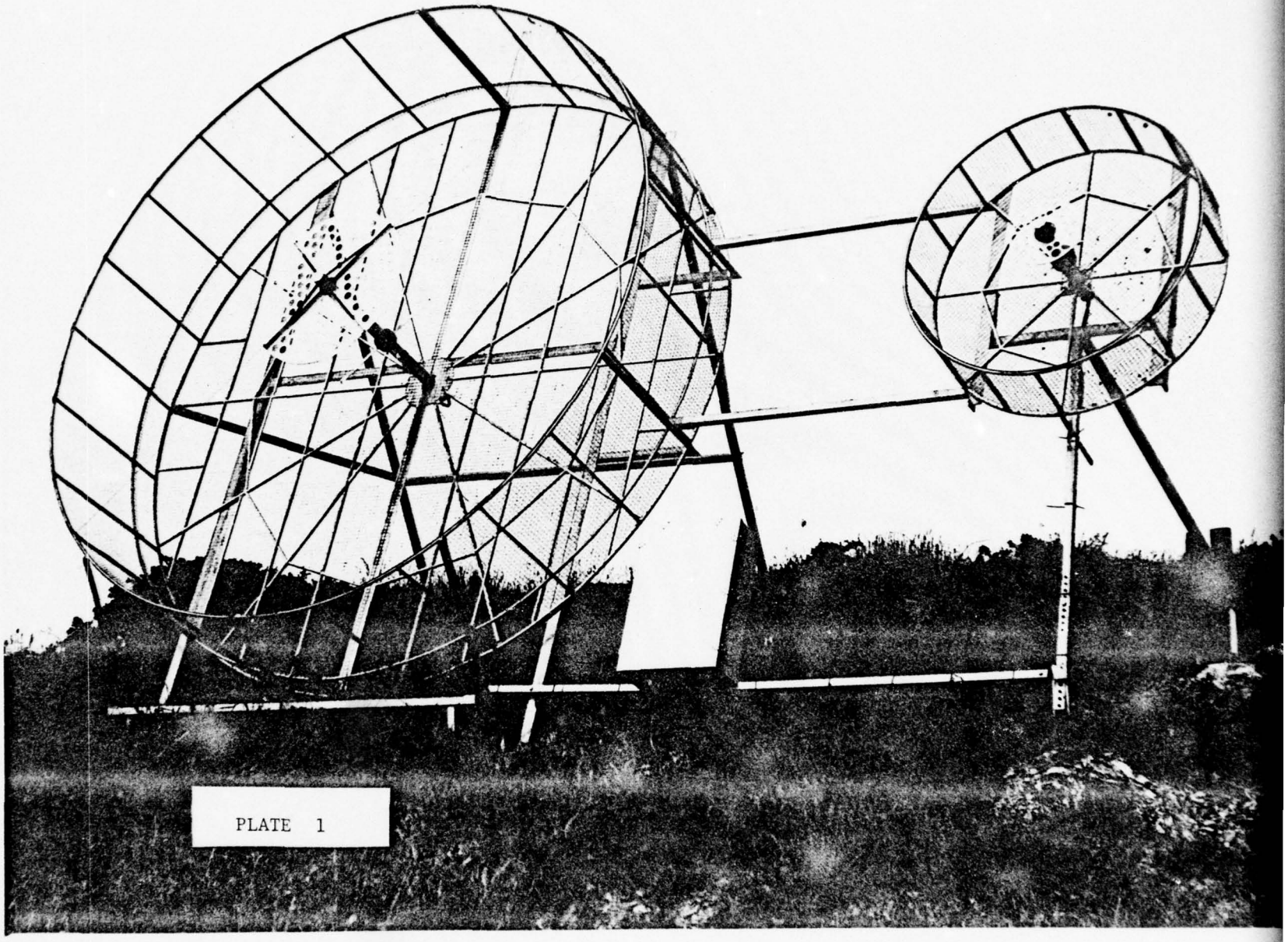

PLATE 1

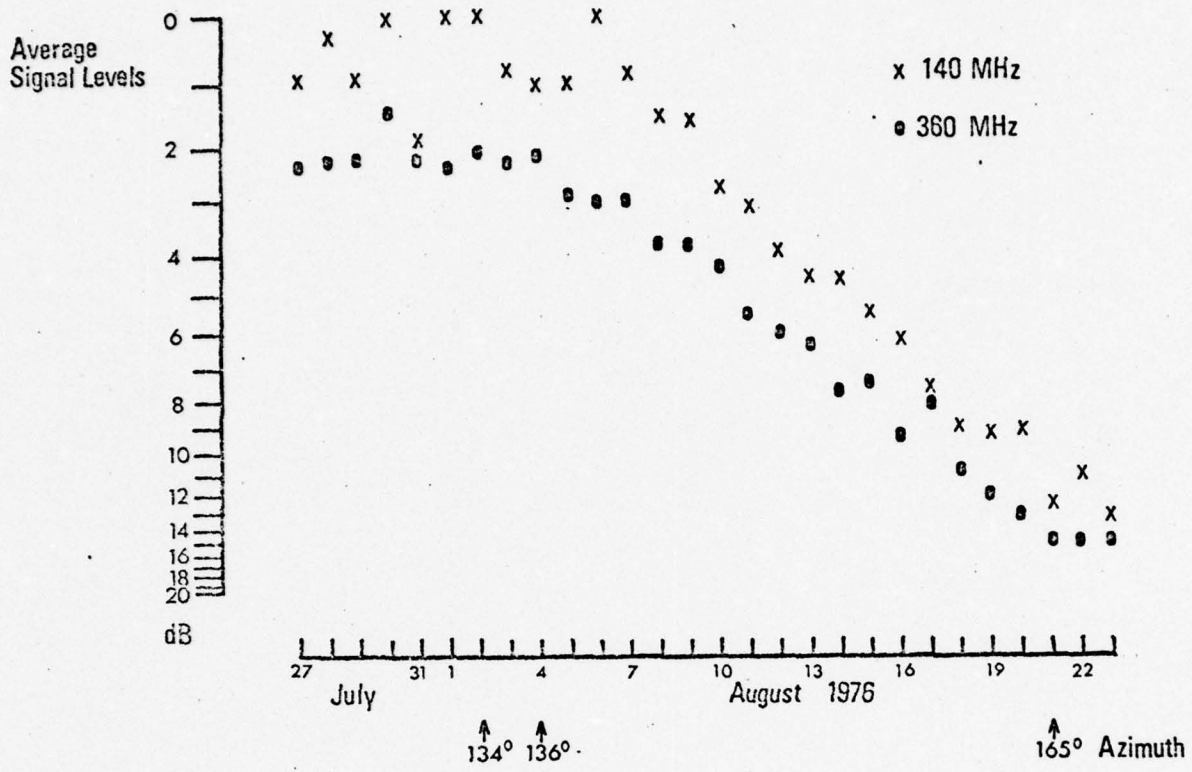

Fig.2. Average relative signal levels of 140MHz and 360MHz carriers for each day during 27 July to 23 August 1976. The ATS-6 Satellite was subject to positional drift manoeuvers on 2 and 4 July 1976.

reflected signals on the ATS-6 experiment have been discussed in detail by REES et al. (1977).

b. Receiver

The design of the receiving equipment used at Aberystwyth is based on the ATS-6 receiving system developed at the Space Environment Laboratory, NOAA, Boulder, USA (GRUBB et al. 1972). The actual receiver used was constructed in modular form by Dunford Hatfield Ltd., Sheffield, U.K. under the supervision of Mr. L. J. Martin, Appleton Laboratory, Slough, U.K.

The receiver uses phase locked loop techniques for the accurate determination of phase differences between very low level signals; the ATS-6 signal levels at the ground being typically $\sim 0.6 \times 10^{-16}$ Wm^{-2} (DAVIES et al., 1972). A schematic block diagram of the receiver is shown in Fig. 3. The Faraday rotation and modulation phase systems can be considered separately.

(i) Faraday rotation

In the Faraday rotation receiving system the two circularly polarised components of the 140 MHz signal are converted to an intermediate frequency of 11.700 MHz using a voltage controlled local oscillator. The signal in one i.f. channel is locked to a reference fixed frequency crystal oscillator with the out of balance voltage from the phase detector fed back with suitable time constant to the voltage controlled local oscillator. The other signal with opposite polarisation is brought to the same i.f. using this common local oscillator and its phase compared to that of the 11.700 MHz reference in a phase detector. The amplified outputs in the form of two quasi-d.c. voltages give the quadrature components (X and Y) from which the amplitude of the

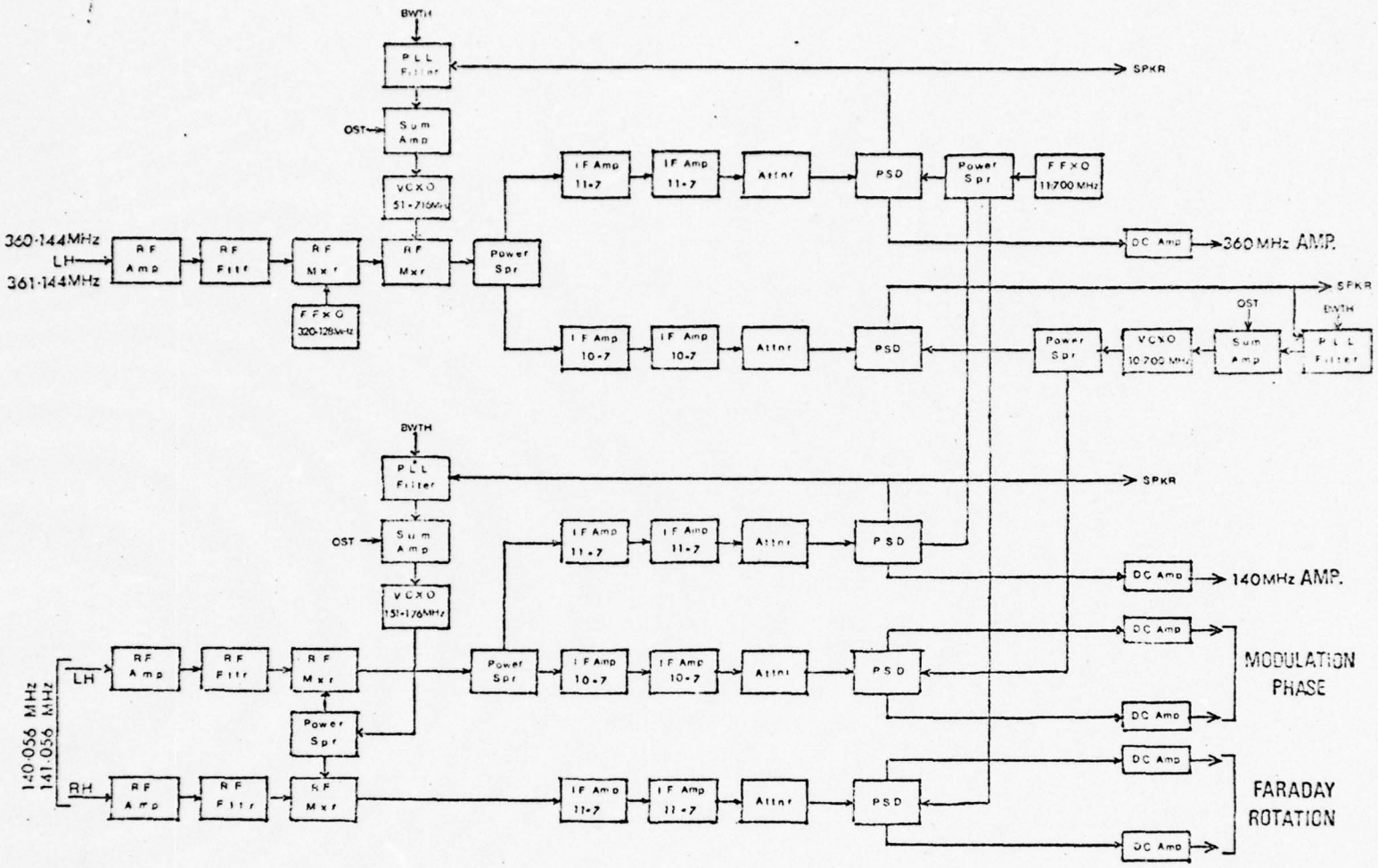

Fig.3. Schematic block diagram of ATS-6 receiver.

second signal (A) and its phase with respect to that of the other component (θ) are obtained from $A = (X^2 + Y^2)^{\frac{1}{2}}$ and $\theta = \arctan (Y/X)$; the latter yielding the Faraday rotation ($\Omega = \theta/2$).

(ii) Modulation phase

The carriers and their respective upper sidebands are received in the modulation phase circuits. The 360 MHz carrier and its sideband are brought to intermediate frequencies of 11.700 MHz and 10.700 MHz respectively by common two stage conversion, the second stage by mixing with a signal from a voltage controlled crystal oscillator operating in a phase locked loop. The conversion of one 140 MHz carrier to 11.700 MHz described above also brings the modulation on this carrier to an i.f. of 10.700 MHz. The 361 MHz sideband, converted to 10.700 MHz is now used in a loop to lock a voltage controlled crystal oscillator at this frequency which in turn provides a reference for phase comparison with the signal in the i.f. channel corresponding to the sideband on the lower frequency carrier. In this way the quadrature component outputs from a phase detector give the phase of the 1 MHz modulation on 140 MHz with respect to that on 360 MHz.

The entire receiving system was designed as a modular integrated package in which the circuits have been simplified by using common modules and avoiding duplication of channels.

The original equipment allowed for acquisition of the signals by manual opening of the phase locked loops and adjustment of suitable d.c. levels fed to the summing amplifiers. However, additional circuitry was built for automatic signal acquisition allowing the equipment to be used reliably at an unattended field station with the often interrupted ATS-6 transmissions.

The settings of the time constants in the phase locked loops are a compromise between narrow loop bandwidth and thus improved signal to noise ratio, and rapid signal acquisition and holding. It was found that loop bandwidth settings of 3 Hz for the two carrier loops and 10 Hz for the sideband loop represented the optimum compromise in the operation of the receiver. The attenuators in the i.f. channels were adjusted at an early stage to give signal amplitudes at the outputs in the range 3 to 5V and thereafter kept constant. The quadrature outputs from the phase detectors are brought to a typical level of several volts in the d.c. amplifiers. In the original design the amplifier time constant was 1s, however this was modified to 10s for the phase measurements in the Aberystwyth system providing some smoothing of the output voltages.

c. Data Logging, Coordinate Converters and Recorders

The output levels of several volts are convenient for storage of data after analogue to digital conversion on magnetic tape for subsequent computer processing. Readings of six voltages corresponding to two pairs of quadrature components and two carrier levels were stored on the data logging system. For quick look monitoring of the performance of the equipment and ionospheric changes each pair of quadrature components were fed to an analogue rectangular to polar coordinate converter whose output voltage, a linear function of angle, was fed to a pen recorder. A two channel Servoscribe chart recorder was used to give simultaneous records of Faraday rotation and modulation phase angles. A chart width of 20 cm for both channels, corresponding to 360^{o} phase difference, gave good angular resolution while the temporal speed was 2mm min^{-1}.

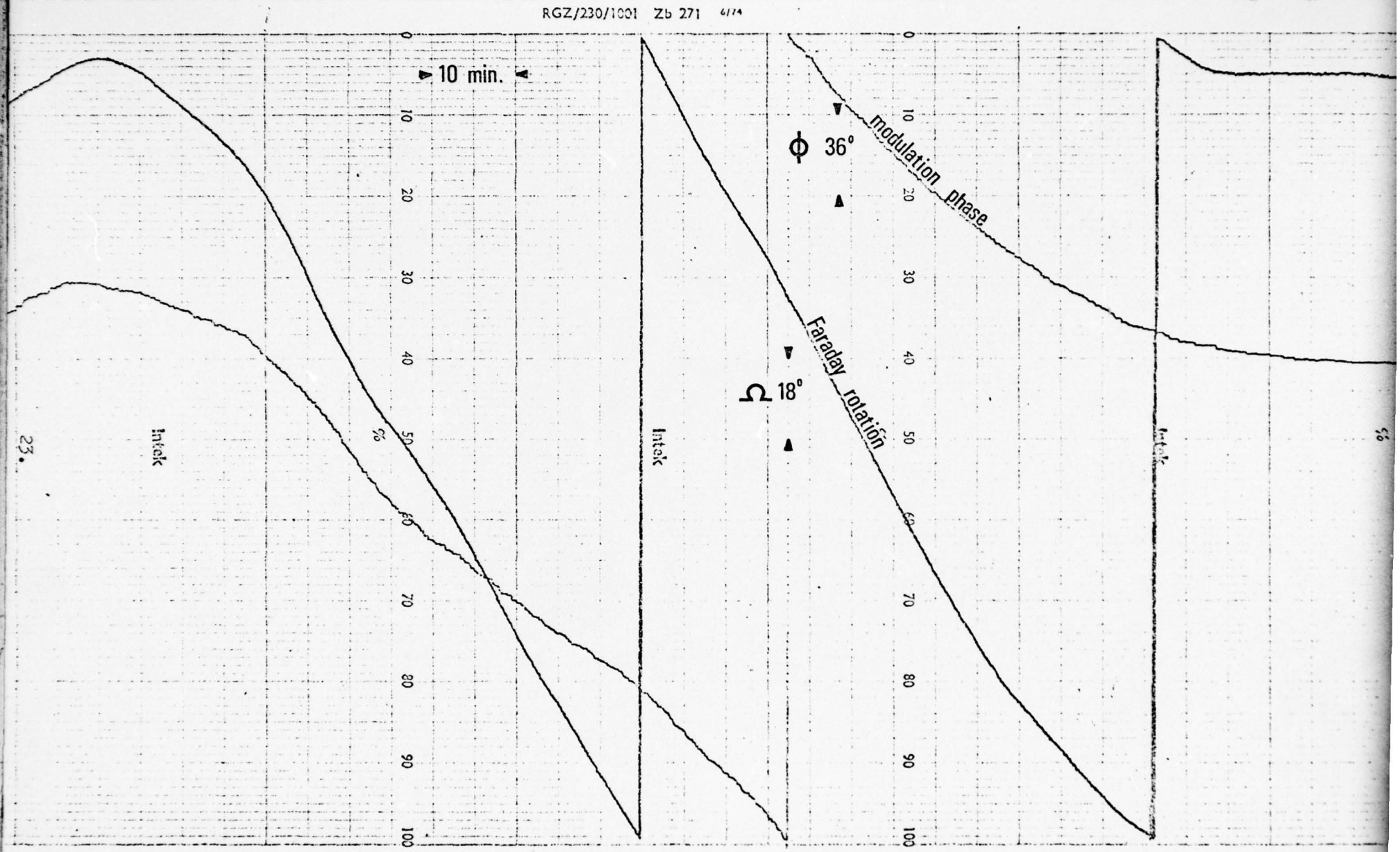

Fig.4. Sample chart recording of modulation phase and Faraday rotation.

A sample record is shown in Fig. 4. A second recorder monitored the amplitudes of the 140 MHz and 360 MHz carriers.

5. CALIBRATION AND ACCURACY

In the ATS-6 experiment the accuracy of the absolute measurements of modulation phase and Faraday rotation is of great importance. As the protonospheric electron content is determined from the difference between the total and Faraday contents, and during daytime may represent only 10% to 20% of the former, to achieve an accuracy of 10% in N_p requires the determination of N_T and N_F to about 1%. The overall accuracy of ATS-6 measurements is dependent on various factors like the spacecraft transmitter and antennas, the performance of the receiving antennas and the calibration of the receiving system. These will be discussed below. In addition, the effect of the choice of mean ionospheric height on the Faraday observation will be considered in detail in the interpretation of the results. The calibration and accuracy of the modulation phase and Faraday rotation measurements are considered separately below.

a. Modulation Phase

The ionospheric phase delay (ϕ) of the 141 MHz signal can be obtained from the phase angle measured at the receiver outputs (ϕ_M) if various systems calibrations are known. The relationship can be written in the form

$$\phi = \phi_M - [\phi_T + \phi_A + \phi_C + \phi_R] \pm 360 \times M \qquad 16$$

where ϕ_T represents the transmitter delay, ϕ_A takes account of the group delays of the receiving antennas and their physical separation, ϕ_C allows for differences in cable lengths, ϕ_R gives

the receiver delay and the final term with M integer accounts for complete cycle ambiguities. Each of these factors can be treated separately.

(i) Transmitter delay

The ATS-6 radio beacon was subject to careful prelaunch calibration to ascertain the phase relationship of the signals at the transmitting antennas and the long term phase stability of the transmitter. The transmitter delay was found to be $\phi_T = -68^o$ (DAVIES et al., 1975b) with a temperature stability of the $\pm 2^o$ over the expected operating range. This value of transmitter delay has been used in the present study.

(ii) Receiving antennas

The choice of short-backfire antennas for the receiving system was conditioned in part by the favourable phase/frequency characteristic of this design in comparison to other high gain antenna systems.

The problem of antenna phase centre displacement for carrier and sideband, representing a frequency dependence of s in the first term of Equation 4, and its interpretation in terms of antenna group delay has been discussed in detail by GRUBB (1975). Experimental measurements of the group delays of short-backfire antennas of optimised design for the ATS-6 frequencies have been made by HARTMANN and ENGELHARDT (1974 and 1975). They report a group delay of 5.8 ns for the 1 MHz sideband on 360 MHz while the corresponding delay for the 140 MHz antenna was 15 ns, values which scale approximately according to wavelength. Thus the group delay appropriate to ATS-6 measurements has a magnitude 15 - 5.8 = 9.2 ns, which for a modulation frequency of 1 MHz

amounts to a phase delay of -2.9^{o}.

The antennas for 360 MHz and 140 MHz were mounted with their active elements coplanar normal to the propagation direction. Since the phase centre of the short-backfire can be considered to be in the plane of the large reflector (GRUBB, 1975) the Aberystwyth antennas must be considered as physically separate in the propagation direction with the 360 MHz antenna ahead of the other by $\sim$ 0.34m. This corresponds to an additional delay $\sim$ 1 ns which represents a phase at 1 MHz $\sim -0.3^{o}$. Thus to an accuracy appropriate to the experiment, allowing for neglect of the second order term evaluated for only one frequency by HARTMANN and ENGELHARDT (1974) and taking into account small differences in antenna design and feed arrangements compared to those of Hartmann and Engelhardt, the value of ϕ_A used in the present study has been taken to be -3^{o}.

As identical lengths of cables were used in comparable situations throughout the receiving system ϕ_C has been taken to be zero in the interpretation of the Aberystwyth data.

(iii) Receiver calibration

To obtain the group delay of the receiving system, from the inputs to the preamplifiers to the outputs to the data logger and chart recorder, it is necessary to generate a spectrum of signals to simulate the satellite transmissions. This is done by a receiver calibrator which was built as part of the receiving equipment to the specifications of the design of GRUBB et al. (1972).

In use, the calibrator, kept physically well away from the actual receiver to minimise cross coupling of stray signals, was connected to the inputs to the preamplifiers via the attenuator and power splitter network shown in Fig. 5a. The attenuators

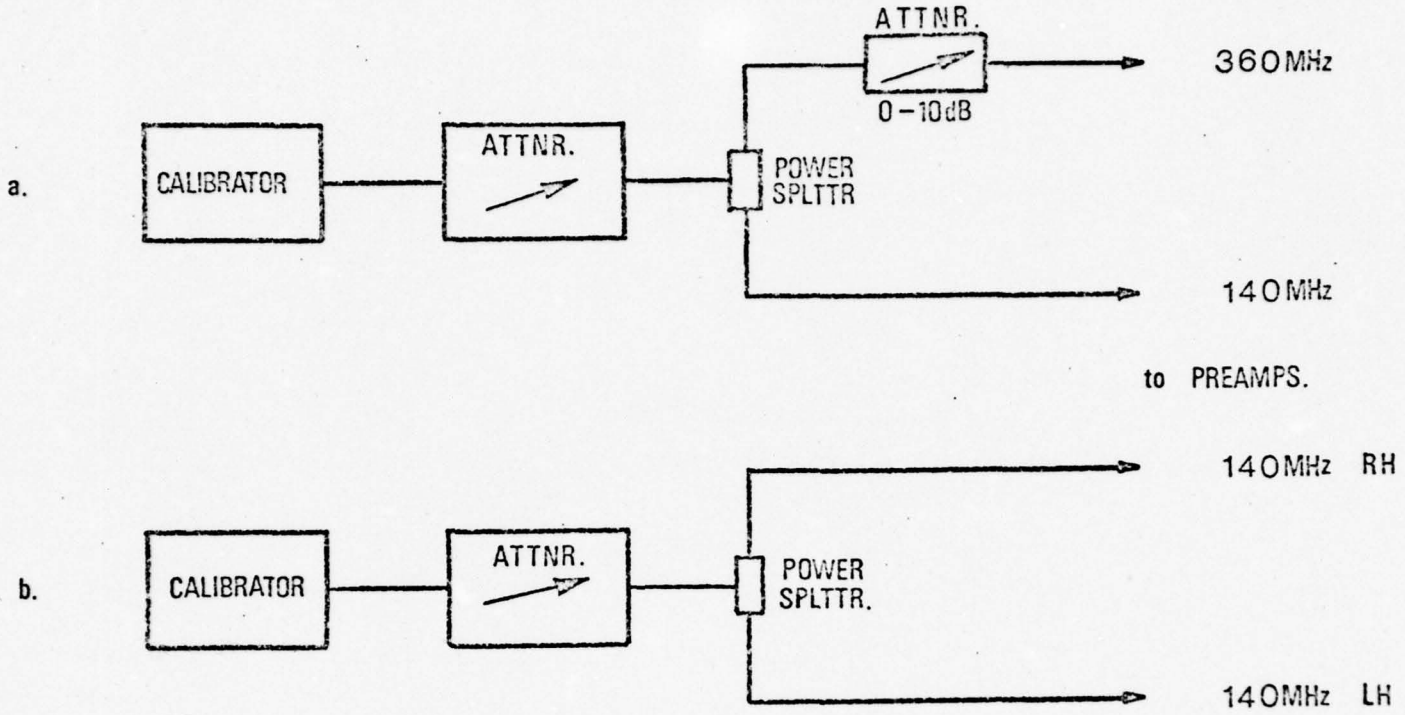

Fig.5. Calibration networks for a. Modulation phase b. Faraday rotation.

were adjusted to give receiver output signal levels for the two carriers comparable to those obtained with the actual satellite transmission and the resulting modulation phase delay for the receiver determined. Calibrations carried out throughout the entire period of ATS-6 observation gave consistent results. Additional comparisons were made on several occasions using an ALDI design calibrator on loan from Air Force Geophysical Laboratory, Bedford, USA which in general gave consistent results with the Aberystwyth calibrator and discrepancies could be traced to the performance of the ALDI instrument. Tests with the master standard calibrator, made available to ATS-6 observers by the Boulder group, gave a modulation phase delay for the receiver which was within the error limits obtained using the Aberystwyth calibrator.

It was noticed in the operation of the ATS-6 receiver that amplitude and phase were not strictly independent in that the modulation phase angle showed a small dependence on the 360 MHz carrier amplitude. The form of this dependence, which appeared to be attributable to the 360 MHz preamplifier, can be seen from Fig.6 which shows the receiver calibration modulation phase angle as a function of signal level defined by the setting of the attenuator in the 360 MHz arm (Fig. 5a). The results displayed in Fig.6 were obtained using the standard Boulder calibrator. The individual points give a mean value and its standard deviation obtained from the average of some 60 readings taken over a period of about 5 minutes. Comparable data for the variation of signal level in the 140 MHz channel presented in Fig.7 shows an essential independence of phase and amplitude.

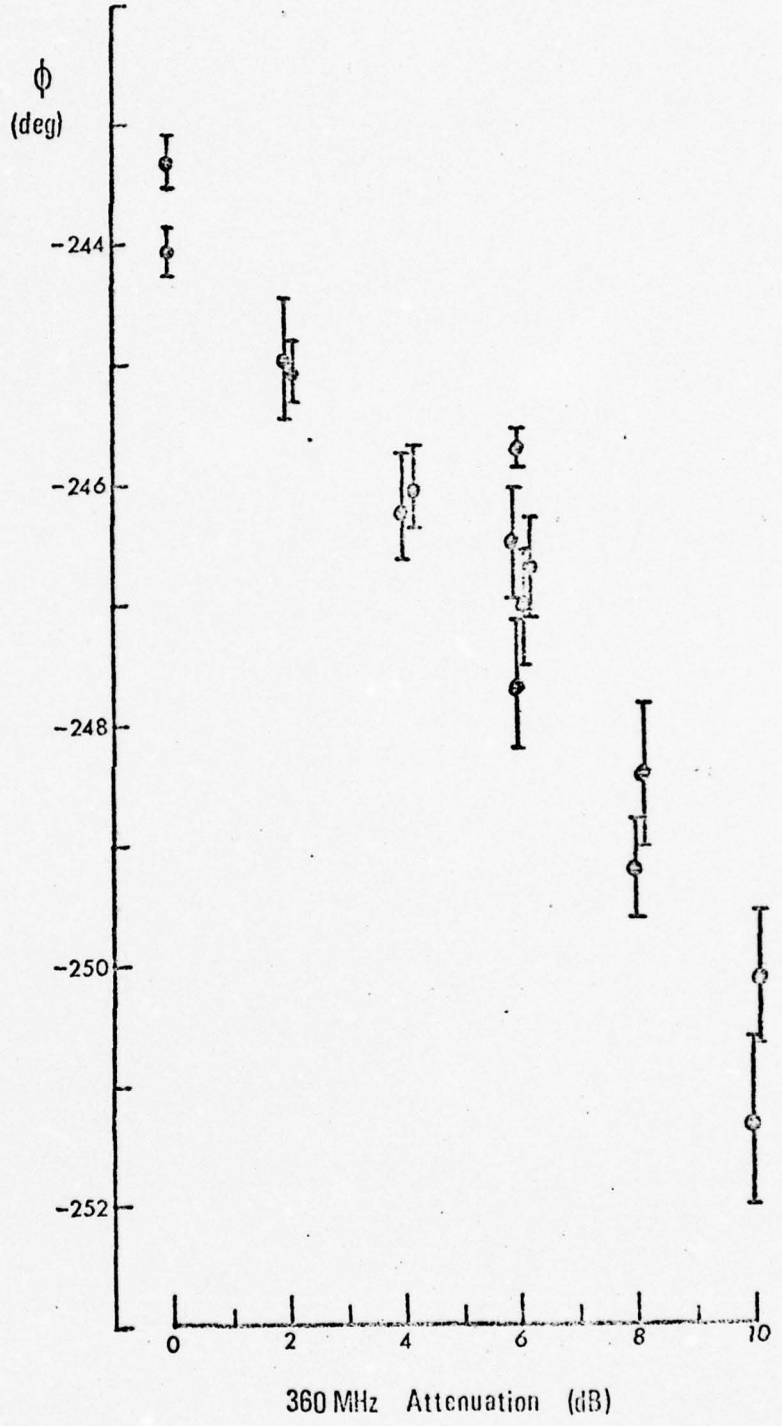

Fig.6. Receiver modulation phase delay as a function of attenuation in 360MHz channel.

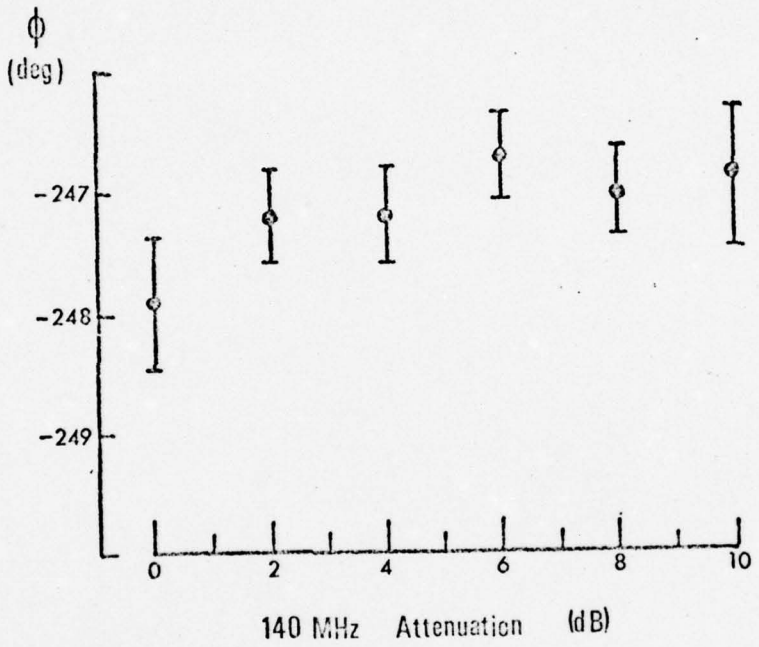

Fig.7. Receiver modulation phase delay as a function of attenuation in 140MHz channel, with 0 - 10 dB attenuator (Fig.5a) in 140MHz arm.

The received signal level at 360 MHz was subject to variations within a typical range of about 3dB which have been attributed to changes in satellite pointing and possibly radiated power, so that a small error in modulation phase is introduced from the amplitude/phase coupling. While it is possible to take account of this variation, for the purposes of the present study which is primarily concerned with averaged observations, a calibration value has been used which is representative of the approximate mean 360 MHz signal level received throughout the observing period.

In the long term, the receiver calibration was found to have good stability with only small dependence on external temperature.

Taking account of the factors discussed above a value of modulation phase delay in the receiver $\phi_R = -248^o$ has been used for the analysis of the results described in this report. It is believed that this value is representative of the receiver calibration applicable to this study of averaged data throughout the nine months of observation to an accuracy of about $\pm 3^o$. However, in the investigation of isolated individual events, particularly at times of scintillation of the 360 MHz signal, the errors could be somewhat larger.

b. Faraday Rotation

The calibration of the Faraday rotation system to obtain absolute values of measured phase difference of the ordinary and extraordinary modes involves consideration of the orientations of the transmitting and receiving antennas together with the phase delay of the receiver.

(i) Transmitting antenna orientation

The measurement of the radiated polarisation was carried out as one of the pre-launch calibrations of the satellite radio beacon so that its orientation is known with respect to the satellite axes (DAVIES et al. 1975a). It is thus possible to calculate the orientation of the transmitted polarisation as viewed by an observer for known satellite and observer locations. For geometry applicable to the ATS-6 satellite stationed at 35°E viewed from Aberystwyth the effective 140 MHz transmitting antenna orientation makes an angle of 26° with the local station horizontal measured in a counter clockwise direction looking towards the satellite.

(ii) Receiving antenna orientation

The active elements of the 140 MHz receiving antenna are crossed linear dipoles followed by a quadrature hybrid in which the linearly polarised incoming signal is converted to its circularly polarised components. A zero phase difference between these polarisation modes implies that the angle of the received linear polarisation bisects the crossed dipoles. The dipoles were set to be symmetrically inclined at nominal angles of ± 45° with respect to the local horizontal, however measurements with an inclinometer showed that there was an assymmetry of 2° in the adjustment. Thus the angle corresponding to zero phase difference between the circular modes was found to be 92° from the local horizontal, counter-clockwise viewed from behind the antenna, that is in the direction of increasing Faraday rotation.

Thus the difference between the effective polarisations of the transmitting and receiving antennas amounts to 92 - 26 = 66° which must be allowed for in estimating absolute Faraday rotation.

(iii) Receiver calibration

The phase comparison of the signals in the 140 MHz channels of the receiver was calibrated using the calibrator described earlier. A signal from the calibrator, brought to an appropriate level in attenuators was fed from a power splitter to the inputs of the two 140 MHz preamplifiers (Fig. 5b) and the corresponding output from the Faraday rotation channels noted. A value of 342^{o} phase difference between the polarisation modes corresponding to a Faraday rotation angle of 171^{o} has been used for the present study. This value was representative of the early calibration runs to an accuracy of about $\pm 2^{o}$ rotation. However, it should be noted that angles outside this range towards lower values were obtained in later calibration work with an extreme value of 166^{o} being measured on one occasion. The physical situation of the receiving equipment at Aberystwyth in a small field site hut made regular calibration impractical so that it has been necessary to assume a fixed value for the present work.

An additional factor affecting the polarisation measurement was the operation for some months of a second group delay receiver of ALDI design in parallel with our own equipment using the extraordinary mode polarisation from the same antenna system. It was found that a change of about 2^{o} was introduced in the polarisation angle measurement when one of the 140 MHz signals was divided between the two receivers.

An independent check of the Faraday rotation calibration was made using a separate receiving system fed from a dipole which could be manually rotated. The polarisation angle of the radiation received from the satellite was determined by swinging the dipole through a signal null between equal levels at the receiver output.

Measurements over an extended period with changing polarisation were then compared with the chart record of Faraday rotation. The results of one such calibration check representing some 80 independent measurements taken over a 10 hour period are plotted in Fig. 8. A best fit straight line yields an intercept of $13^{o} \pm 2^{o}$ for the angular difference between the two measurements. This angle can be compared to a corresponding value of 11^{o} obtained from the calibration measurements of receiver and receiving antenna.

c. Resolution of Ambiguities

Having determined the origins for the measurements of modulation phase and polarisation rotation one further consideration remains in the determination of absolute values of these angles, namely ambiguities of complete cycles. This point dictated the choice of frequencies for ATS-6 and its resolution was facilitated by the recording of two angles with differing sensitivities to ionospheric changes so that it was relatively easy to select the correct cycles to give reasonable values for both ionospheric and protonospheric parameters. Furthermore, the results reported here were obtained for conditions of minimum solar activity so that the predawn modulation phase angles were usually within the first cycle. Thus in spite of the frequent interruptions of the transmissions the resolution of complete cycle ambiguities has presented no real problems.

6. IONOSPHERIC PARAMETERS - RESULTS

a. Data Base

The ionospheric data presented here have been obtained from the chart records of the angular parameters ϕ and Ω reduced at one hour intervals for the period November 1975 to July 1976 when

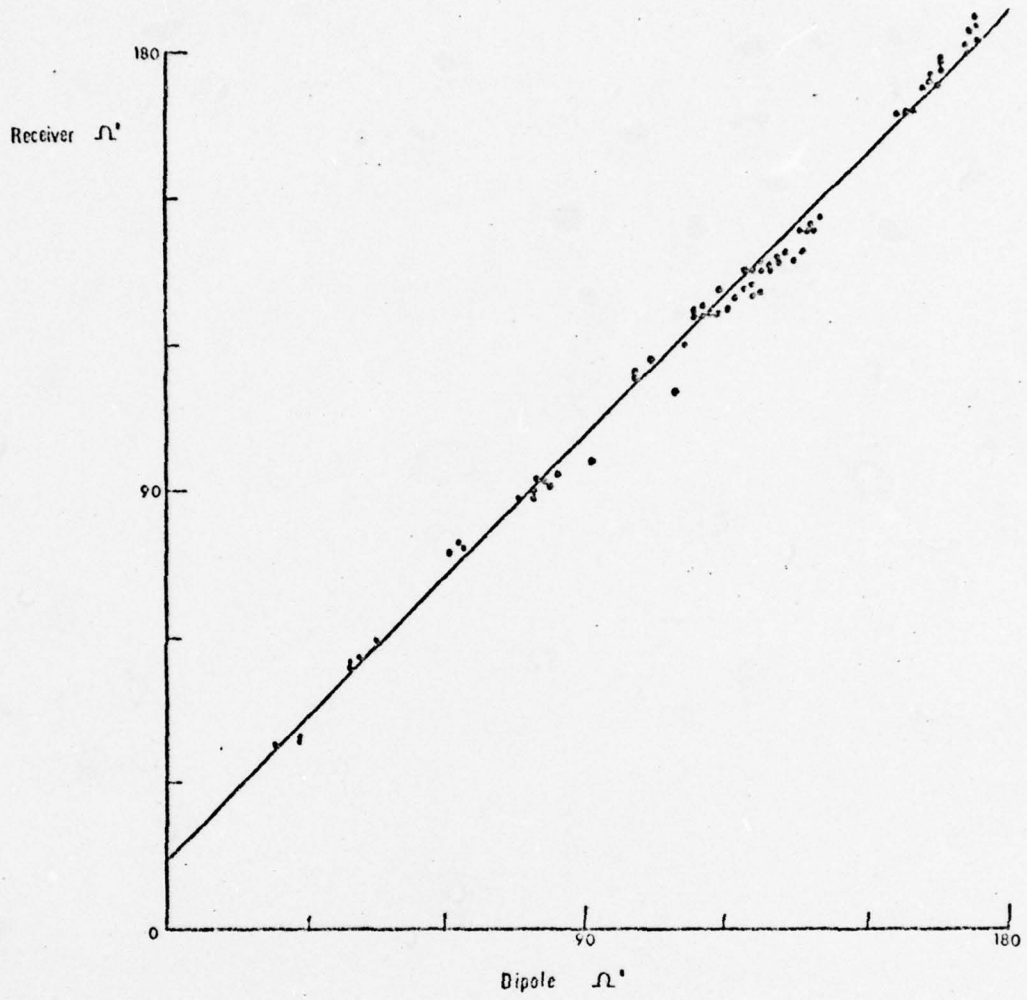

Fig.8. ATS-6 receiver Faraday rotation angles compared to independent measurements obtained using a rotating dipole.

satellite transmissions were available and records were obtained.

Hourly values of N_T, N_F and N_p together with F have been calculated. The F-factor has been presented in two equivalent forms, F itself and h_{BL} (or h_{eff} after DAVIES et al. (1976)), the height for which the observed value of F equals the longitudinal gyrofrequency. Tables of these parameters on a monthly basis have been prepared which also contain a statistical summary of the data for each hour, namely mean and standard deviation, median and quartile values. Sample tabulations of N_T, N_F, N_p and F for the month of November 1975 are presented in Tables 2 to 5.

b. Day to Day Variability

The day to day variability of the parameters can be gauged from superposed multiplots of the diurnal variation for each day in a month. Plots of N_T, N_F and N_p for three months, representing winter, equinox and summer are shown in Fig. 9. The large day to day variability of N_T and N_F agrees with the findings of many beacon satellite workers but as yet no completely satisfactory explanation is available (RISHBETH and KOHL, 1976). Apart from obvious solar and geomagnetic dependencies it has been suggested that the variability reflects the erratic nature of the global neutral wind system (KANE, 1975).

Fig. 9 shows that the variability is most pronounced in N_p, to an extent that the general shape of the individual diurnal plots is masked by the day to day variations. In addition, the local mean times of the maximum and minimum values of N_p show considerable ranges, although a more consistent picture is found in the monthly averaged data.

TABLE 2

HOURLY VALUES OF SLANT NT
UNITS IN ELECTRON PER SQUARE METER X 10*15
NOVEMBER 1975

DAY	0	1	2	3	4	5	6	7	8	9	10	11	12	13	14	15	16	17	18	19	20	21	22	23
1	130	133	133	138	124		112	135	177	177	209													
2	NO RECORDS AVAILABLE																							
3										172	161	203	198	195			193	195	160	160	135	107		
4		51	40	33	26	30	37										160	128	91	56	44	30	30	30
5	30	37	25	25	25	28	37	98	160	198	202	233	282	254	226	191	160	145	121	95	89	86	84	79
6	79	72	68	60	51	51	61	103	138	163	186	216	202	242	263	219	160	126	98					
7	89	86	75	72	60	58	70	119	145	163	200	202	221	224	270	238	177	117	100	86	82	84	82	81
8	84	79	75	77	67	67	72	119	153	174	205	224	247	226	261	247	177	130	110	107	100	100	103	103
9	109	107	107	110	98	98	105					230	242	309	282	268								
10				60	49	47	54	96	131	193	200	238	254	251	238	221	209	177	147	137	124	124	114	107
11	93	89	86	82	67	60	60	103	165	193	230	256	249	216	223	240	184	172				107	100	95
12	102	89	93	93	79	75	79	114	158	299	223	223	231	237	235	226	182	142	123	119	107	107	107	107
13	107	107	107	107	95	95	98	135	170	201	224	242	238	221	258	247	247	177						
14										196	230	261	247	247	247	226	209	137	119	119	123	124	124	131
15	133	135	137	135	128	124	124	147	172	185	219	251	272	212	216	219	195	151	133	124	128	135	133	138
16	142	144	142	140	137	137	135	145	202	235	258	312	266	272	249	247	219	167	165	175	179	188	188	189
17	174	198	200	193	170	160	156	174	219			282	298	331	377	380	354	295	165	138	133	130	130	119
18	117		86	74	79	74	72	126	281	186				256	231	181	153	138				118	107	107
19	107	102	103	96	84	79	81	114	179	200								133	126	103	93	96	98	105
20	103	103	107	102	81	62	77	107	147	175					207	195	153	133					93	96
21	96	98	103	89	88	93	83	131	188	275	296	328	287	258	247	233	205	177	142	137	128	126	131	124
22	128	133	137	128	123	114	112	130	172	238	212	272	302	317	370	275	223	202	86	103	103	100	98	95
23	79	72	77	67	67	63	54	75	124	163	207	223	200	191	172	207	149	119	96	82	68	63	60	60
24	63	61	65	60	58	60	61	89	131	182	214			212	240	235	195	181	145	119	96	88	96	102
25	98	89	95	89	68	67	70	93	119	151	170	177	219	203	216	189	161	144					96	96
26	98	93	96	86	77	75	72	88	131	154	212	268	224	247	268	200	135	118	110	107	96	95	96	96
27	93	86	93	84	74	77	86	103	147	172	219	207	233	214	184	182	181		116	110	100	100	100	102
28	103	105	107	102	95	91	88	95	130	160	191	189	172	189	172	181	147	133	117	103	100	102	98	107
29	107	107	121	121	121	117	110	114	151	216	267	263	235	298	254	191	174	156	128	131	130	119	107	107
30	116	116	107	89	68	67	75	93	131	164	182	195	209	195	212	230	235	217	130	110	88	79	79	81
COUNT	25	25	26	27	27	26	27	25	25	26	23	23	23	25	25	25	26	26	22	21	21	23	24	24
MEAN	103	99	99	93	84	80	84	114	158	168	215	239	240	241	245	227	190	158	124	115	107	104	102	102
RMS.	27	33	34	35	33	31	28	22	28	29	30	37	33	39	47	41	43	38	22	26	28	29	28	28
MEDIAN	103	98	100	89	79	75	77	114	153	188	212	233	238	237	240	226	181	145	122	110	100	102	99	103
UPQRT.	117	100	107	110	98	95	105	131	174	204	224	263	266	257	262	244	209	177	142	134	128	124	110	107
LOWQRT	91	82	77	72	67	60	61	96	131	168	200	207	219	212	216	193	160	133	110	103	91	88	95	95

TABLE 3

HOURLY VALUES OF SLANT NF

UNITS IN ELECTRON PER SQUARE METERX10*15

NOVEMBER 1975

DAY	0	1	2	3	4	5	6	7	8	9	10	11	12	13	14	15	16	17	18	19	20	21	22	23.
1	83	89	90	90	76	66	64	94	128	133	172	225	239	204	194									
2	75	80	80	81	71	68	64	113	146	168	196	207	216	215	263	229	187	173	151	144	115	115	106	95
3	74	45	40	30	22	24	38	81	112	144	150	178	168	162	156	173	157	162	128	131	117	90	79	66
4		43	34	24	37	19	29	72	103	114	149	156				171	144	117	77	50	36	25	25	26
5	24	22	20	17	15	17	25	79	137	170	179	205	248	225	198	164	136	123	93	71	67	59	62	59
6	56	58	47	39	30	30	38	76	111	139	162	185	174	213	233	191	132	94	72					
7	64	63	54	47	38	33	44	90	122	137	171	173	195	194	235	208	148	87	72	60	54	57	67	57
8	58	56	51	49	39	36	38	81	115	135	167	189	211	191	219	208	140	92	72	71	65	64	67	72
9	72	74	72	71	62	60	66					189	207	269	232	223								
10				39	30	29	35	73	109	140	174	216	225	222	213	195	180	150	126	112	99	95	88	75
11	66	65	59	55	45	30	36	77	138	163	222	225	222	189	198	210	156	149				84	78	72
12	72	67	67	64	55	50	53	82	126	174	121	193	202	208	207	197	151	115	95	90	78	75	78	78
13	77	76	77	72	64	62	63	95	135	132	182	204	290	167	219	208	207	141						
14										156	189	221	215	210	209	189	165	100	81	78	86	88	89	98
15	98	99	102	96	86	81	84	114	138	148	176	213	232	174	176	180	150	111	93	82	87	89	90	98
16	99	105	106	98	92	90	89	107	162	194	217	269	225	226	207	203	168	124	121	128	130	137	138	139
17	130	148	149	146	125	108	110	128	174		216	233	250	266	326	330	312	253	137	110	105	102	106	91
18	88		59	42	52	47	47	102	195	162	216	258	233	228	204	153	129	115				83	81	82
19	81	77	73	69	55	49	53	85	153	171		236	191	209	183	171	155	104	98	72	62	67	72	75
20	78	80	89	72	81	52	49	76	121	151		227	229	198	175	162	124	105					62	65
21	65	65	66	56	47	46	49	82	140	224	247	281	233	216	208	191	162	135	104	98	86	90	96	89
22	95	98	97	85	75	70	70	93	135	200	175	231	238	273	326	235	186	171	61	79	79	77	75	71
23	55	53	57	54	48	46	39	82	114	151	189	205	179	169	153	189	131	101	79	65	53	48	46	46
24	47	48	49	43	38	38	39	64	109	156	181	182	182	178	212	204	164	152	122	95	69	64	72	77
25	71	65	66	63	45	43	46	62	95	123	142	147	187	174	184	155	130	112					67	68
26	67	68	65	60	50	47	47	61	104	126	177	231	189	210	231	164	99	81	76	72	62	61	65	64
27	62	56	59	53	43	45	50	64	111	133	171	162	189	167	144	138	137		84	69	61	63	64	68
28	69	70	71	67	59	55	51	60	95	127	153	154	134	151	133	143	114	94	80	68	65	68	64	71
29	72	74	84	83	78	70	63	72	111	165	242	222	195	249	216	150	138	120	96	102	99	90	81	79
30	86	81	72	61	43	42	44	64	103	151	150	165	178	165	180	207	205	184	101	81	71	55	56	59
COUNT	27	27	28	29	29	29	29	28	28	28	27	30	29	29	29	29	28	27	23	22	22	24	26	26
MEAN	74	71	69	63	54	50	53	83	126	154	183	206	207	205	208	191	157	128	96	88	79	77	76	75
RMS.	19	23	25	25	23	21	18	23	25	25	25	33	25	43	37	39	37	24	24	23	23	23	21	20
MEDIAN	72	67	67	61	50	47	49	80	121	151	176	206	207	208	207	191	151	117	93	80	74	76	74	72
UPQRT.	83	80	80	77	67	64	63	93	137	166	196	227	230	223	225	208	167	150	121	102	99	90	88	82
LOWQRT	64	54	55	48	39	37	39	68	110	136	167	182	198	176	182	164	134	101	76	71	62	62	64	65

TABLE 4

HOURLY VALUES OF SLANT NP

UNITS IN ELECTRON PER SQUARE METERX10*14

NOVEMBER 1975

DAY	0	1	2	3	4	5	6	7	8	9	10	11	12	13	14	15	16	17	18	19	20	21	22	23
1	465	447	429	481	484		487	410	481	438	368													
2	NO RECORDS AVAILABLE																							
3										378	303	253	299	327			354	327	316	289	178	166		
4		79	63	92	93	110	82										155	108	142	60	80	48	48	39
5	56	74	49	79	93	111	118	194	227	272	227	283	244	296	284	274	235	220	279	240	223	269	274	198
6	225	191	218	202	204	213	229	274	276	244	239	304	280	290	304	286	271	323	257					
7	259	233	217	254	220	247	263	269	236	262	295	289	259	303	347	309	294	307	284	260	287	269	251	234
8	260	225	244	272	273	308	334	387	344	386	378	356	361	347	420	387	375	376	380	363	346	364	363	319
9	362	327	345	398	364	362	300					409	353	505	455									
10				202	187	187	195	231	223	226	254	228	296	288	255	259	288	268	211	249	252	296	263	318
11	267	241	269	269	219	211	238	265	270	300	275	314	271	269	249	299	284	233				211	231	231
12	292	223	258	294	234	253	261	316	316	342	312	294	292	291	293	293	311	275	279	289	291	318	291	291
13	300	359	360	354	311	329	355	366	390	379	419	379	380	393	385	387	405	357						
14										407	409	402	325	369	378	374	431	365	378	414	368	368	350	340
15	357	357	346	393	421	431	404	330	358	382	411	378	400	386	394	393	443	398	402	422	412	464	409	410
16	427	391	364	418	446	464	455	381	397	408	403	428	419	454	423	441	509	422	440	474	491	507	498	489
17	438	467	513	479	448	513	463	456	458			496	475	451	513	503	419	413	279	285	286	277	242	280
18	298		259	244	270	262	245	242	259	230				278	274	276	237	231				270	255	246
19	255	247	301	275	296	297	279	290	298	290								295	287	319	312	293	297	300
20	256	238	273	292	303	305	279	309	245	241					345	327	282	286					312	311
21	311	329	390	330	411	473	496	492	480	471	498	469	540	421	367	426	432	420	382	383	421	359	358	350
22	331	348	481	421	476	442	424	376	367	380	309	409	439	444	443	399	366	307	251	247	247	230	230	240
23	234	164	199	165	183	175	150	137	144	171	161	178	209	220	188	181	184	181	177	171	156	148	140	140
24	157	130	157	167	194	220	220	259	273	287	332			341	281	309	309	285	238	244	275	241	248	247
25	275	241	275	268	236	237	245	312	244	273	278	303	322	342	313	346	316	319					253	284
26	311	276	311	260	270	280	254	280	277	281	350	374	356	369	374	361	357	376	344	354	347	333	311	329
27	312	295	339	312	307	324	358	399	388	385	483	449	444	466	480	445	437		414	416	391	373	385	337
28	345	354	363	346	356	365	367	347	322	325	381	355	376	381	385	374	336	393	378	354	346	337	347	345
29	354	327	369	378	431	477	478	415	396	512	460	411	399	493	386	408	358	361	322	295	304	260	285	282
30	298	290	345	286	254	246	315	294	313	329	320	300	306	291	323	318	300	331	286	290	170	243	225	216
COUNT	25	25	26	27	27	26	27	25	25	26	23	23	23	25	25	25	26	26	22	21	21	23	24	24
MEAN	298	273	293	294	296	302	310	322	314	326	346	351	354	356	352	353	334	315	306	305	294	290	282	282
RMS.	84	99	102	108	111	112	89	80	85	81	82	78	75	70	78	73	83	76	76	92	96	97	89	87
MEDIAN	298	276	300	286	273	268	279	312	313	313	350	356	353	347	374	361	326	321	287	290	291	289	260	288
UPQRT.	350	338	363	378	411	382	404	384	385	385	429	409	400	407	397	404	405	376	378	373	358	356	348	333
LOWQRT.	257	224	244	244	215	220	238	269	251	267	278	294	296	291	283	296	284	275	257	248	235	241	236	237

TABLE 5

HOURLY VALUES OF F-FACTOR

UNITS IN KILO-HZ

NOVEMBER 1975

DAY	0	1	2	3	4	5	6	7	8	9	10	11	12	13	14	15	16	17	18	19	20	21	22	23
1	524	543	554	533	499		463	569	591	615	673													
2	NO RECORDS AVAILABLE																							
3										683	680	716	694	680			667	680	655	669	710	691		
4		690	689	598	528	515	636										738	748	690	730	667	687	657	711
5	662	613	695	566	576	495	556	655	701	705	725	718	718	722	715	700	697	693	629	610	613	562	600	612
6	584	600	567	540	489	475	512	681	659	695	712	702	704	719	723	711	678	608	603					
7	581	595	582	529	515	468	511	619	683	666	699	700	722	707	712	711	681	604	585	570	532	556	568	580
8	565	564	553	521	483	439	437	532	633	636	667	688	696	692	606	687	644	581	536	540	534	520	530	566
9	545	567	554	523	514	499	514					672	696	713	671	679								
10				540	506	494	525	622	673	706	713	739	722	723	730	722	704	694	700	668	632	623	629	574
11	582	597	662	550	519	627	491	604	683	699	720	717	728	715	726	715	691	706				656	637	618
12	582	613	590	559	575	543	647	690	653	683	753	709	714	717	719	711	678	659	632	619	595	574	595	595
13	588	601	588	547	548	533	501	596	642	662	665	689	687	672	695	689	683	652						
14										648	672	691	710	695	692	682	646	599	558	534	572	576	597	606
15	598	601	610	587	548	535	542	631	647	651	684	694	697	669	646	671	631	601	571	540	554	536	554	575
16	572	595	506	573	551	540	542	603	656	675	689	705	689	661	678	671	627	610	599	596	593	596	680	604
17	611	615	607	618	602	555	576	602	647			674	687	706	706	709	721	703	679	649	642	643	665	626
18	610		562	546	538	526	539	669	722	712				728	720	692	690	681				616	622	629
19	622	616	657	584	530	510	535	610	699	699								637	631	566	543	569	603	564
20	615	629	629	632	545	515	571	581	670	758					693	680	666	642					543	554
21	554	544	509	515	434	401	410	512	608	677	681	700	664	684	689	668	645	624	597	588	548	585	555	587
22	606	604	577	548	500	500	502	586	643	687	665	694	698	703	720	699	663	693	579	622	622	629	626	610
23	575	631	687	615	593	591	502	669	723	734	746	752	732	723	728	746	716	693	667	648	631	626	626	626
24	614	643	620	682	543	515	524	681	678	698	691			[illegible]	722	710	688	688	683	650	584	592	607	618
25	528	597	572	572	535	527	732	543	650	669	684	677	697	[illegible]	629	668	657	636					569	576
26	559	576	554	570	531	614	529	656	645	667	687	703	688	695	703	670	601	559	563	547	523	525	554	538
27	543	556	519	513	477	474	477	502	616	634	637	640	662	639	640	618	620		525	510	498	512	507	547
28	544	542	540	539	510	482	475	517	614	651	654	664	638	653	634	648	631	576	554	537	534	547	529	549
29	547	567	568	562	526	466	443	520	601	624	687	690	679	662	693	643	649	628	611	634	626	619	622	602
30	607	607	554	556	513	516	475	559	623	671	674	691	607	695	693	708	713	693	637	602	659	565	594	598
COUNT	25	25	26	27	27	26	27	25	25	26	23	23	23	25	25	25	26	26	22	21	21	23	24	24
MEAN	583	693	530	550	526	507	517	506	636	676	686	697	697	695	608	688	671	650	613	602	592	592	594	595
RMS.	31	34	30	29	35	37	47	45	35	29	23	23	22	22	25	28	34	48	50	55	55	49	41	35
MEDIAN	502	697	575	556	528	514	521	590	690	680	662	494	607	695	699	689	678	647	607	602	593	585	507	597
UPQRT.	606	614	607	580	548	527	542	615	661	694	703	709	714	716	720	710	691	693	655	649	637	626	624	615
LOWQRT.	556	571	554	539	506	489	477	554	628	651	667	683	687	681	688	670	645	608	571	544	539	556	561	575

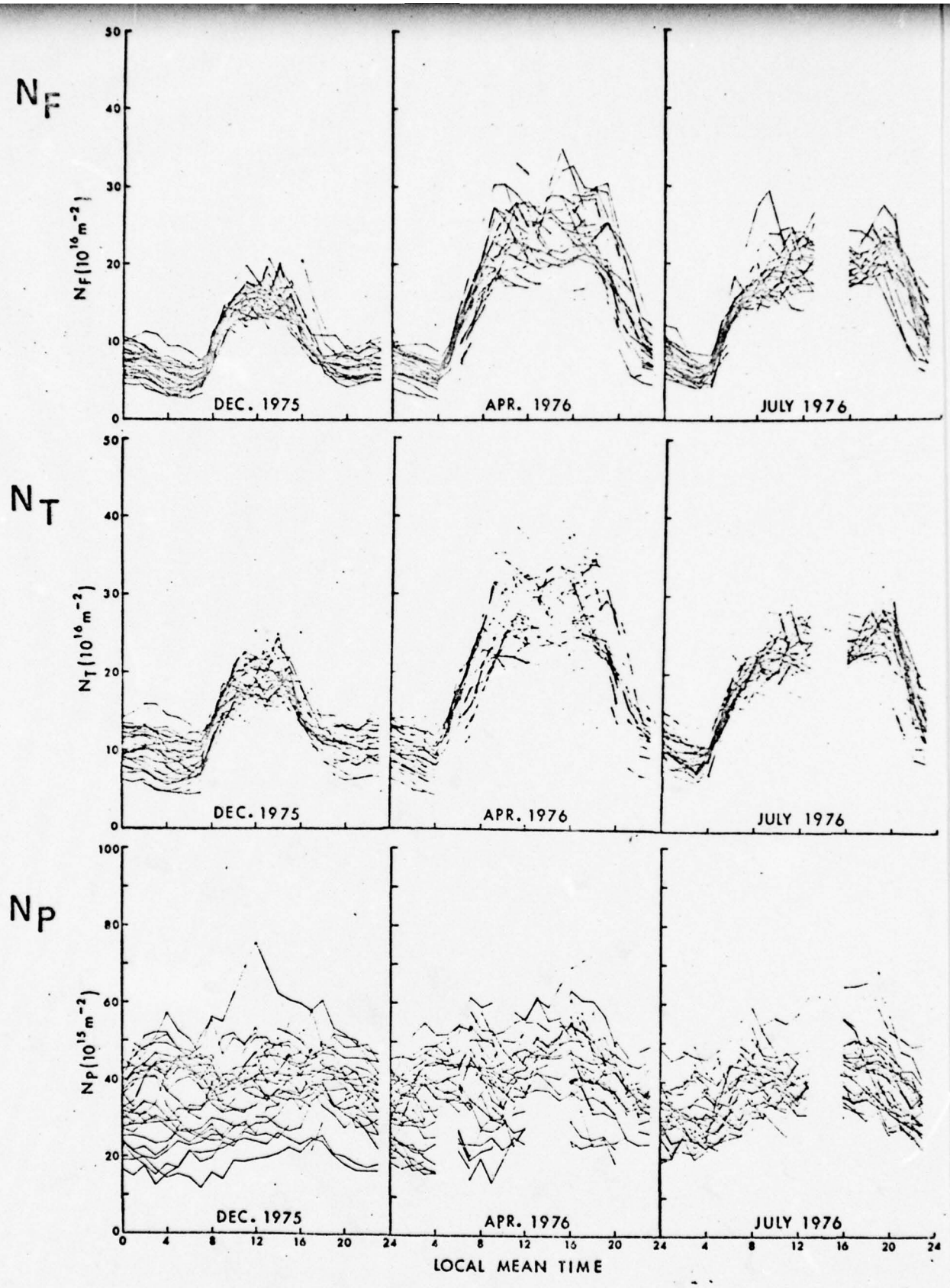

Fig.9. Multiplots of diurnal variations of N_F, N_T and N_P for Aberystwyth for selected months.

In Table 6 standard deviation of the noon values of each of the parameters by month is compared to the corresponding diurnal range of the monthly mean values. For N_T and N_F the variability is much less than the diurnal range with the smallest standard deviations in winter and largest at equinox suggesting that the magnitude of the day to day variations is related to the electron content level. However, for N_P in winter the noon time variability is comparable to the mean diurnal range with the deviations representing some 30% to 50% of this range at other seasons. The variability of N_P from day to day is dependent on many factors and in discussing this parameter account must be taken of the local and conjugate ionospheres together with the rapid depletion and slow refilling of the plasmasphere after geomagnetic activity, points which will be considered in detail later. In addition, double peaked diurnal curves and nighttime maxima in N_P are observed on occasion, features which correspond to the light-ion spectrometer measurements of CHEN et al. (1976), however such variations are smoothed out in the median curves.

c. Monthly Median Behaviour

Because of the large day to day variability in the parameters it was decided to concentrate study, at least initially, on values representing averaged data for each month.

The diurnal plots of the median values for each month are plotted in Figs. 10 to 18. These show N_T, N_F, N_P, N_P/N_T%, F and h_{BL} (i.e. h_{eff}) for each of the nine months under study. The dotted sections of the curves, particularly for March 1976, join median points based on less than ten individual daily values,

Table 6 Standard deviations of the noon values of N_T, N_F and N_P compared to diurnal range of mean data for each month.

	N_T 10^{16} m^{-2}		N_F 10^{16} m^{-2}		N_P 10^{15} m^{-2}	
	RMS	Range	RMS	Range	RMS	Range
Nov. 75	3.3	16.5	2.8	15.8	7.5	8.3
Dec. 75	2.4	10.7	1.7	10.3	10.6	9.5
Jan. 76	2.0	15.0	1.5	11.6	6.8	10.0
Feb. 76	2.2	14.0	2.2	13.3	5.2	8.8
Mar. 76	3.1	17.5	3.2	16.3	5.3	14.8
Apr. 76	4.1	21.1	3.5	19.0	9.5	19.2
May 76	3.6	20.3	2.9	18.3	8.6	20.5
June 76	4.8	17.8	4.6	16.0	7.0	18.0
Jul 76	2.8	17.4	2.6	16.1	6.0	14.3

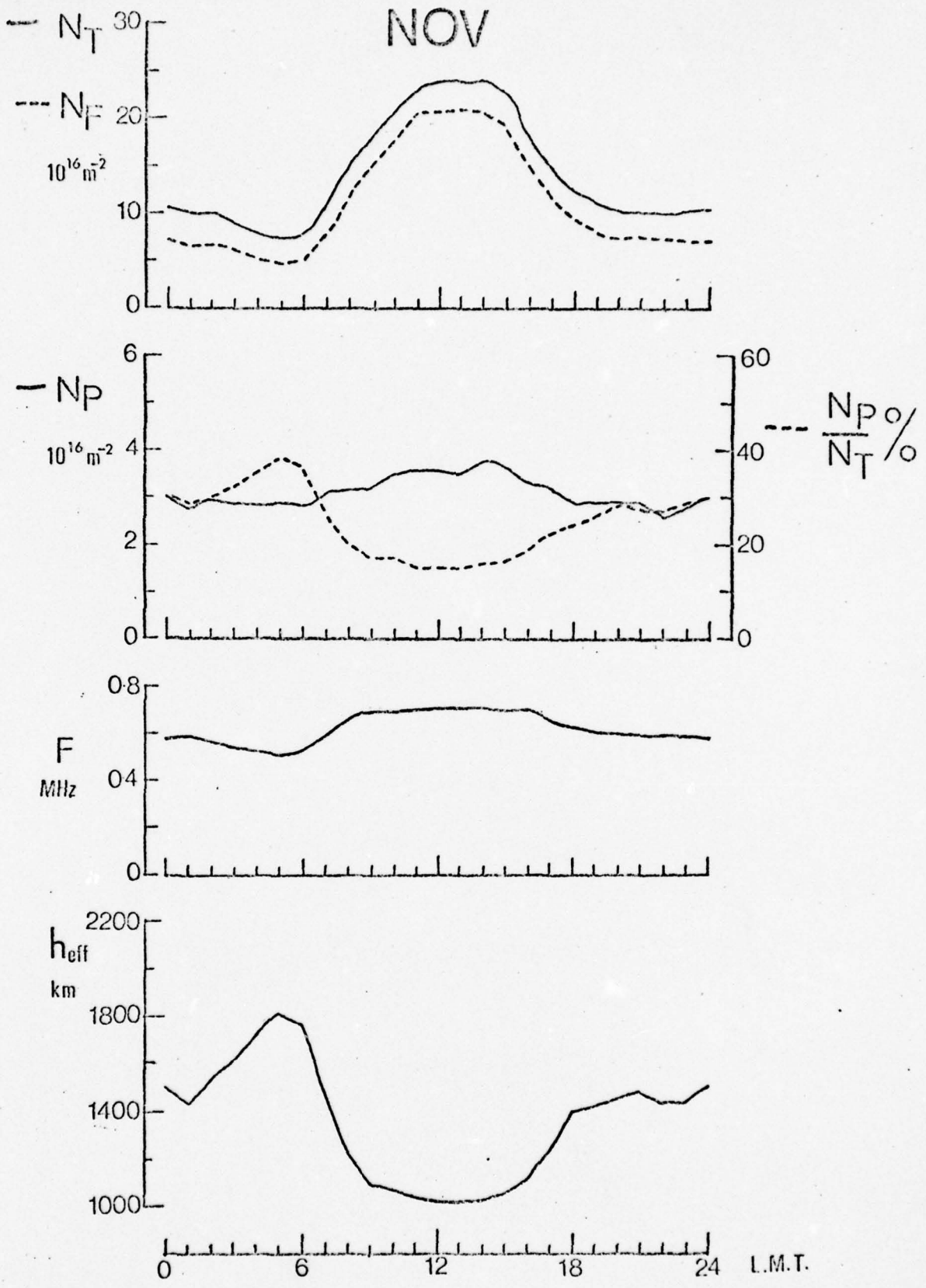

Fig.10. Monthly median hourly values of N_T, N_F, N_P, N_P/N_T%, F and h_{eff} for Aberystwyth for November 1975.

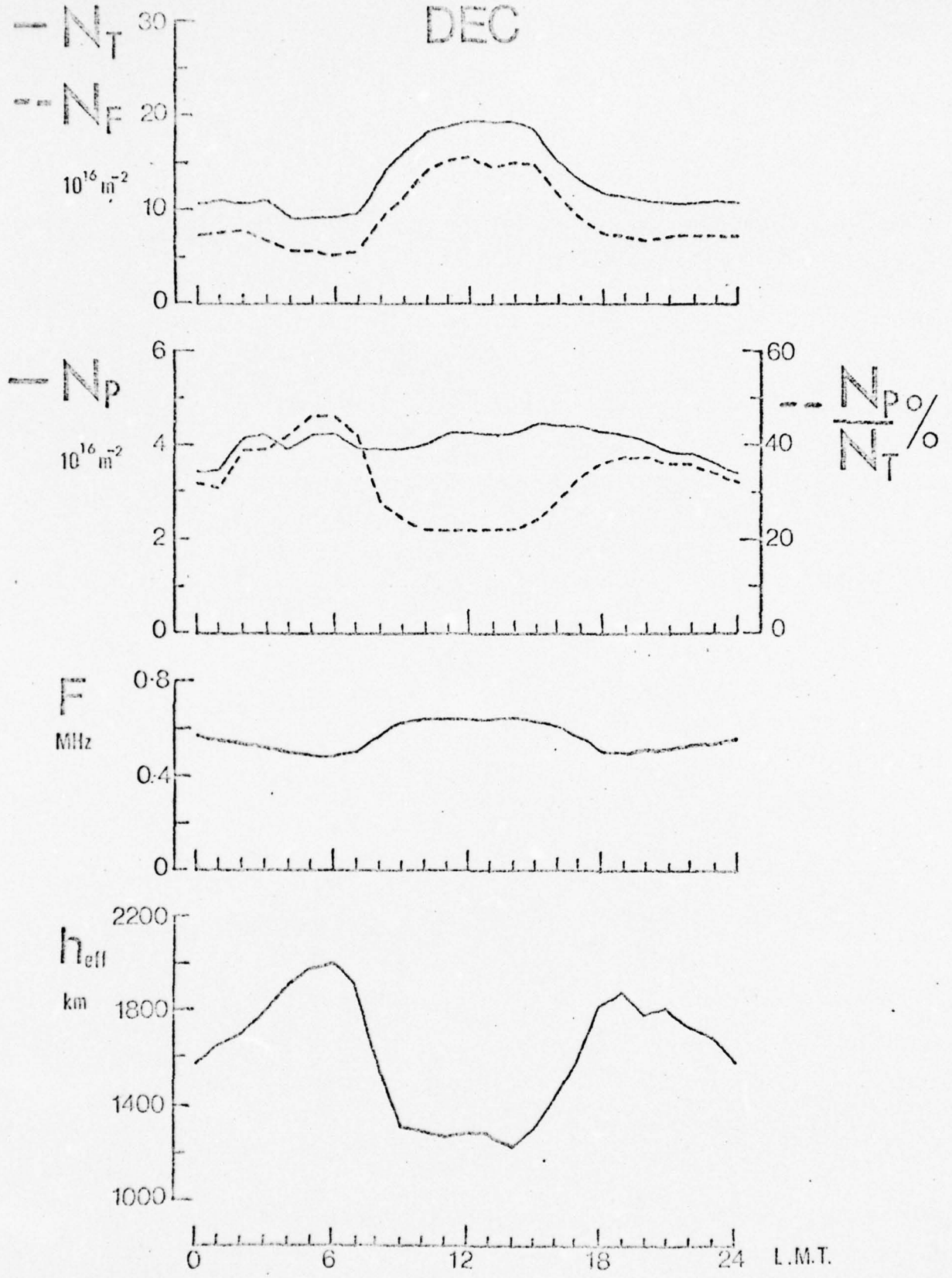

Fig.11. Monthly median hourly values of N_T, N_F, N_P, N_P/N_T%, F and h_{eff} for Aberystwyth for December 1975.

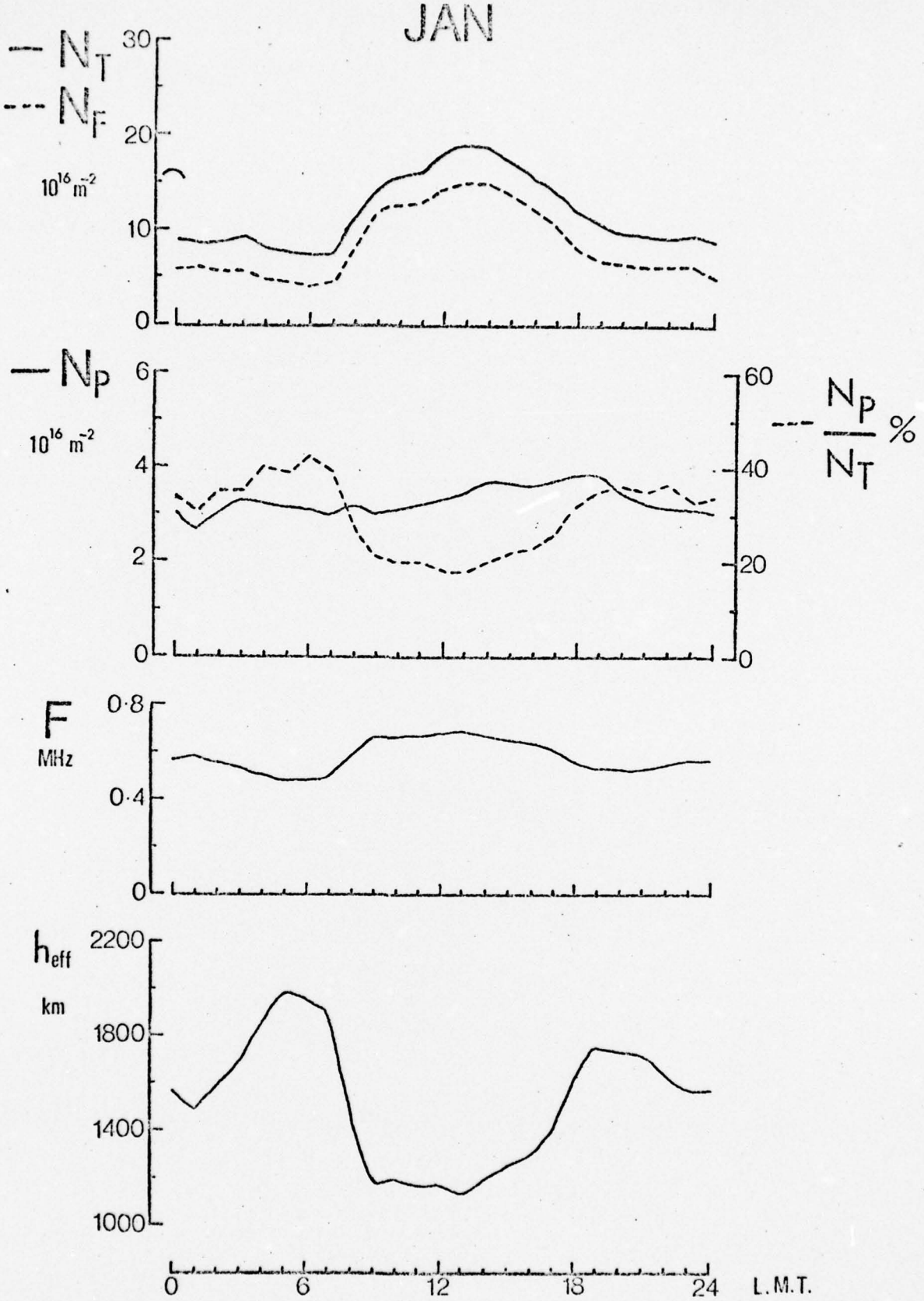

Fig.12. Monthly median hourly values of N_T, N_F, N_P N_P/N_T%, F and h_{eff} for Aberystwyth for January 1976.

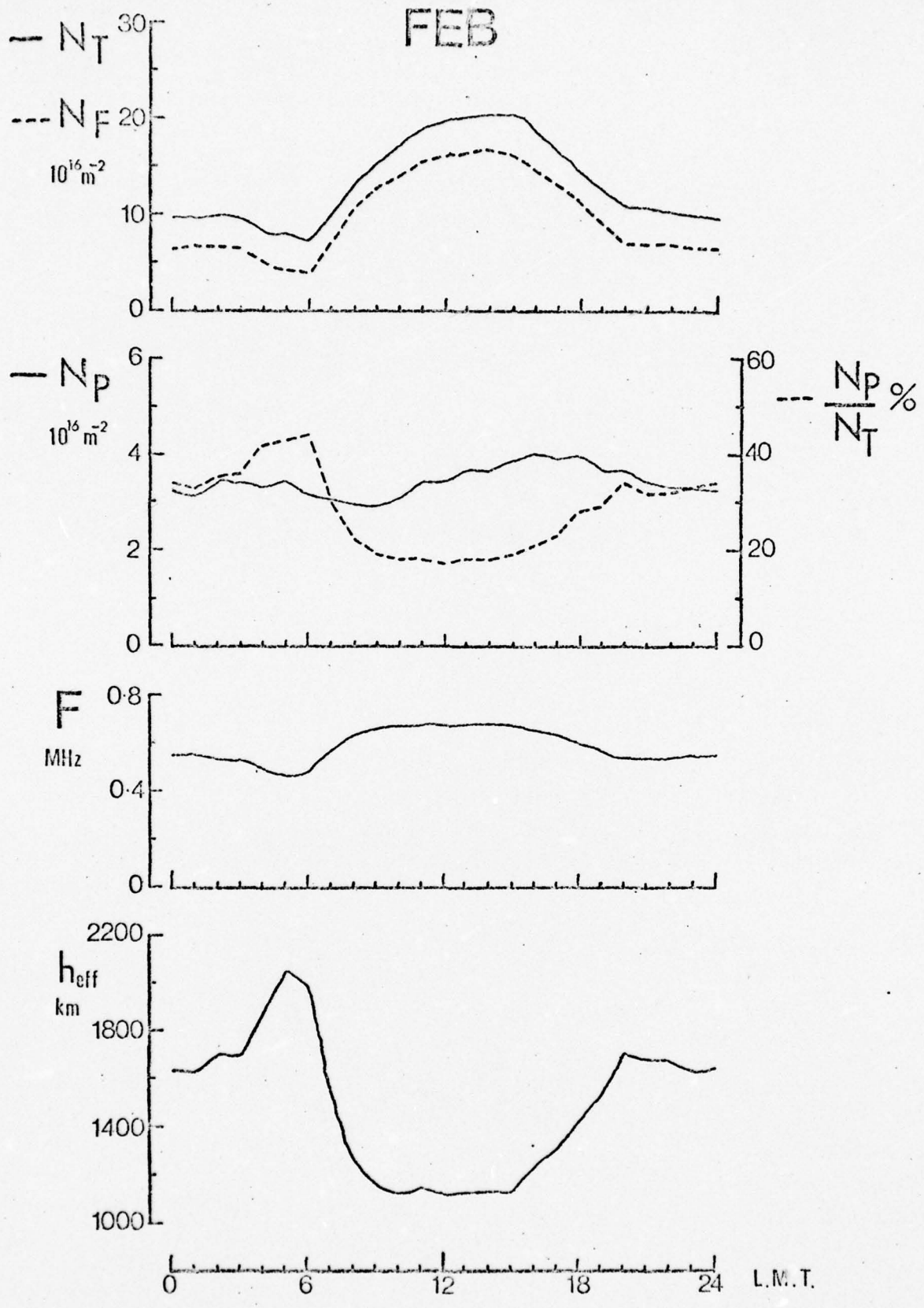

Fig.13. Monthly median hourly values of N_T, N_F, N_P, N_P/N_T%, F and h_{eff} for Aberystwyth for February 1976.

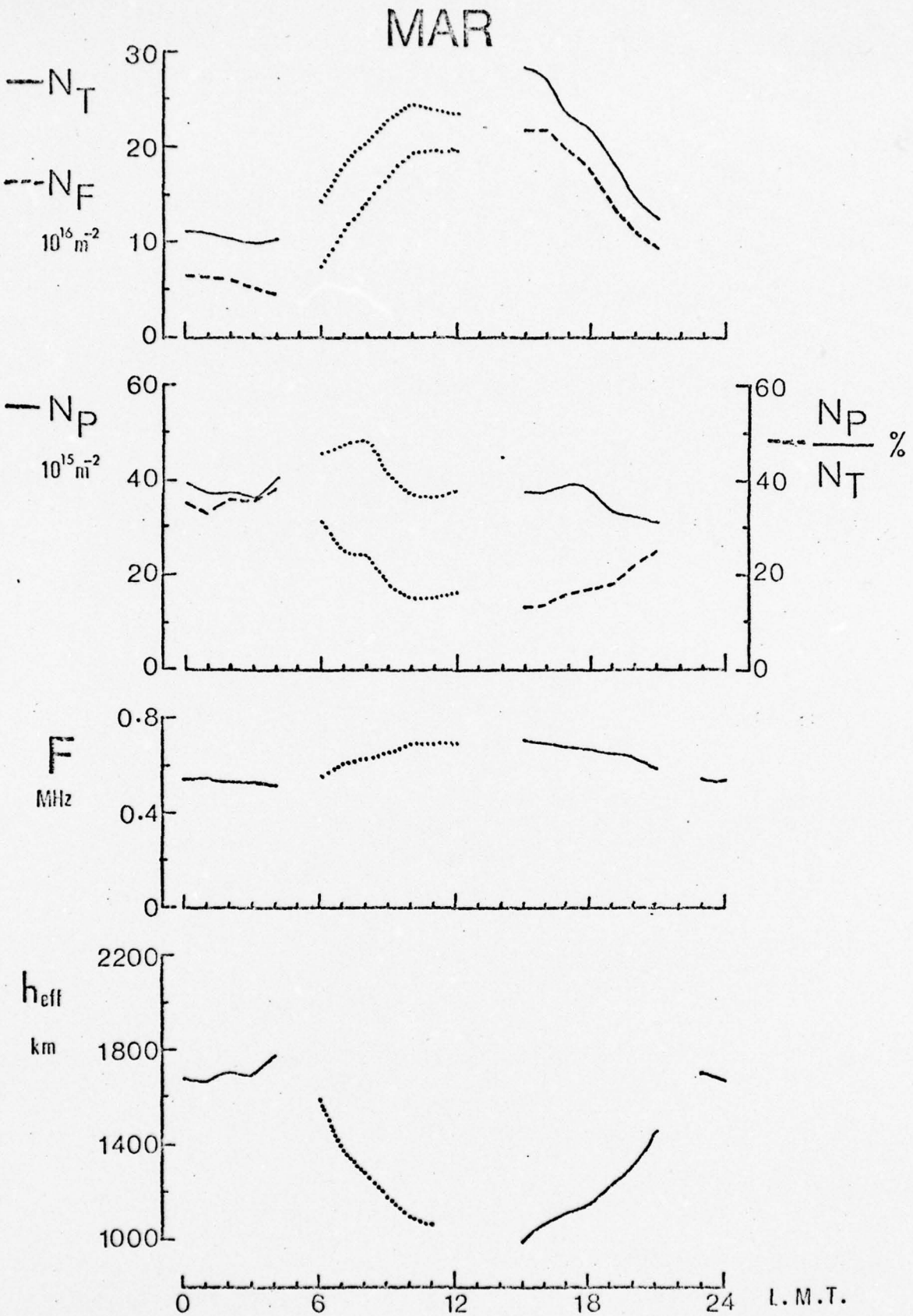

Fig.14. Monthly median hourly values of N_T, N_P, N_P N_P/N_T %, F and h_{eff} for Aberystwyth for March 1976.

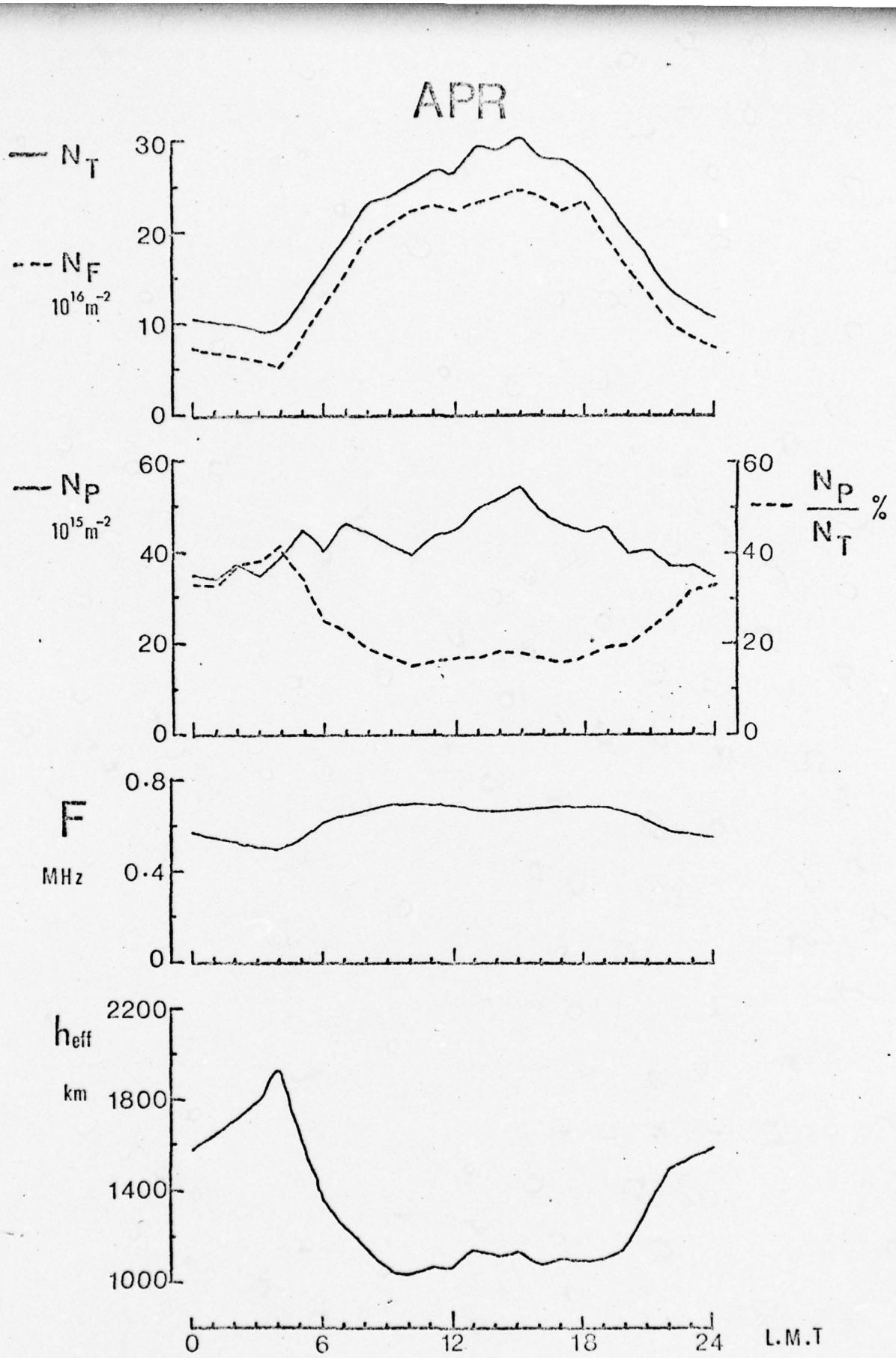

Fig.15. Monthly median hourly values of N_T, N_F, N_P, N_P/N_T%, F and h_{eff} for Aberystwyth for April 1976.

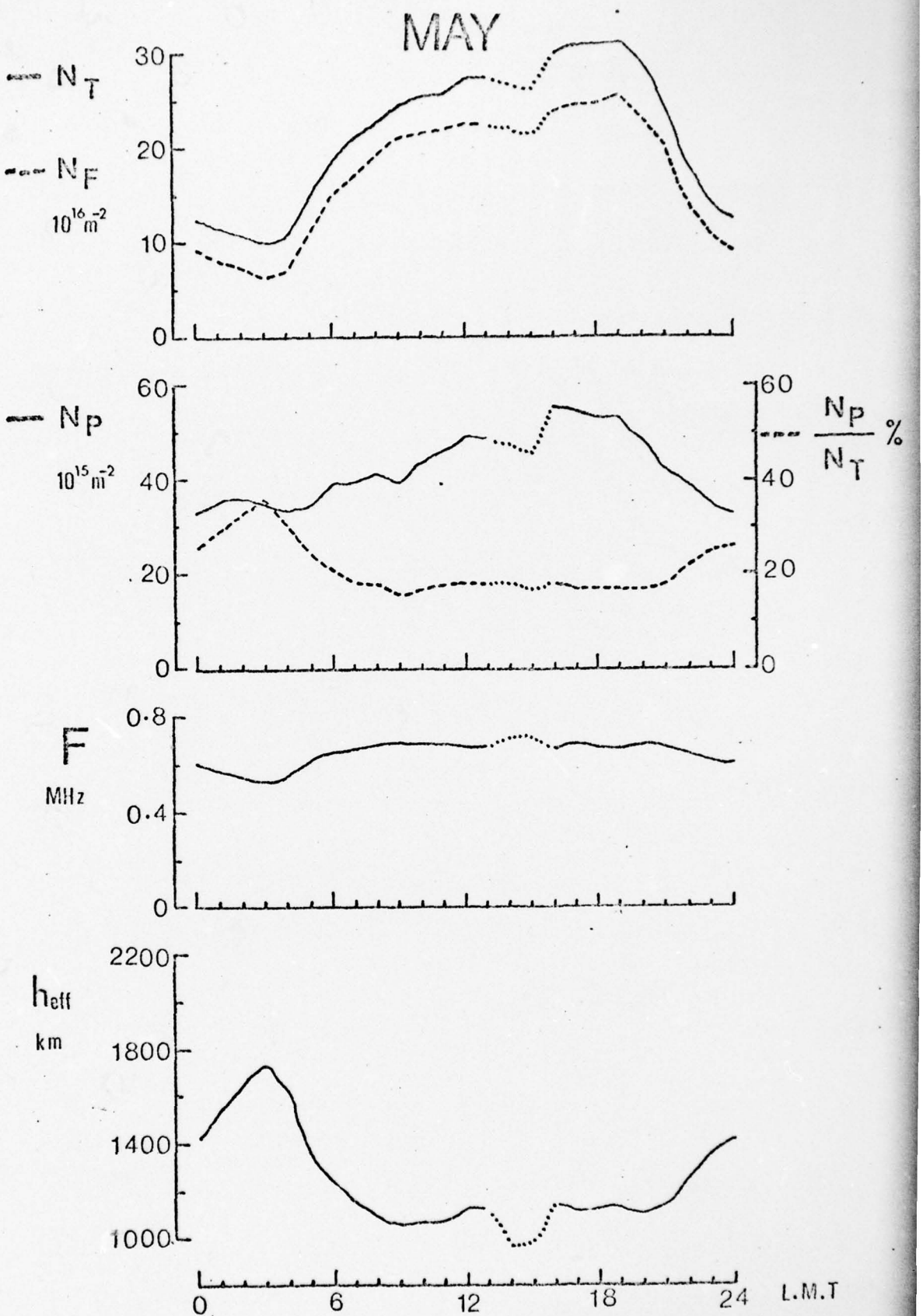

Fig.16. Monthly median hourly values of N_T, N_F, N_P, N_P/N_T%, F and h_{eff} for Aberystwyth for May 1976.

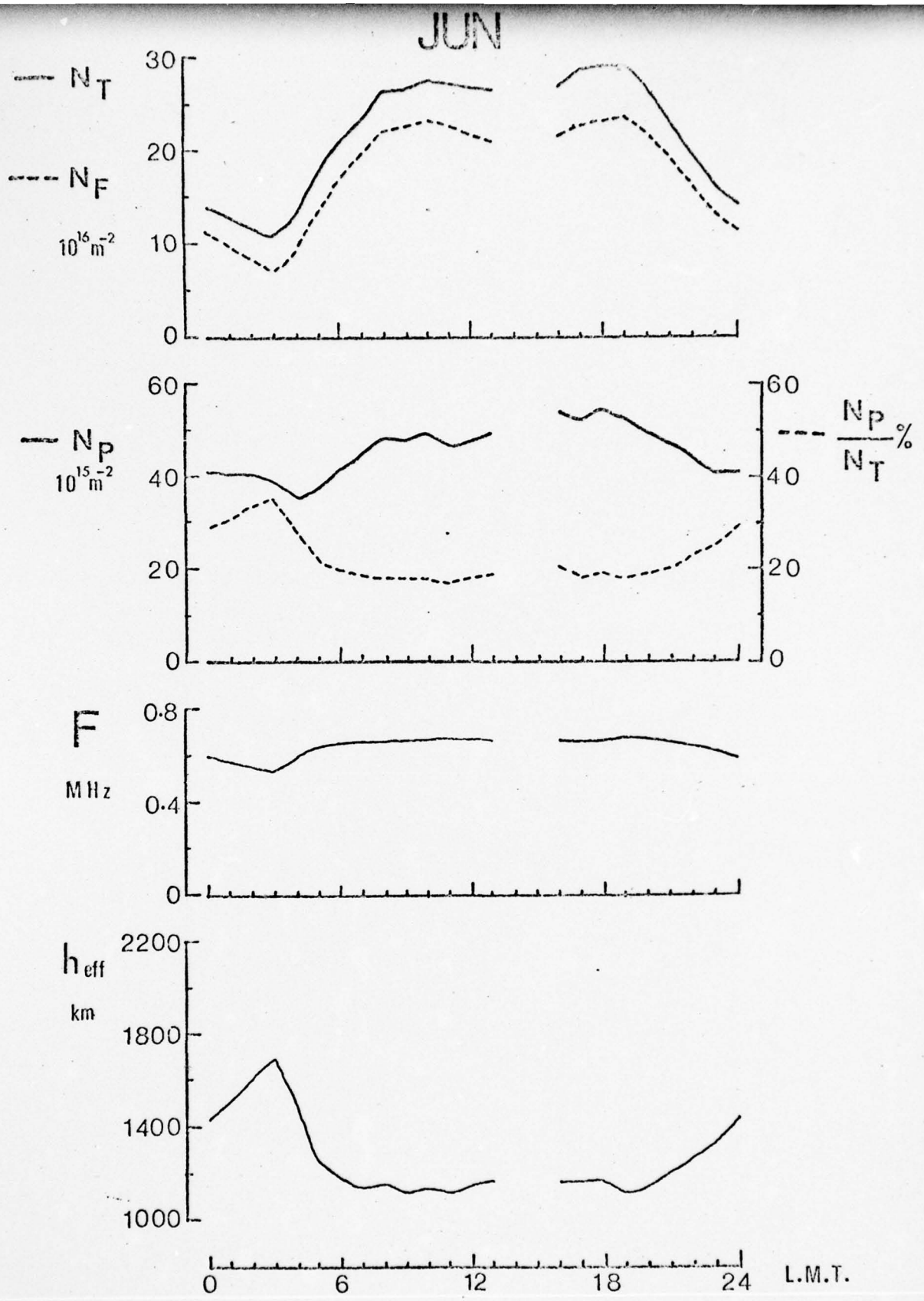

Fig.17. Monthly median hourly values of N_T, N_F, N_P, N_P/N_T%, F and h_{eff} for Aberystwyth for June 1976.

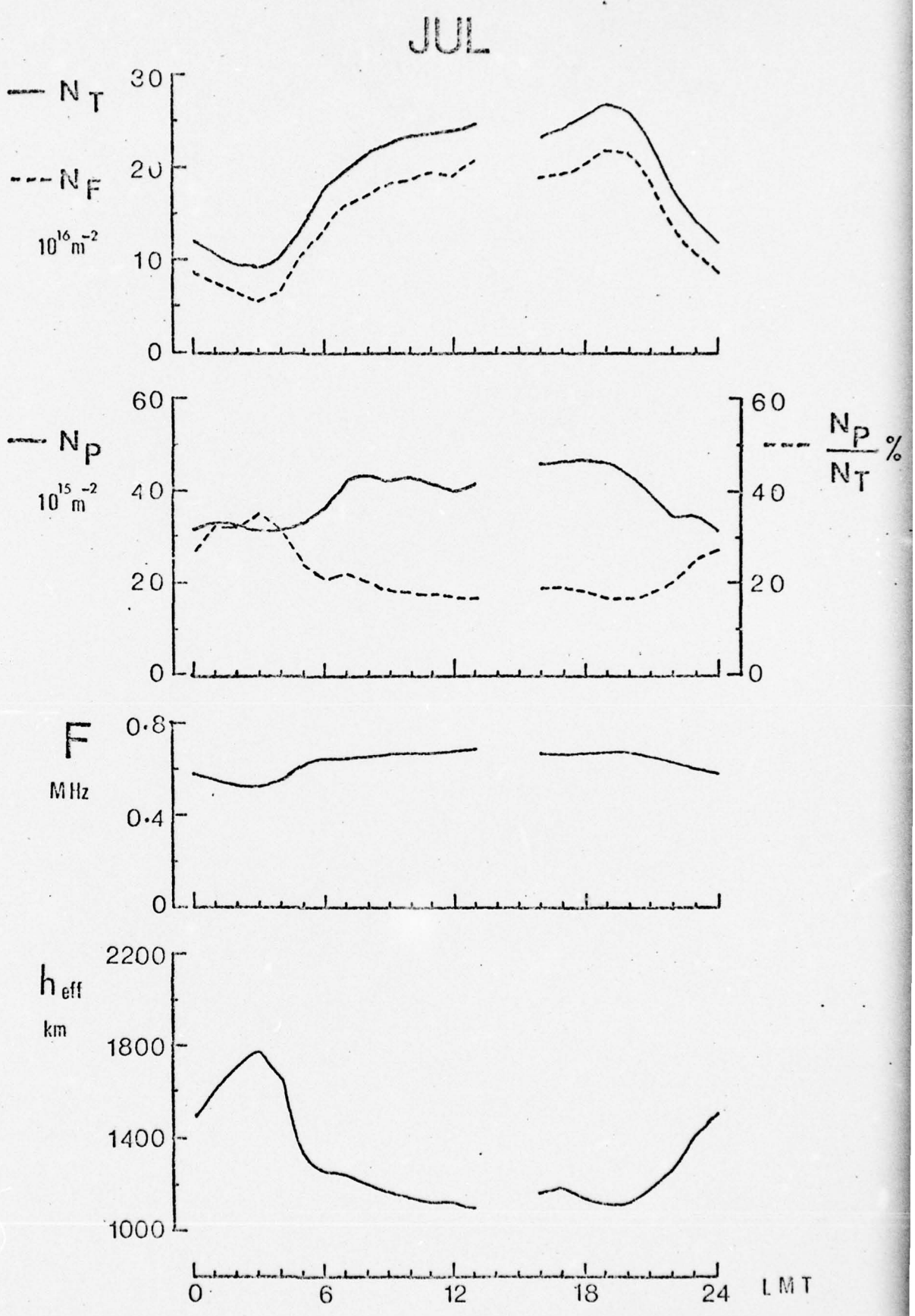

Fig.18. Monthly median hourly values of N_T, N_F, N_P, N_P/N_T%, F and h_{eff} for Aberystwyth for July 1976.

while sections missing indicate that no transmissions were available at these hours throughout the month.

The diurnal variations of N_T and N_F are essentially similar in character indicating that as expected the ionospheric contribution dominates the total electron content at least during daytime. By contrast, N_P shows only a small diurnal variation with minimum values in the predawn hours around 3×10^{16} m^{-2} for all months and a maximum generally in late afternoon, of about 4×10^{16} m^{-2} in winter rising to approximately 5×10^{16} m^{-2} in summer. The protonospheric content expressed as a percentage of the total has values by day typically in the range 15 to 20% while the predawn maximum of about 35% in summer exceeds 40% in winter.

The diurnal variations of F show a predawn minimum about 0.5MHz corresponding to an effective height of about 1800 km while the daytime value is generally in the region of 0.66 MHz representing an effective height around 1200 km. It is interesting to note that F is approximately proportional to the $\overline{M}_e$ factor studied by KERSLEY and SAMBROOK (1971) who found a 30% diurnal variation in this parameter which is in close agreement with the present measured change in F. The effective heights can be compared to those quoted by HARGREAVES and HOLMAN (1972) from model studies which were in the range 1000 to 1400 km.

d. Seasonal Variations

The daytime values of N_T and N_F are smallest in winter with the maximum just after noon. The larger single peak later in the afternoon at equinox gives way to a twin peak diurnal variation in summer when the polewards neutral wind causes a depression in the early afternoon values. The seasonal variations of ionospheric N_F are best appreciated by the contour plot of the median values

as a function of time of day and month. Superposed on Fig. 19 are the times of sunrise and sunset at the 300 km sub-ionospheric point estimated from COLIN et al. (1966). The basic solar control of the N_F photo-ionisation is immediately apparent.

No clear relationship is seen between each of N_T, N_F and N_P and either mean solar flux or mean A_P although changes in solar activity are small over this nine month period at solar minimum.

The noon time values of N_P show a variation by month which follows closely the corresponding changes in N_F. However it is apparent from an examination of a contour plot of N_P by hour and month (Fig. 20) that this parameter does not show the same direct solar control as N_F. Furthermore, the daytime maximum in N_P in November and December extends considerably beyond the sunlit hours of the short winter day, so that even if the time constants involved are several hours it is still difficult to explain the observed diurnal variation purely in terms of interaction with the local ionosphere.

Several studies have been concerned with plasma exchange between two conjugate ionospheres along a field line (e.g. YOUNG et al., 1970, PARK, 1970, MAYR et al., 1972) and it is reasonable to assume that the intervening protonosphere is dependent on both local and conjugate ionospheric conditions. In a first attempt to account, at least qualitatively, for the general form of the N_P variations, particularly for winter, ionospheric data for Slough (51.5^{o}N, 0.6^{o}W), representing conditions in the general vicinity of the local 300 km sub-ionospheric point (47.9^{o}N, 2.5^{o}E) was considered in conjunction with similar data for Cape Town (33.9^{o}S, 18.4^{o}E), suitably time shifted to Aberystwyth local mean

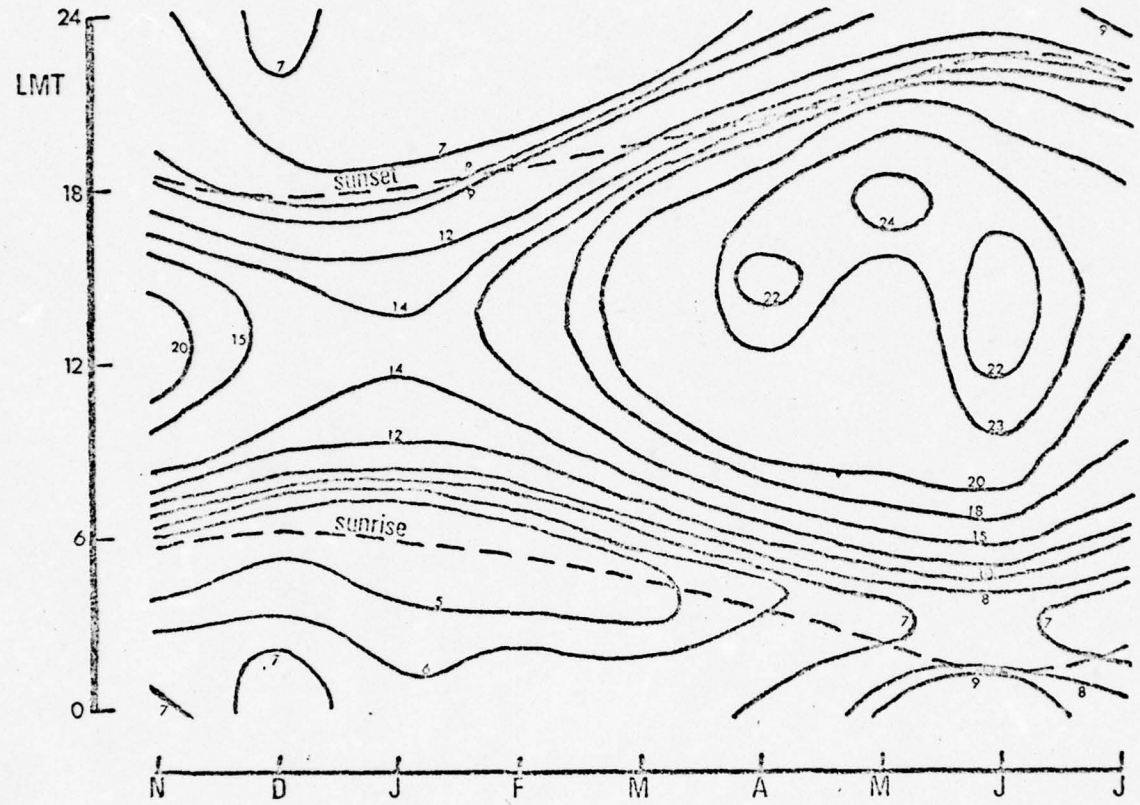

Fig.19. Plot of selected contours of N_F ($10^{16} m^{-2}$) by time of day and month for Aberystwyth. Also plotted are times of sunrise and sunset at 300 km along ray path.

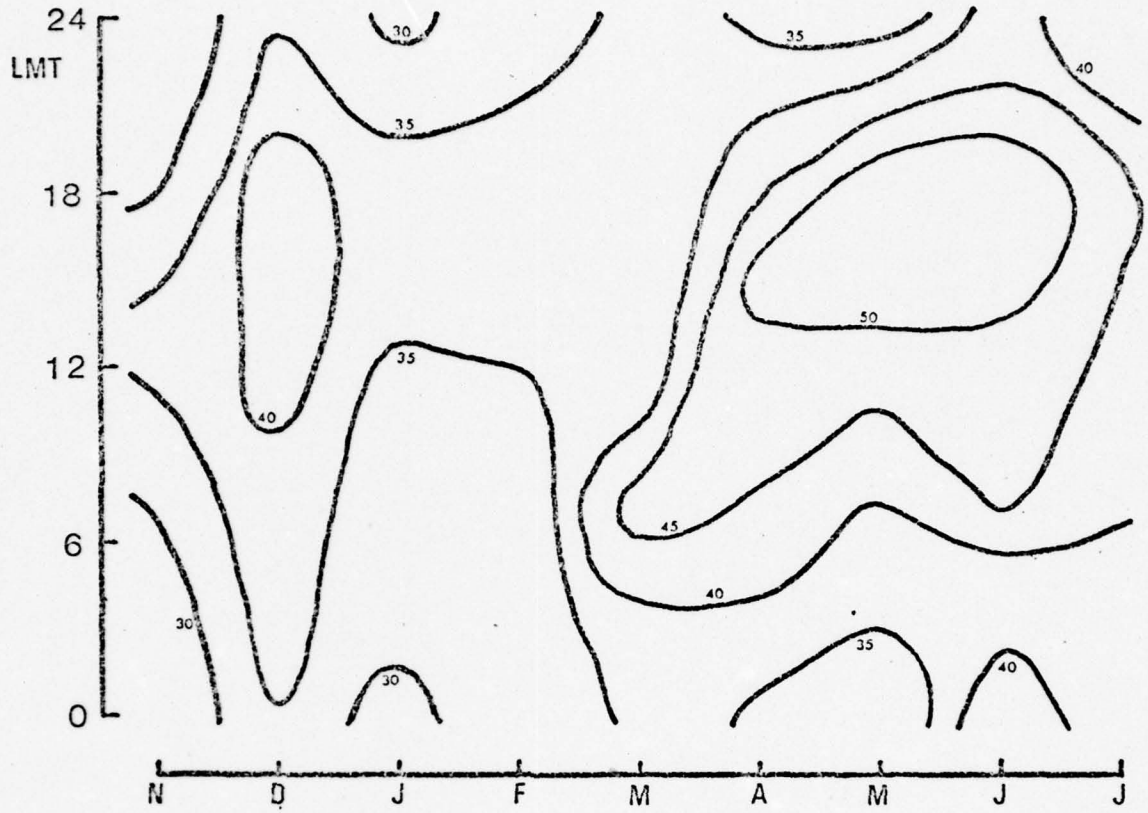

Fig.20. Plot of selected contours of N_p ($10^{15}m^{-2}$) by time of day and month for Aberystwyth.

time, and taken to be indicative of conditions in the conjugate ionosphere ($36^{o}S$, $20^{o}E$). As no current ionospheric data were available for Cape Town corresponding values from the previous solar cycle were used. Various studies were made using these data sets and it was found that a contour plot which broadly shows some of the features of the N_P variations is obtained using averaged values of corresponding maximum electron densities for the two stations which are time delayed by about two hours. In particular the length of the summer day in the conjugate hemisphere helps account for the N_P variations in November and December. The results of this work suggest that account must be taken of both local and conjugate ionospheres in an explanation of the observed N_P variations. However, this study has not been pursued further in this form because, concentrating as it does on only one field line, it has limited application to the actual physical situation and furthermore its application requires a more realistic assessment of the time constants involved in protonospheric filling and depletion.

e. Accuracy of N_P Data

Since N_P is obtained from the difference of N_T and N_F and, during daytime at least, has a magnitude generally less than 20% of N_T, it is important to consider the accuracy of the measurements of N_T and N_F and the consequent accuracy in N_P. The errors fall into two categories, systematic observational errors in the absolute determination of the angular parameters and errors associated with the choice of mean ionospheric height in the reduction of the Faraday rotation angles.

(i) Observational errors

The effects of errors in the absolute values of the measured angular parameters have been estimated and their implications on the monthly median diurnal variations of N_p considered.

Fig. 21 shows the effects of various constant systematic errors in the measured angles on the diurnal variations of the median N_p values for December 1975, April 1976 and July 1976. Each curve represents the percentage error in N_p resulting from an assumed error in one of the angles ϕ and Ω; the curves for an error of given sign in ϕ and an equal error of opposite sign in Ω are virtually identical since the numerical constants in Equations 7 and 12 are almost equal. It is believed that the errors in the measured parameters of the present study can be conservatively estimated, in most circumstances, at less than $\pm 7^{\circ}$ in each of the angles so that the resulting absolute accuracy of the N_p data is generally better than about ± 15%. The short term relative errors are, in general, much smaller than this value.

(ii) Effects of constant $\overline{f}_L$ factor

An additional error could arise in the data from the use of a constant $\overline{f}_L$ in the Faraday content estimated. Two factors must be considered here. Firstly there are the consequences of a change in the mean ionospheric height in the choice of a constant $\overline{f}_L$, and secondly the implications of a changing-height of the F2-layer peak with a resulting diurnal variation in $\overline{f}_L$ must be discussed. This latter point is of particular importance in ascertaining the validity of the small diurnal variations found in N_p.

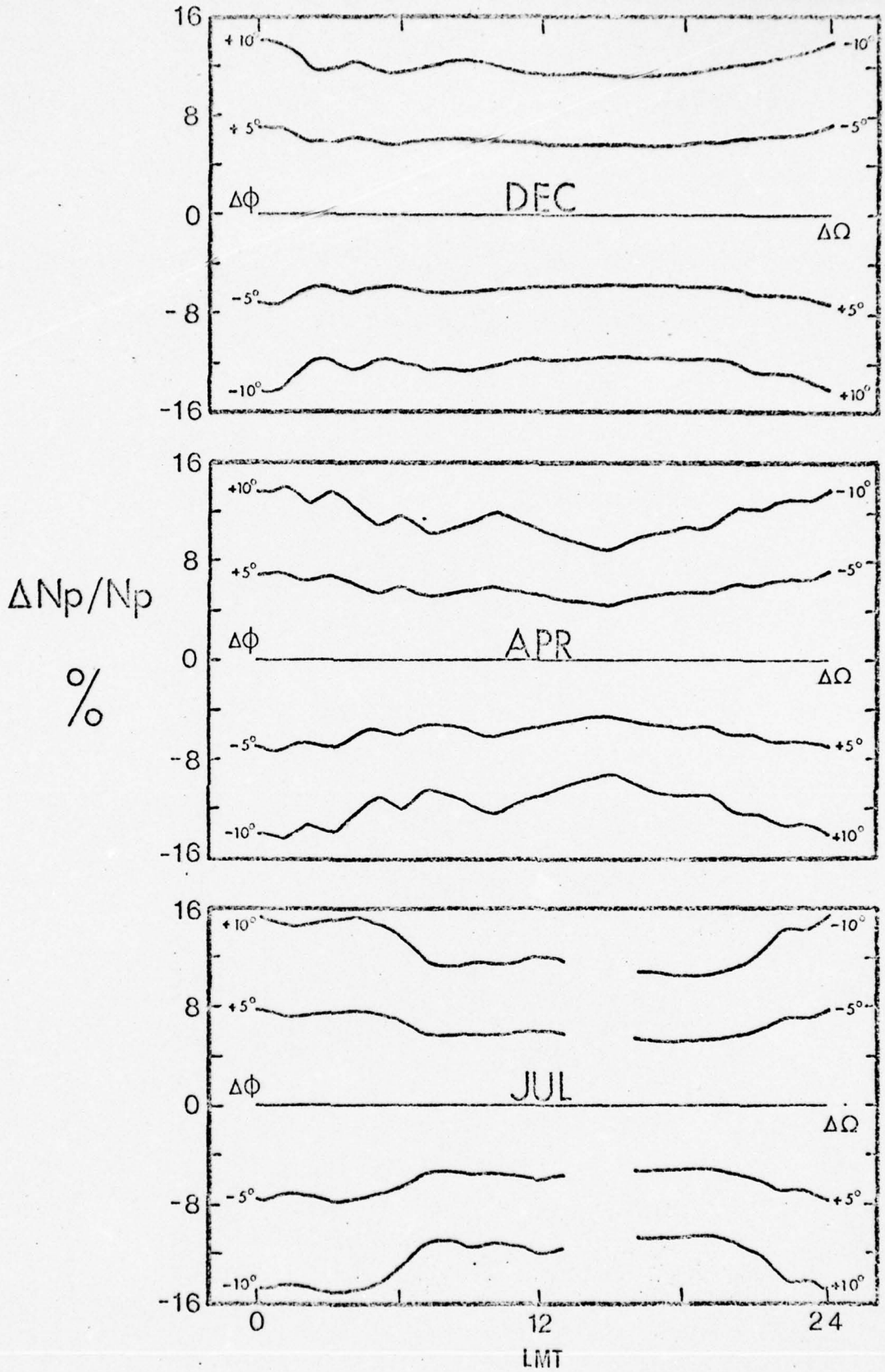

Fig.21. Diurnal variations of percentage errors in N_p resulting from errors in measured angular parameters for selected months.

Examination of Fig. 1 shows that in the region 300 to 500 km, the value of $\overline{f}_L$ differs from the value at 420 km by less than ± 1.3%, so that resulting uncertainty in N_p during daytime is less than 10% and much smaller at night. Most workers have chosen a mean ionospheric height between 350 to 400 km, and in this range the dependence of $\overline{f}_L$ on height is small for the ATS-6 to Aberystwyth geometry, representing a change in $\overline{f}_L$ of less than 1%. The effect on the diurnal variation of N_p and N_p/N_T% of the use of different mean ionospheric heights over a wide range from 200 to 600 km is shown in Figs. 22 to 24 for winter (December, 1975), equinox (April 1976) and summer (July 1976).

The height of the maximum ionisation in the F-layer shows a diurnal variation so that it is reasonable to assume a similar change in the mean ionospheric height for the precise evaluation of $\overline{f}_L$ in Faraday content measurements. KERSLEY and TAYLOR (1974) compared incoherent scatter profiles with Faraday data for satellites in low orbit and found that on average the mean ionospheric height was some 80 km above the height of the layer peak (h_m) although the difference between the heights for individual measurements ranged from 60 to 120 km. In the present study h_m has been determined from ionosonde data and the consequences on N_p of the use of three height increments, 50, 100 and 150 km above the layer peak assessed.

To obtain monthly median representative values of h_m, a true height reduction of the ionosonde data from Slough has been performed, employing a model suggested in its original form by SHIMAZAKI (1955). The virtual height of reflection is given by

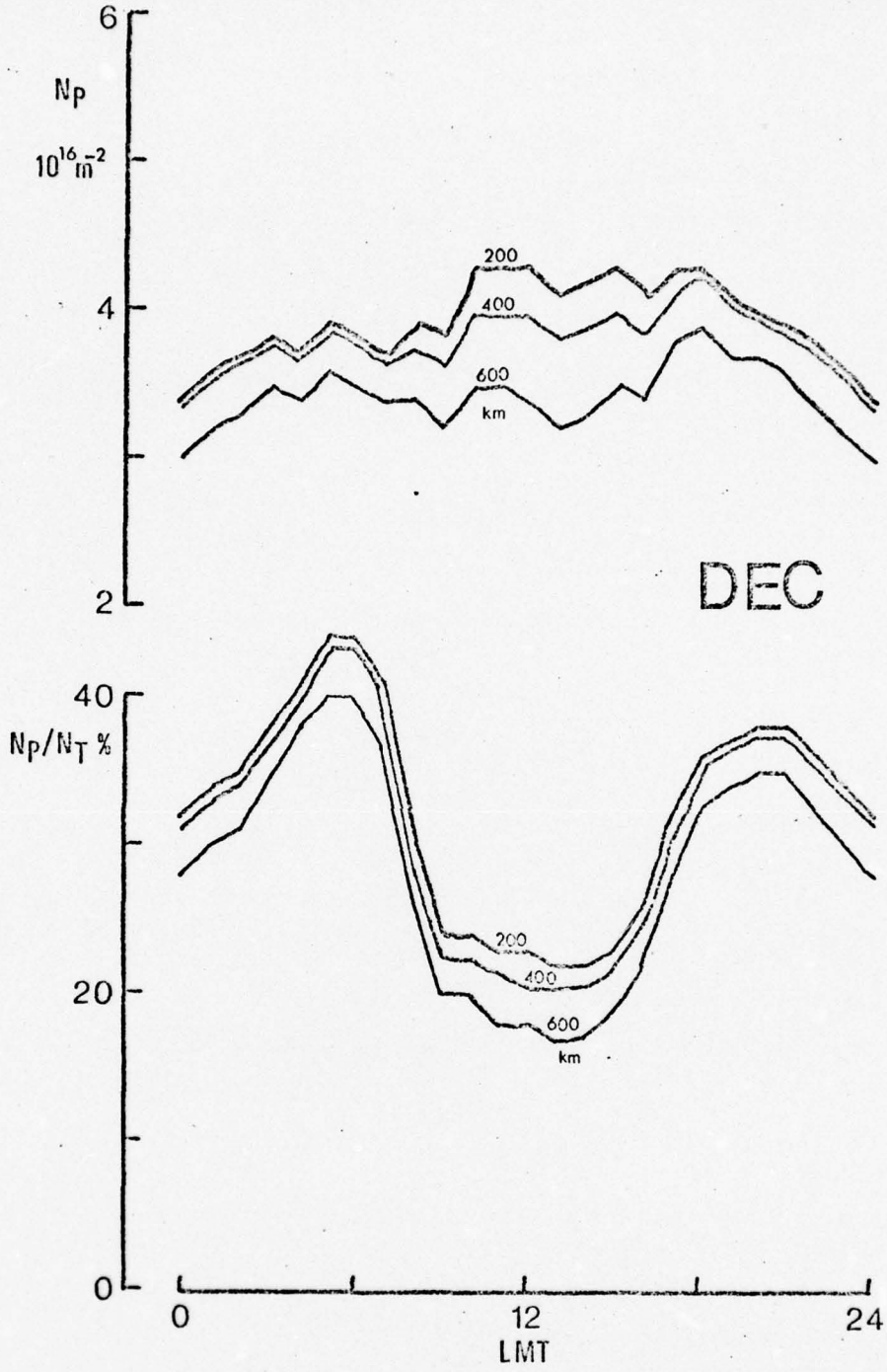

Fig.22. Diurnal variations of N_p and N_p/N_T% for $\bar{f}_L$ evaluated at three different heights for Aberystwyth for December 1975.

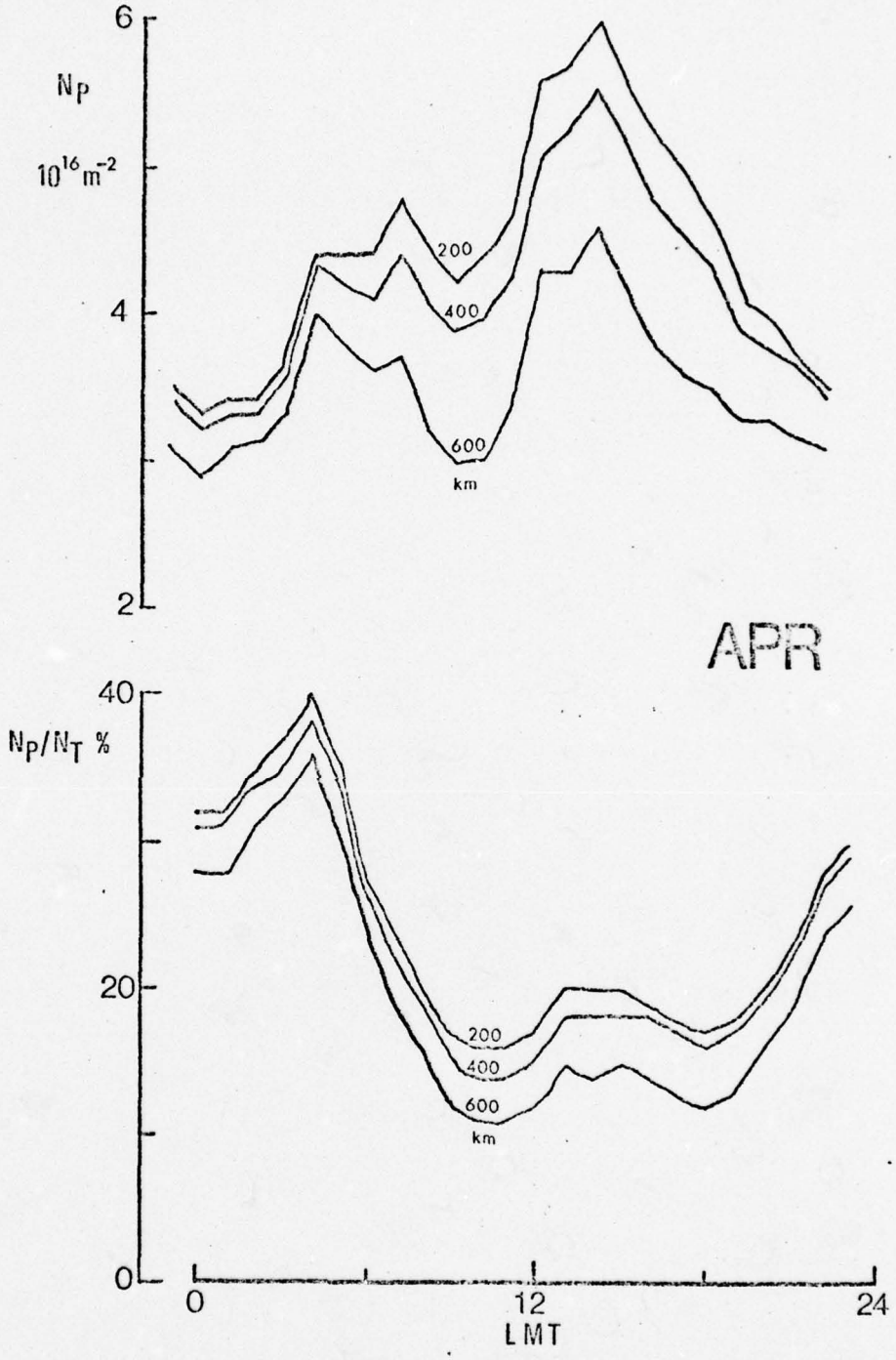

Fig.23. Diurnal variations of N_p and N_p/N_T% for $\overline{f}_L$ evaluated at three different heights for Aberystwyth for April 1976.

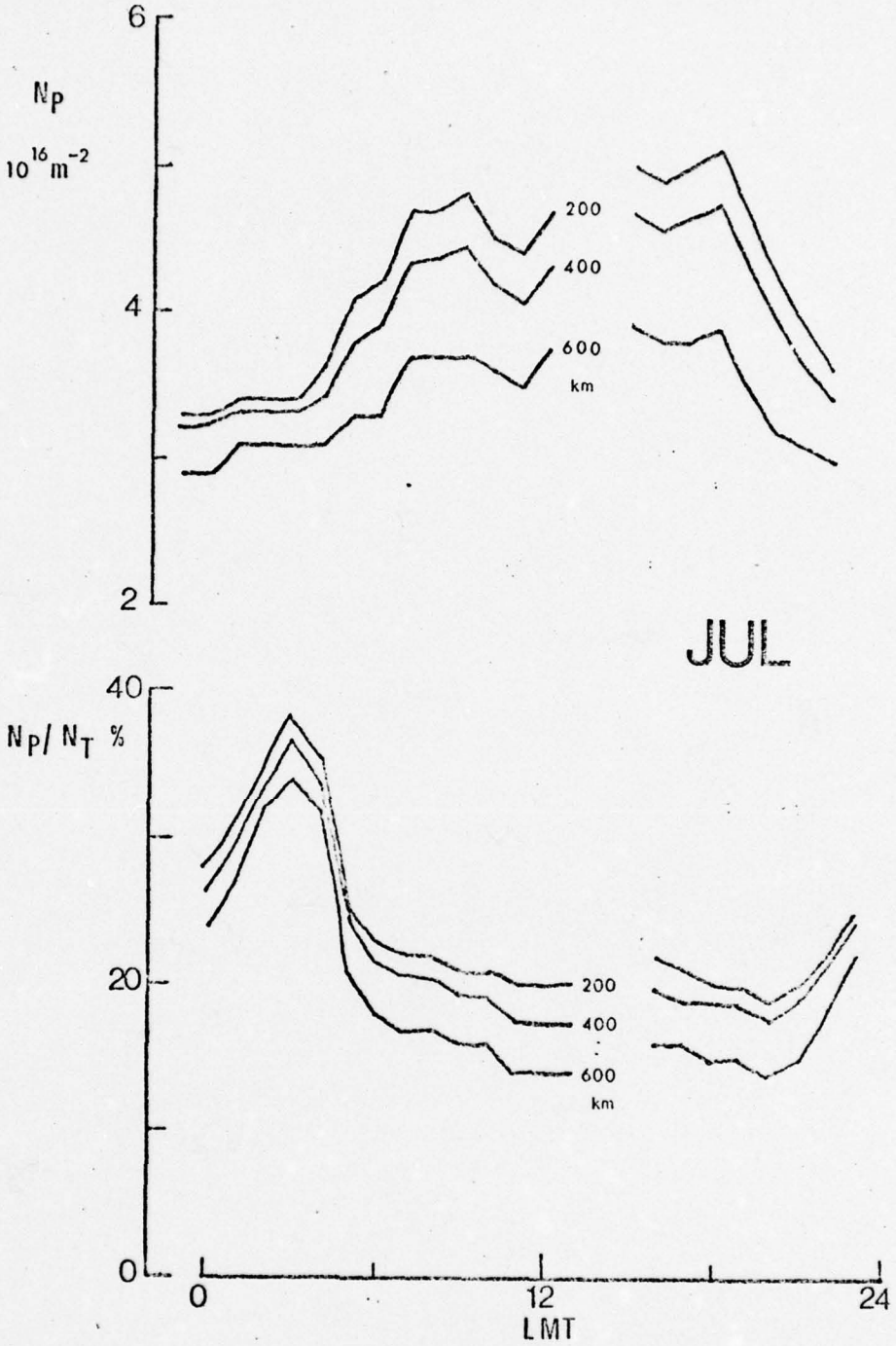

Fig.24. Diurnal variations of N_p and N_p/N_T% for $\overline{f}_L$ evaluated at three different heights for Aberystwyth for July 1976.

$$h'F2 = \frac{1490}{M(3000)F2} - 176 \text{ km}$$

where M(3000)F2 is the maximum usable frequency factor in MHz. The virtual height at a frequency of 0.834 f_oF2 is numerically equal to h_m in the absence of E and F1 ionisation. BRADLEY and DUDENEY (1973) introduced a correction to account for the daytime E-layer ionisation and it is this equation which has been used in the present work. Their expression gives h_m directly, with errors less than 20 km, and is of the form

$$h_m = \frac{1490}{M(3000)F2+\Delta M} - 176 \text{ km}$$

with $\Delta M = 0.18/(X-1.4)$ and $X = f_oF2/f_oE$.

Median hourly values of h_m on a monthly basis have been obtained using Slough ionosonde data and the diurnal variation of $\overline{f}_L$ assessed for the three constant height increments. The resulting curves showing the effect of layer height changes on the diurnal variation of N_P are presented in Figs. 25 to 27 for the three months representing winter, equinox and summer. These show that the diurnal variation found in N_P is enhanced by the use of a variable mean ionospheric height when compared to the values obtained for a constant height. Following the work of KERSLEY and TAYLOR (1974) an increment of 100 km would seem appropriate when using data from a geostationary satellite so that the lowering of the F2-layer peak during daytime appears to give values of N_P increased by some 6% while at night the values depart little from those obtained with a fixed $\overline{f}_L$ evaluated at 420 km.

The important conclusions for this work are that for the Aberystwyth observations the values of N_P are not particularly

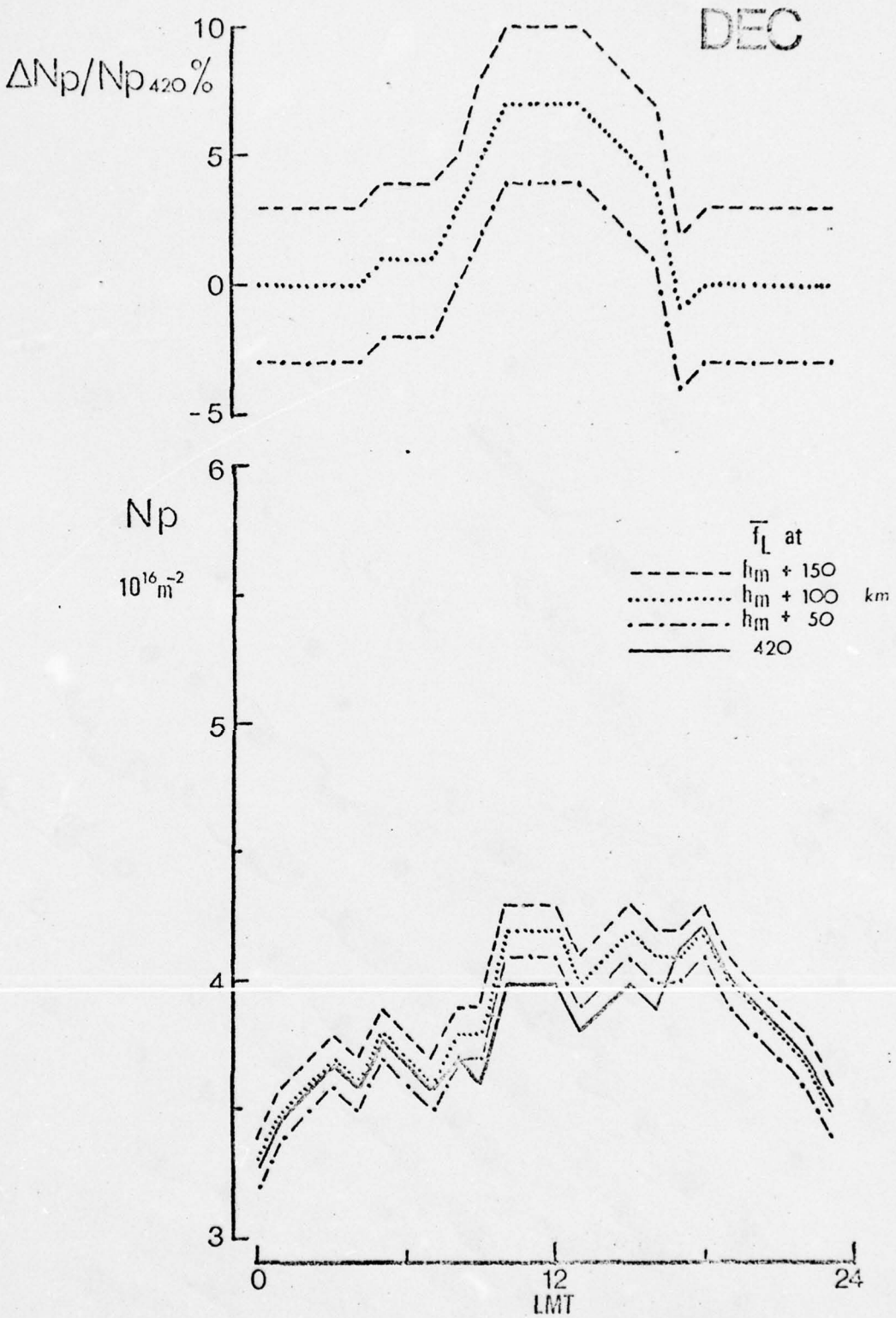

Fig.25. Effect of variable $\bar{f}_L$, evaluated for three height increments to h_m, on diurnal variation of N_p for Aberystwyth for December 1975.

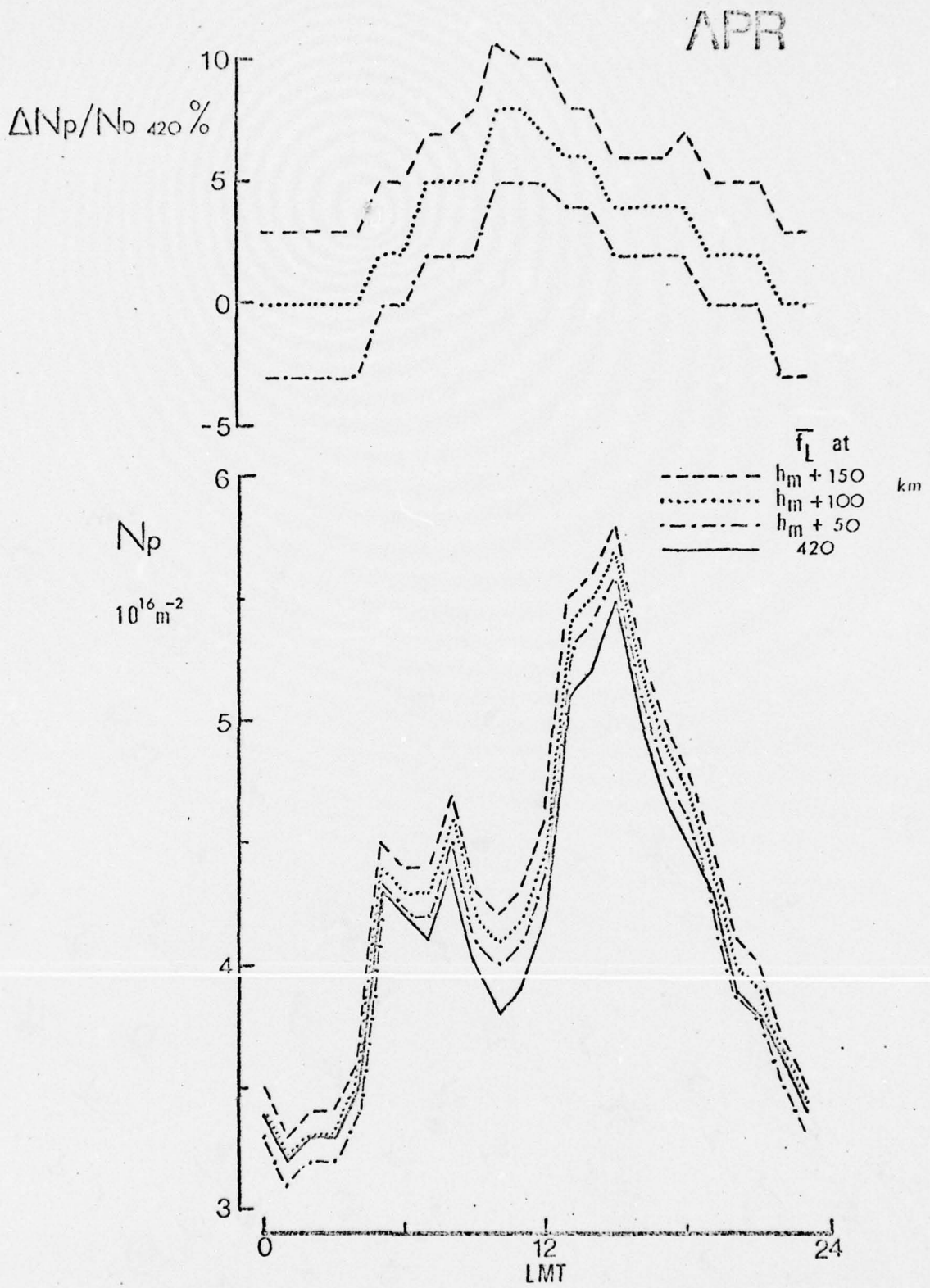

Fig.26. Effect of variable $\overline{f}_L$, evaluated for three height increments to h_m, on diurnal variation of N_p for Aberystwyth for April 1976.

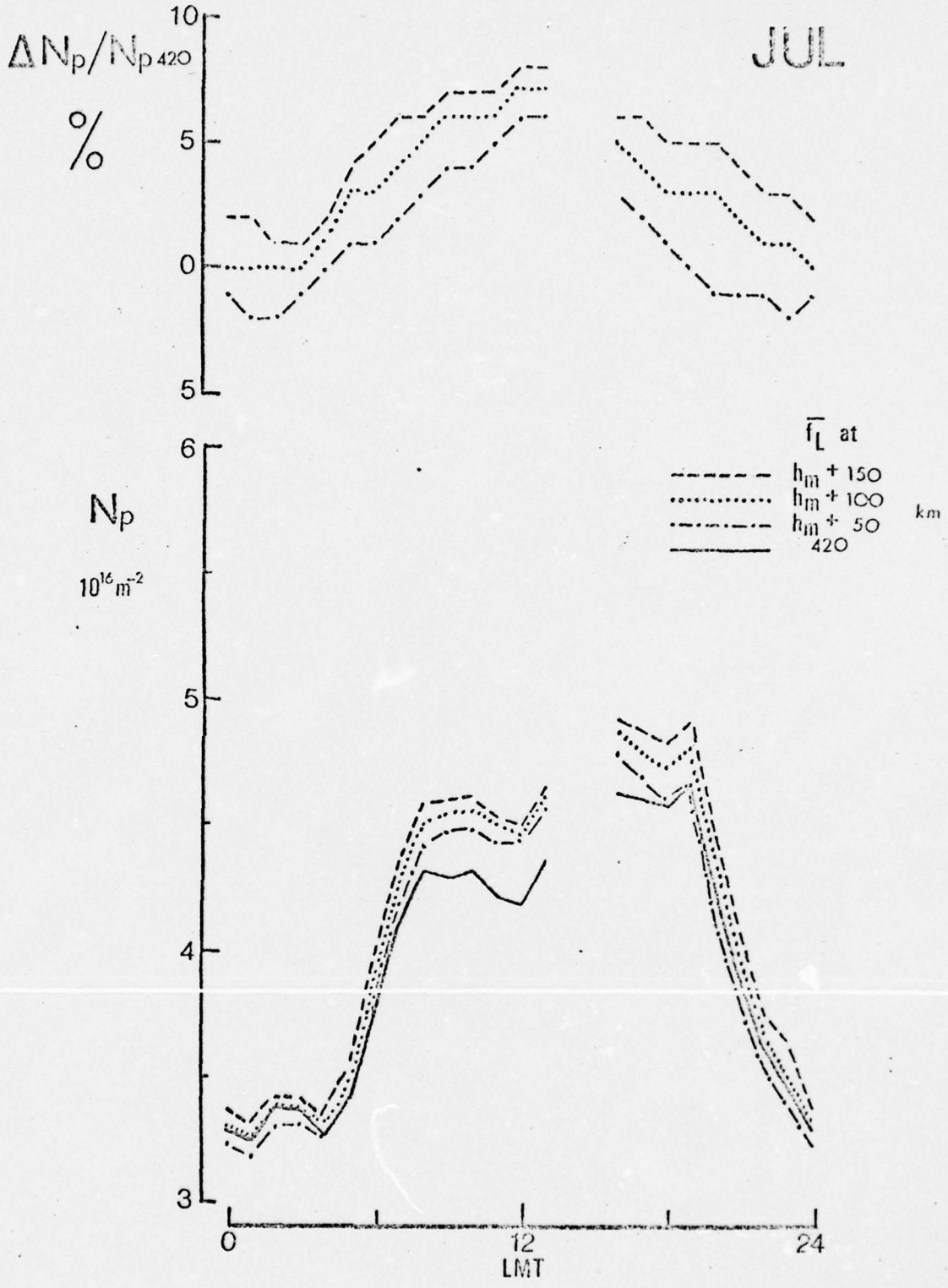

Fig.27. Effect of variable $\bar{f}_L$, evaluated for three height increments to h_m, on diurnal variation of N_p for Aberystwyth for July 1976.

sensitive to the choice of mean ionospheric height and the diurnal variation of this parameter is enhanced by the use of a variable height so that it can be concluded that this observed diurnal variation represents a true reflection of protonospheric behaviour and is not simply a product of the observational geometry and the analysis techniques.

7. IONOSPHERIC/PROTONOSPHERIC FLUX

a. Introduction

Plasma produced by photo-ionisation in the ionospheric part of the plasmasphere can travel up or down by three possible mechanisms.

1. Electric fields, originating from either the dynamo region or at higher latitudes the solar wind induced dawn-dusk field in the magnetosphere, can cause vertical plasma drifts. However, the magnitude is small at mid-latitudes because of the inclination of the geomagnetic field lines but outside the plasmapause the plasma can escape freely. EVANS (1972) has reported electric field induced vertical drifts in the F-region with a magnitude of about 25 ms^{-1}.

2. The thermospheric neutral wind, resulting from atmospheric horizontal temperature gradients, results in the plasma being dragged up and down the field lines. However, the neutral wind is most pronounced at ionospheric heights and is not capable of transferring ionisation all the way to the protonosphere. It can remove plasma to heights where the recombination loss coefficient is different, thus enhancing or reducing the plasma pressure necessary for the diffusion mechanism.

3. Diffusion of plasma along the geomagnetic field lines is the most efficient way in which plasma can travel up and down in the plasmasphere in response to pressure changes. Diffusive motion

is not particularly important at F-layer heights because of reactions caused by the random movement of the dense plasma but at higher altitudes the diffusive mechanism is of great importance in plasma interchange between ionosphere and protonosphere because the ion gyrofrequency exceeds the collision frequency with neutral particles.

Between 600 km and 1000 km there is a transition region at which charge exchange occurs between oxygen and hydrogen. That is, $O^+ + H \rightleftharpoons O + H^+$, so that the ion flux is predominantly O^+ below and H^+ above this transition height. BANKS and DOUPNIK (1974) calculated these fluxes and found that, with a plasma density exceeding 9×10^3 cm^{-3} in a flux tube above 3000 km, plasma could be readily transferred to F-region heights. Thus the protonosphere acts as a reservoir of ions which drains and refills through interaction with the ionosphere at both ends of the flux tube.

The plasmaspheric flux has been measured on a limited basis using whistlers (PARK, 1970) and incoherent scatter (EVANS, 1975a) but continuous observations allowing systematic study of the diurnal and seasonal variations are lacking.

The ATS-6 experiment provides a method of estimating integrated net protonospheric fluxes on a continuous basis as the temporal change of protonospheric content is indicative of the filling and draining of this region where production and loss processes are unimportant. However, it should be noted that the protonospheric content measured in the ATS-6 experiment refers to the slant path to the satellite which intersects a wide range of L-value flux tubes, as shown in Fig. 28 for Aberystwyth geometry

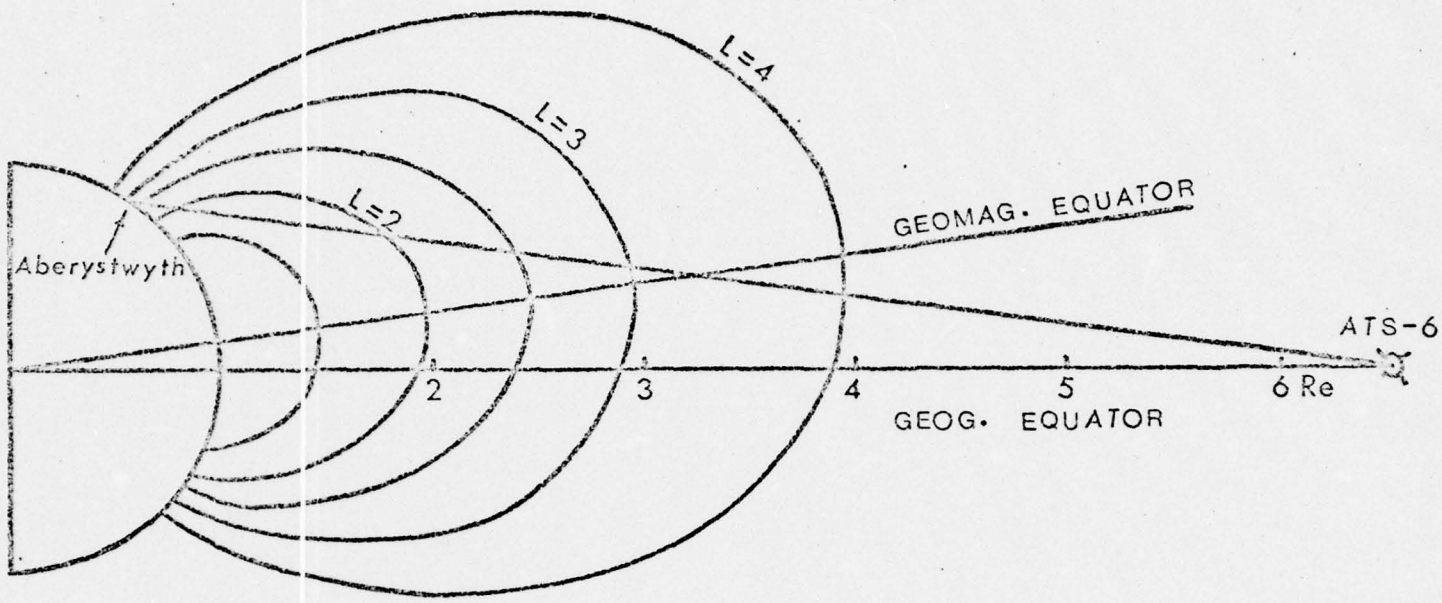

Fig.28. Geomagnetic field line configuration for ATS-6 to Aberystwyth ray path.

up to L = 4. The protonospheric flux estimated from ATS-6 measurements is thus an integrated parameter over these tubes in contrast to the more direct measurements of flux essentially along a particular field tube given by the whistler and incoherent scatter techniques.

b. Results and Discussion

The monthly median diurnal values of N_p have been used to estimate the temporal rate of change of this parameter (dN_p/dt), calculated for each hour, which gives an indication of the net integrated ionisation flux in and out of the protonosphere. To reduce the scatter in the data points the N_p data were first filtered using a 3-hour running mean before calculating the gradients. The results for the nine months of observation are presented in Fig. 29 where positive values, indicative of an upwards flux filling the tubes, are found for the most part by day with negative values, corresponding to downwards depletion, generally more prevalent at night. Mention must be made of the negative values found during daytime in March. As has already been noted (Fig. 14), the median N_p values for these hours are based on only a small sample of daily values at a time of high geomagnetic activity and so must be treated with caution. Similarly the impression of a strong downwards flux during mid-morning in April is in reality based on only one data point.

In an attempt to explain some of the observed features of the diurnal variations of the integrated flux, the sunrise and sunset times at ionospheric height (300 km) along the ray path estimated from the curves of COLIN et al. (1966) are indicated on Fig. 29. Since the protonospheric flux tubes interact with the ionosphere at both ends of the field lines the sunrise and

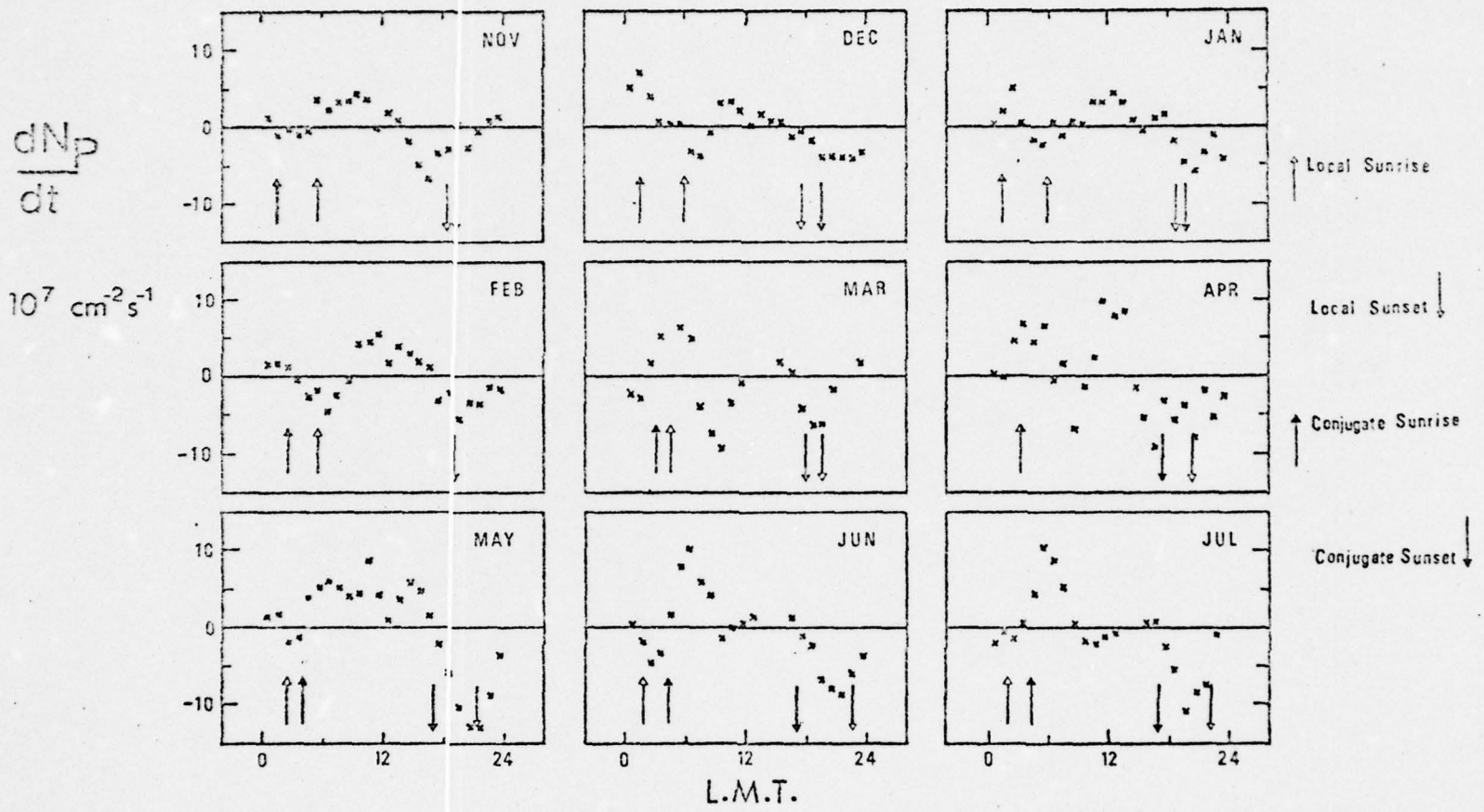

Fig.29. Diurnal variations of integrated protonospheric flux (dN_p/dt) for Aberystwyth by month from November 1975 to July 1976.

sunset times at 300 km in the conjugate ionosphere (36^{o}S, 20^{o}E) are also shown. The non-alignment of the geographic and geomagnetic axes results in sunrise and sunset times at the two points conjugate to each other which differ progressively for different months from a sunrise coincidence in April and a sunset coincidence in February. It must be remembered in interpreting this presentation that the ray path crosses many field lines at different heights, the ionospheric feet of which become sunlit at different times. Fig. 28 gives an indication of the range of latitude of the ionospheric terminations of the field lines up to L = 4, but taking account of the longitude range as well, the spread of sunrise and sunset times for the feet of the relevant field lines in both local and conjugate hemispheres can exceed ± 1 hour about the times shown in Fig. 29.

A second factor to bear in mind is the time constant between an increase in ionospheric ionisation and the appearance of enhanced protonospheric plasma. A time constant $\sim$ 1 hour has been suggested for the diffusive barrier at the O^{+}/H^{+} transition height (KOHL, 1966), while the travel time of the ions to the high protonosphere even at thermal speed may considerably exceed 1 hour depending on the field line path. Thus the overall time constant may be of the order of several hours.

It might be expected that changes in plasmapause position would be reflected in the observed data. For quiet magnetic conditions the plasmapause has a minimum radius (L $\sim$ 3) around 0600 LT with a bulge to L $\sim$ 5 in the evening sector (1800 - 2400 LT) (CARPENTER, 1966). The consequences to the protonospheric content

along the line of sight to a geostationary satellite might be expected to give a positive gradient till the time of the dusk bulge with subsequent reduction of N_p as the plasmapause contracts to 0600 LT. An examination of Fig. 29 shows that the observed gradients are not wholly consistent with these conclusions, particularly with regard to the large negative gradients found in the late afternoon and evening sector. It is suggested that, for Aberystwyth/ATS-6 geometry, the contribution to N_p and its time gradient resulting from plasmapause dynamics is relatively small and that the results can be interpreted for the most part in terms of interaction between the ionosphere and protonosphere along flux tubes lying well inside the plasmasphere.

Considering first the northern hemisphere summer curves represented by June and July in Fig. 29, it can be seen that upwards fluxes start some two hours after local sunrise with maximum values some two hours after conjugate sunrise. The subsequent decrease in the flux rate may be indicative that the relatively short small volume tubes of low L- value (say $L \lesssim 2$) become well filled so that the upwards flux to them is decreased and the subsequent small increases in protonospheric content occurs on the larger volume higher L- value flux tubes (CARPENTER and PARK, 1973). The rates of change do not differ significantly from zero in the middle of the summer day when the neutral wind is depressing the F- layer ionisation, but after conjugate sunset a large downwards protonospheric flux quickly develops. It is interesting to note that this downwards flux maximises at about the time of the second daytime ionisation peak in the still sunlit local ionosphere. This suggests that the protonospheric depletion at this time is to the conjugate ionosphere and the

shape of the flux variation, quickly maximising downwards with subsequent reduced values, appears to indicate that the short inner tubes are quickly drained.

Unfortunately the curves for other months do not show such clear-cut trends and their interpretation is more difficult. The downwards flux onset near either local or conjugate sunset is apparent for all months, while earlier times for November and April may be a reflection of the scatter of the raw data points. It should be noted that March, November and April in that order are months of highest mean geomagnetic activity in the period. An upwards flux associated with sunrise in the local hemisphere can be seen at all months but it is interesting to note that a short-lived secondary peak is found around conjugate sunrise in December and January when the time separation between sunrise in the two hemispheres is a maximum.

It can be concluded from these studies that both local and conjugate ionospheres play a role in the filling and depletion of the protonospheric flux tubes and that in the interpretation of data referring to observations along the line of sight to a geostationary satellite both hemispheres must be considered.

In an attempt to gain further understanding in a qualitative interpretation of the protonospheric observations the ionospheric f_oF2 data for Slough, representing local conditions, and Cape Town (for a previous solar epoch), appropriate to the conjugate ionosphere, are plotted in Fig. 30. For comparison the Cape Town data have been time shifted to refer to the local mean time at Slough. In northern hemisphere winter (November to February) the f_oF2 diurnal variations at Slough show a single-peaked structure with maximum values of $\sim$ 6 MHz around midday. A similar

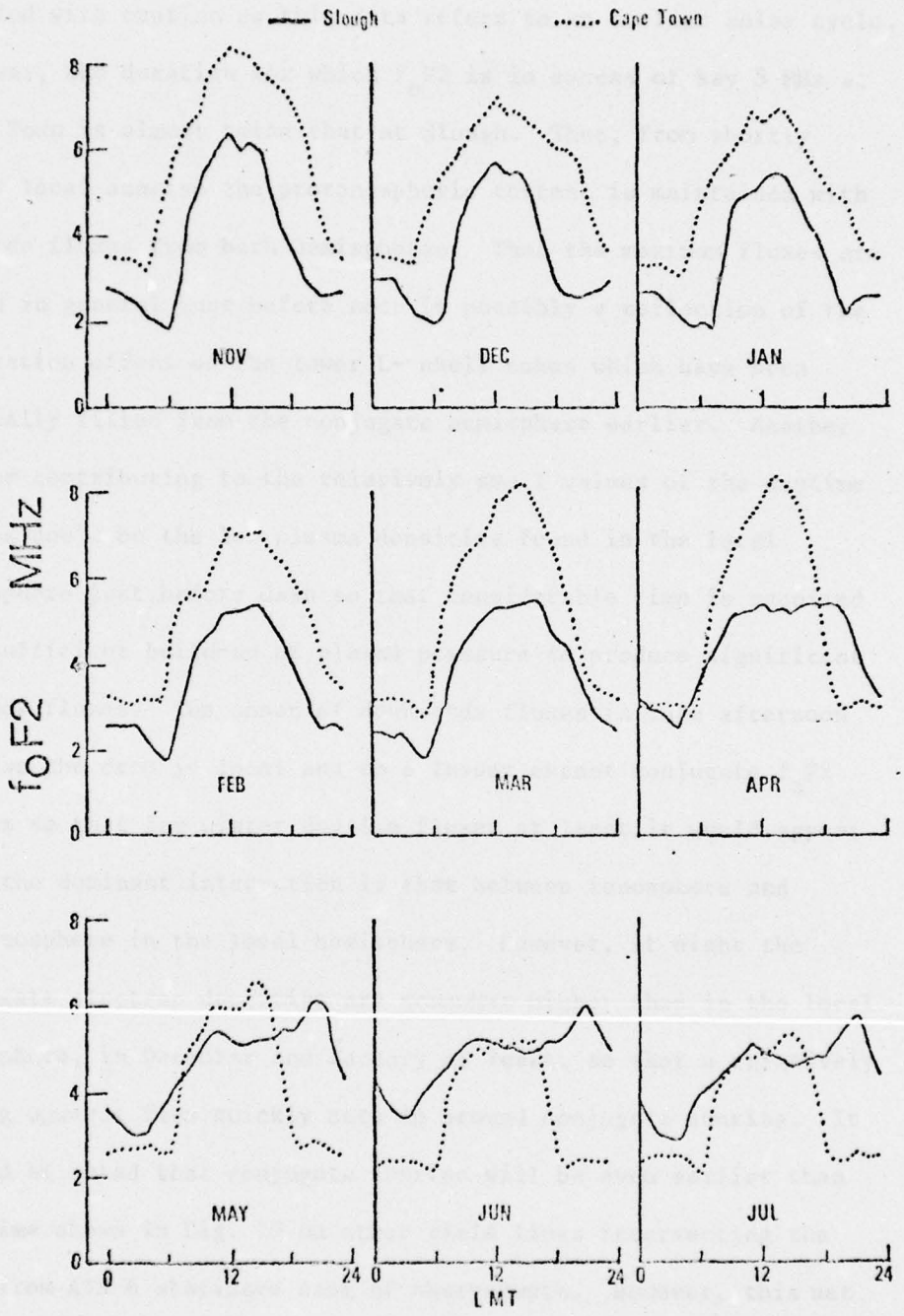

Fig.30. Monthly median hourly values of foF2 for Slough (1975-6) and Cape Town (1963-4), the latter shifted to LMT at Slough.

single-peaked variation is found in the Cape Town data for these months with maximum values ∿ 7 MHz. Precise magnitudes should be treated with caution as this data refers to an earlier solar cycle. However, the duration for which f_oF2 is in excess of say 5 MHz at Cape Town is almost twice that at Slough. Thus, from shortly after local sunrise the protonospheric content is maintained with upwards fluxes from both hemispheres. That the maximum fluxes are found in general just before noon is possibly a reflection of the saturation effect of the lower L- shell tubes which have been partially filled from the conjugate hemisphere earlier. Another factor contributing to the relatively small values of the daytime fluxes could be the low plasma densities found in the local ionosphere just before dawn so that considerable time is required for sufficient build-up of plasma pressure to produce significant upwards fluxes. The onset of downwards fluxes in late afternoon follows the drop in local and to a lesser extent conjugate f_oF2 values so that for winter daytime fluxes at least, it would appear that the dominant interaction is that between ionosphere and protonosphere in the local hemisphere. However, at night the conjugate electron densities are somewhat higher than in the local ionosphere, in December and January at least, so that a relatively strong upwards flux quickly sets in around conjugate sunrise. It should be noted that conjugate sunrise will be even earlier than the time shown in Fig. 29 on other field lines intersecting the path from ATS-6 stationed east of Aberystwyth. However, this net upwards flux is short-lived, the effects of the predawn bite out in f_oF2 in the local ionosphere more than compensating so that a net decrease in protonospheric content is found until after local sunrise.

The uncertainty of some of the March data and the scatter of the observed fluxes in April, a month of above average geomagnetic activity, mean that the fluxes for these months cannot be interpreted in detail. Consistent integrated flux patterns are found for the northern hemisphere summer months of May, June and July. The strong upwards flux following the earlier local sunrise quickly saturates and is followed by depressed or even negative values around midday when the local f_oF2 values are kept almost constant under the dynamic influence of the neutral wind. The evening peak in the local ionosphere is more than compensated by the rapid drop in electron density in the short winter day at the conjugate point so that strong downwards fluxes, it would seem to the conjugate ionosphere, are observed. These quickly maximise then drop indicating an emptying of the inner L- shell tubes.

It is thus apparent that an interpretation of the observed protonospheric variations requires consideration of interactions with the ionosphere in both hemispheres and while in the main the integrated protonospheric content is determined by local conditions, there are times when the conjugate ionosphere is the dominant factor.

Average integrated fluxes, presented in Table 7 for each month, show that to within the accuracy of the estimates the magnitude and duration of the upwards flux by day is broadly compensated by the downwards flux at night. PARK (1970) has calculated average daytime and nighttime fluxes from a limited data base of whistler observations of tube content. He estimates a flux through the 1000 km level with a daytime filling magnitude $\sim 3 \times 10^8$ cm^{-2} s^{-1} and a nighttime draining value reduced by a

Table 7. AVERAGE INTEGRATED PROTONOSPHERIC FLUXES

	Upwards		Downwards	
	x 10^7 cm^{-2} s^{-1}	Duration hr	x 10^7 cm^{-2} s^{-1}	Duration hr
Nov	2.2	12	-2.2	12
Dec	2.3	12	-3.0	11
Jan	1.9	14	-2.8	10
Feb	2.9	11	-2.5	13
Mar	4.0	7	-4.3	11
Apr	5.4	10	-4.2	13
May	4.2	15	-6.1	9
Jun	3.8	9	-4.2	10
Jul	3.9	8	-3.4	13

factor of two. These values are significantly higher than the results of the present study. However, PARK's data refer to a quiet period during which the protonosphere drains and refills in a regular diurnal pattern. Secondly, his results correspond to 1000 km level while the ATS-6 observations are for a flow at about 2000 to 3000 km where the fluxes are probably smaller and the tube area is increased by $\sim$ 5%. Another important factor is that the observations of PARK refer to tubes for L > 4 while the Aberystwyth ray path crosses tubes for L $\gtrsim$ 1.7. CARPENTER and PARK (1973) have argued that the flux is enhanced for higher L-shells because of the relatively less dense plasma in these larger volume tubes. Finally, as will be seen later, the protonospheric content builds up consistently during a long quiet period with the daytime flux exceeding that at night. This trend is interrupted sharply during moderate to severe geomagnetic activity and many days or even weeks are required for recovery. Thus on average the daytime and nighttime fluxes do not differ significantly in magnitude.

8. SLANT SLAB THICKNESS

Slab thickness is a parameter which gives an indication of the shape of the ionospheric profile by normalising the electron content with respect to the peak electron density (N_m). Following the notation of DAVIES et al. (1976) the slant slab thickness (τ_s) is given by

$$\tau_s = N_T/N_m \qquad 16.$$

Values of N_m can be obtained from published F2- layer critical frequency data. For comparison of slant slab thickness with the other measured shape parameter, the F- factor, it is necessary to

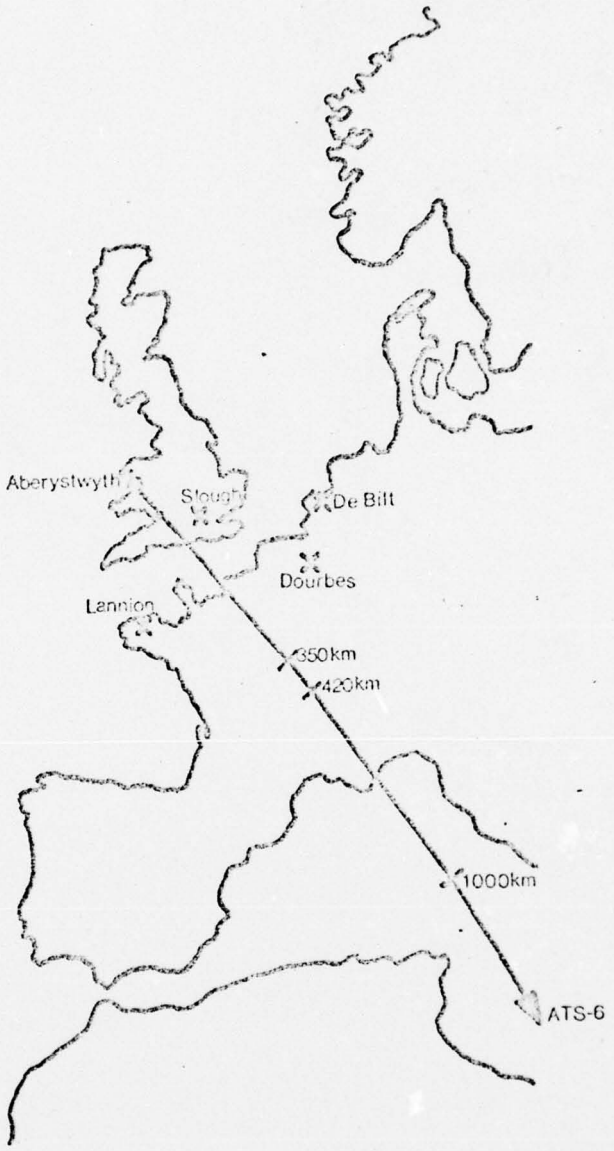

Fig.31. Ground projection of ray path in relation to various ionosonde stations.

evaluate f_oF2 at the sub-ionospheric point of the ray path (47.3°N, 3.3°E for 350 km altitude). However, as there is no convenient ionosonde at this location an extrapolation procedure has been used to generate the required data from values obtained from a number of ionosondes in the general locality.

A prior test of f_oF2 data from several European stations showed a substantial longitudinal gradient in the values for the same local mean time. Therefore, only four stations, with the smallest range in longitudes about the sub-ionospheric point, have been used: De Bilt (52.1°N, 5.2°E), Slough (51.5°N, 0.6°W), Dourbes (50.1°N, 4.6°E) and Lannion (48.7°N, 3.5°W). Fig. 31 shows the geographic locations of these stations with respect to the ground projection of the ray path. Data was unavailable for Lannion for March 1976 and for De Bilt from March 1976. The missing values have been interpolated from the published worldwide contours of f_oF2 (CCIR, 1967) by using the existing data for the other stations.

The monthly median f_oF2 values for each hour from the four stations have been considered as a function of latitude and f_oF2 at the sub-ionospheric latitude obtained from a regression line analysis. When the correlation coefficient was less than 0.7 the f_oF2 value at the sub-ionospheric point was estimated from the CCIR plots. A comparison of the two methods showed that differences were in general within the errors in scaling the contour plots.

It should be noted that to keep the workload reasonable in this preliminary study attention was concentrated on monthly median f_oF2 and N_T values so that the 'median' slab thickness

calculated may differ slightly from the true median of the individual daily values, however, it is unlikely that any conclusions are affected by this approximation. In fact, following DAVIES et al. (1976) a further smoothing has been carried out on the data by calculating a 3- hour running mean of the hourly values for each month.

The smoothed median values of slant slab thickness are presented in Fig. 32. Daytime values < 400 km in winter give way to thicknesses ∿ 800 km in summer while by contrast magnitudes well in excess of 700 km on winter nights contrast to thicknesses < 600 km during darkness in summer. Also of note are the predawn and post sunset peaks in slab thickness which are most prominant in the winter months.

Following DAVIES et al. plots have been made of F against τ_s for each month (Fig. 33). While the daytime values of F are essentially constant τ_s increases from winter to summer but in the predawn sector increases in F are matched by large slab thickness in winter when the protonospheric content assumes greatest proportional importance. The curves show essential similarities to those of DAVIES et al. being 'open loops' in summer and more nearly linear in winter, although the secondary loop found near midnight in winter reflects the decrease in slab thickness observed in the European data and not in the American values.

9. COMPARISON WITH AMERICAN SECTOR DATA

a. Introduction

Although the prime objective of the present work has been the study of ionospheric/protonospheric coupling along the ATS-6 ray path to Aberystwyth it was considered important that the data

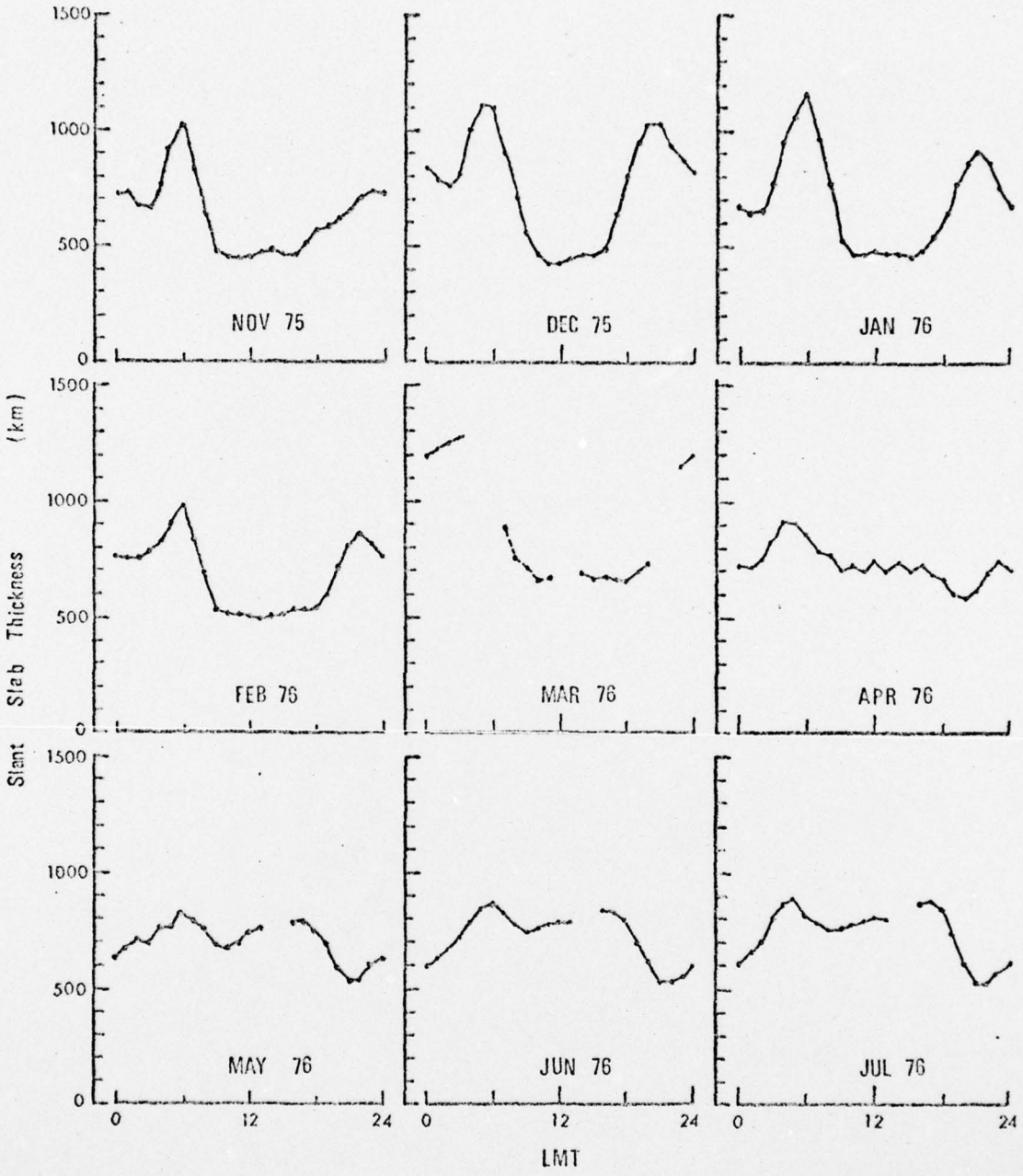

Fig.32. Monthly median hourly values of slant slab thickness (3-hour means) for Aberystwyth from November 1975 to July 1976.

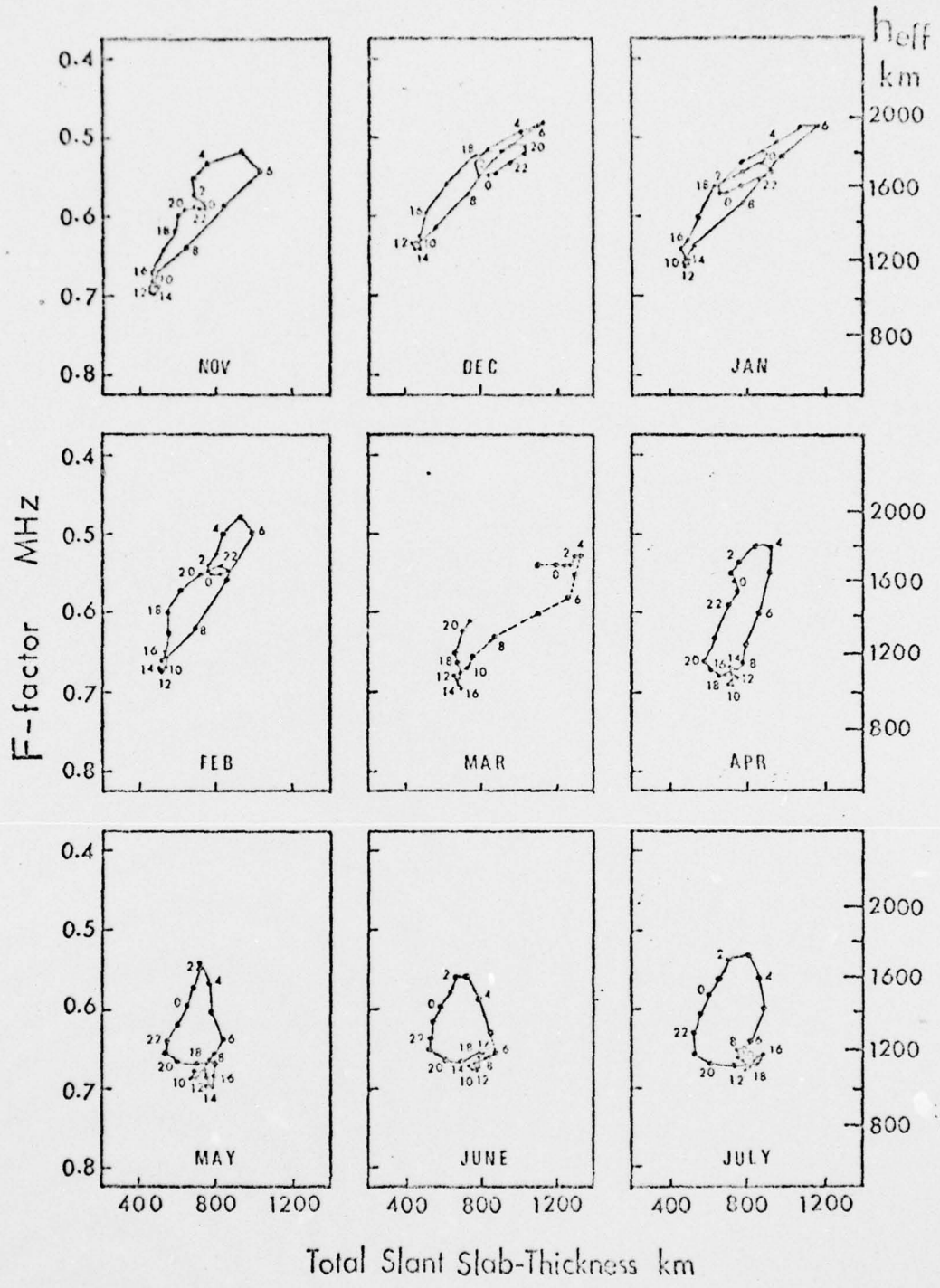

Fig.33. Monthly median hourly F versus slant slab thickness plots (3-hour means), November 1975 to July 1976.

obtained should be compared to other available ATS-6 results. FRITZ (1976) has published a complete set of data for the Boulder, USA station (40°N, 105°W) obtained from July 1974 to May 1975 during the first phase of the ATS-6 project when the satellite was stationed at 94°W longitude. Apart from individual case studies of a few days duration and theoretical model work this experimental data forms the only base, at the time of writing, with which to compare the Aberystwyth results. Surprisingly, at first sight at least, the monthly median Boulder protonospheric content shows a diurnal variation in which minimum values are found by day with a maximum at night, especially for the winter months. This pattern in American sector data has been repeated in the case studies of SOICHER (1976b) and POLETTI-LIUZZI (1976), but has been passed over largely without comment by all three groups of workers. The very limited data to come as yet from the European sector would appear to be in essential agreement with the Aberystwyth results in terms of the form of the diurnal variation (SOICHER, 1976b and HARTMANN et al. 1976).
It thus appears that there is a discrepancy between American and European observations of protonospheric content which requires explanation.

b. Comparison of Results

The published Boulder monthly median N_p data for the ATS-6 Phase I period, converted to local mean time, are compared to corresponding monthly values for Aberystwyth from the later Phase II operations in Fig. 34. The differences in the form of the diurnal variations and in the N_p magnitudes for the two

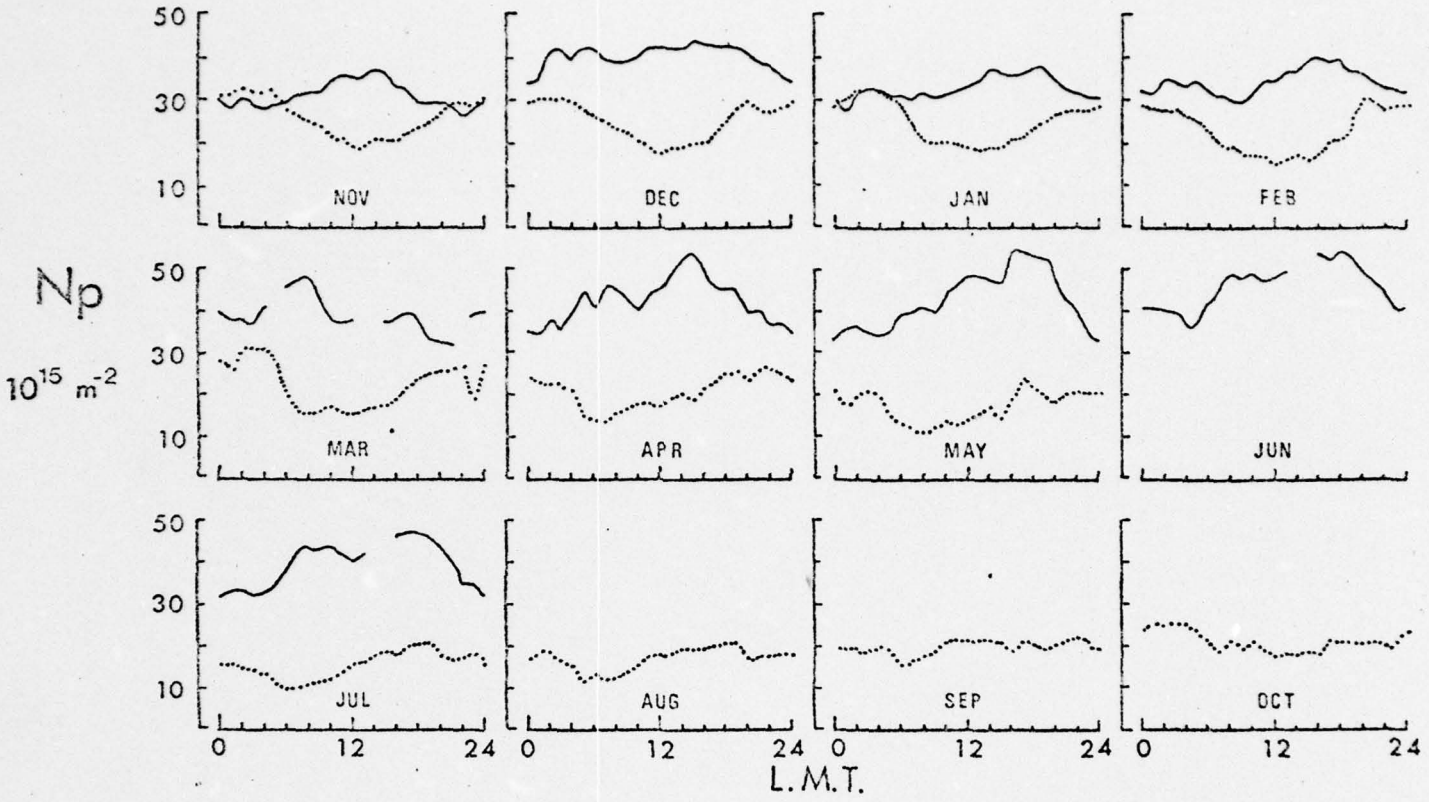

Fig.34. Comparison of median N_p for Aberystwyth (solid) (November 1975 - July 1976) with that for Boulder (dotted) (July 1974 - May 1975).

stations are immediately apparent. An examination has shown that these differences cannot be attributed to differences in the level of solar and geomagnetic activity between the data sets. However, a table corresponding to Table 1 for Aberystwyth, giving the geophysical parameters for the ATS-6 to Boulder geometry allows certain conclusions to be drawn. Firstly, the discrepancies in N_P cannot be attributed to range differences along the slant path. While the range through the ionospheric part of the path up to a height of 2000 km is $\sim$ 2600 km for Boulder compared to $\sim$ 3600 km for Aberystwyth, the range difference of the protonospheric paths is only $\sim$ 3%. Secondly, for the Boulder geometry f_L is a single valued function of height/ Fig.35; the height increase in cos 0 is too small to offset the decrease in gyrofrequency as is the case for the Aberystwyth geometry. As a result, f_L for Boulder is a much more sensitive function of height around 400 km than that for Aberystwyth, so that a change of $\pm$ 100 km in the height at which f_L is evaluated can result in a change of $\pm$ 50% in N_P. Hence in the interpretation of the Boulder diurnal variation of N_P it is of great importance to assess the effect of diurnal changes in the height of the F2- layer. A procedure similar to that already described for the Aberystwyth data was carried out to estimate the true height of the ionospheric peak (h_m) from ionosonde data. Unfortunately, the World Data Centre were unable to provide f_oF2 and f_oE values for either Boulder or White Sands for the period of Phase I ATS-6 observations. However, monthly median ionosonde data from Boulder for corresponding months of the previous solar cycle, eleven years earlier, have been used to estimate h_m and its diurnal variation.

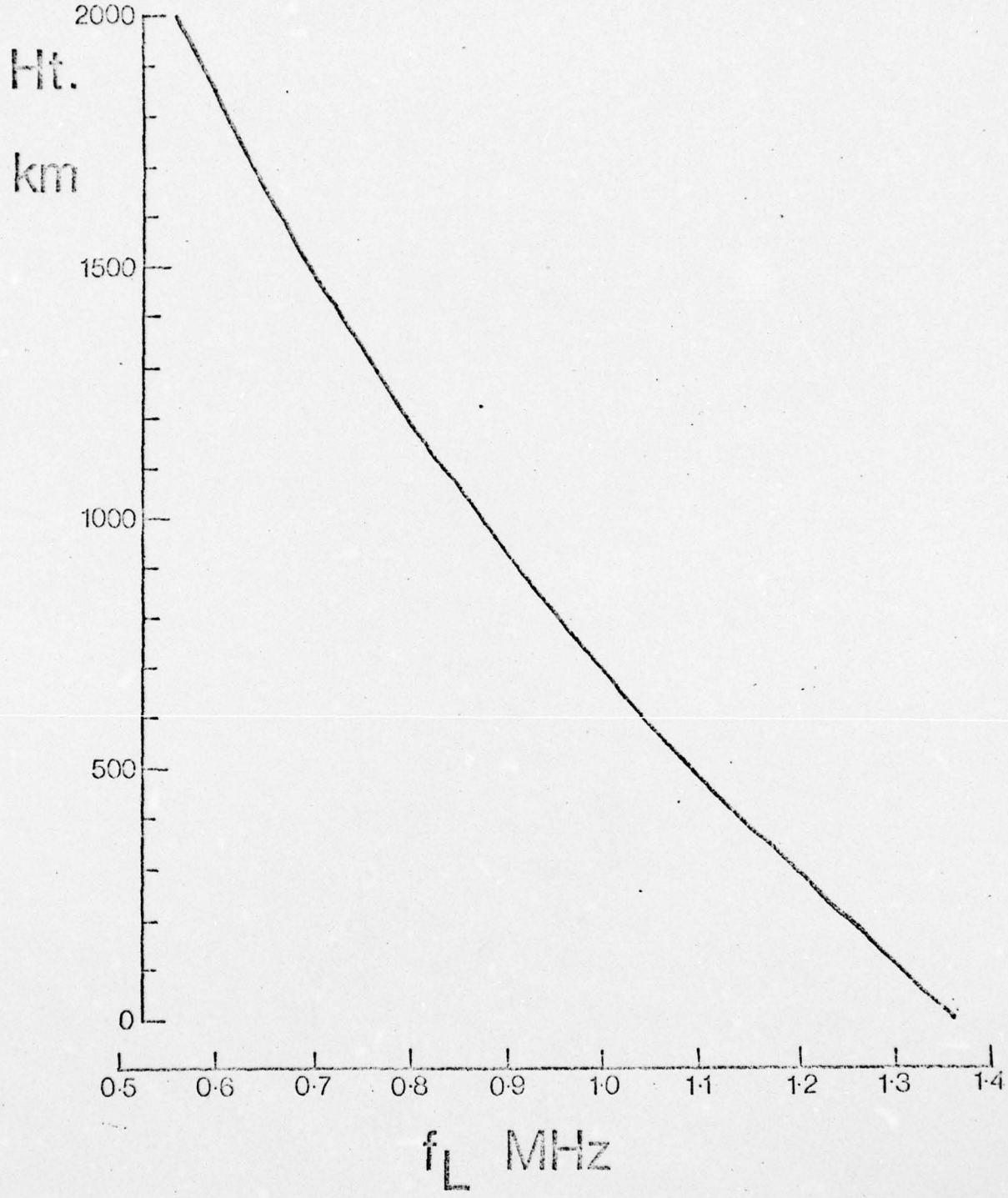

Fig.35. Height variation of longitudinal gyrofrequency for ATS-6 to Boulder path to a height of 2000 km.

The substantial effect of this variation of h_m on the values of N_p, particularly for daytime, is illustrated in Figs. 36 - 38. Choosing h_m + 100km as the height for the estimation of $\overline{f}_L$ it can be seen from Fig. 39 that the afternoon values of N_p are significantly enhanced. For the equinoxial month of March a minimum value of N_p is now found around dawn rather than the broad morning minimum of the raw data for which a constant $\overline{f}_L$ evaluated at about 380 km had been used. In winter a raising of the daytime values is detected, but this still leaves them lower than those found at night and in fact for no reasonable choice of increment to h_m can the diurnal variation be reversed. Thus, while the remarks of KLOBUCHAR and KIDD (1972) and ALMEIDA (1974) are partially confirmed and the diurnal variation of the layer height plays a more significant role for stations in the American sector than Europe, nevertheless, an alternative ionospheric as opposed to observational explanation must be sought to account for the winter daytime minimum in N_p.

Differences in the magnitude of N_p for Aberystwyth and Boulder also require interpretation. It can be seen from Fig. 34 that while nighttime values in winter are comparable, at other hours and seasons, in particular summer, the Boulder content may be less than half that found at Aberystwyth.

Consideration of the ray path geometry with respect to the field lines for Boulder (Fig. 40) shows that at comparable points on the path the intersection is with higher L-shell tubes, with a minimum $L \sim 2$, than for Aberystwyth (Fig. 28) where a considerable portion of the path intersects field lines for which $L < 2$. In addition the field line geometry results in a conjugate ionospheric point at much higher latitude than Boulder itself in

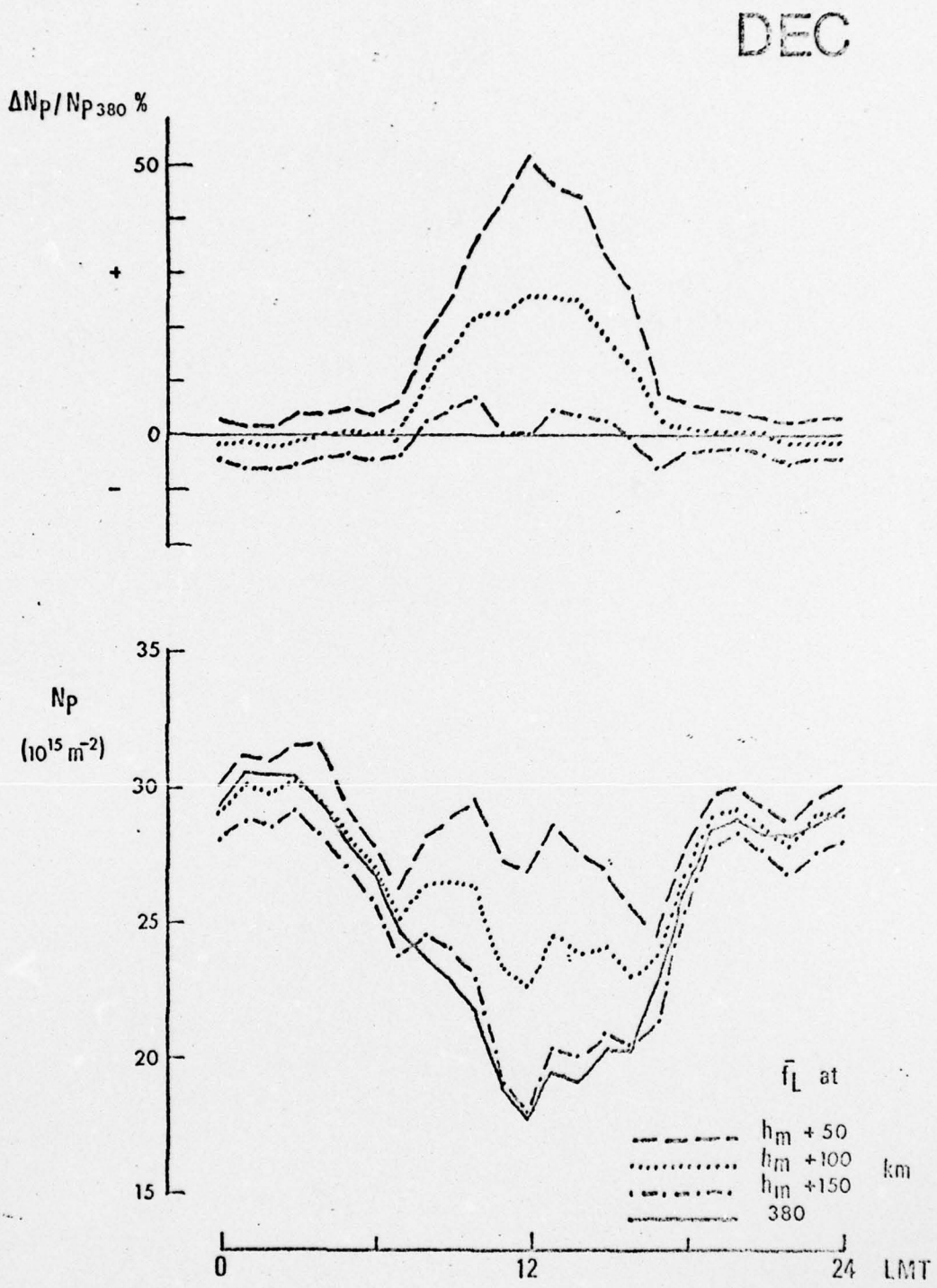

Fig.36. Effect of variable $\bar{f}_L$, evaluated for three height increments to h_m, on diurnal variation of N_P for Boulder for December 1974.

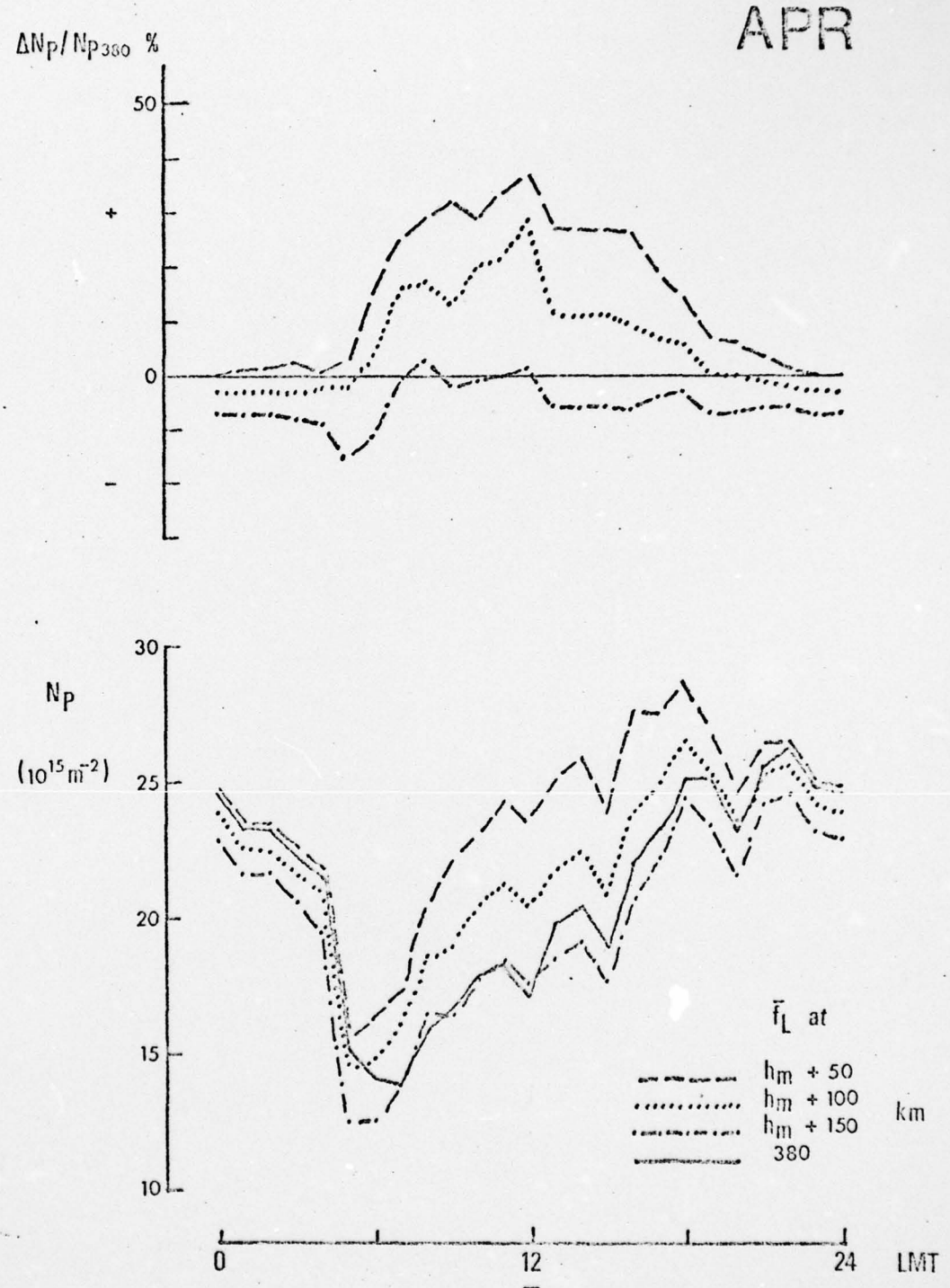

Fig.37. Effect of variable $\bar{f}_L$, evaluated for three height increments to h_m, on diurnal variation of N_p for Boulder for April 1975.

AD-A046 762 UNIVERSITY COLL OF WALES ABERYSTWYTH DEPT OF PHYSICS F/G 20/14
ATS-6 OBSERVATIONS OF IONOSPHERIC/PROTONOSPHERIC ELECTRON CONTE--ETC(U)
FEB 77 L KERSLEY, H KAJEB-HOSSEINIEH AFOSR-72-2267
UNCLASSIFIED AFGL-TR-77-0107 NL

2 OF 2
AD A046 762

END
DATE FILMED
12-77
DDC

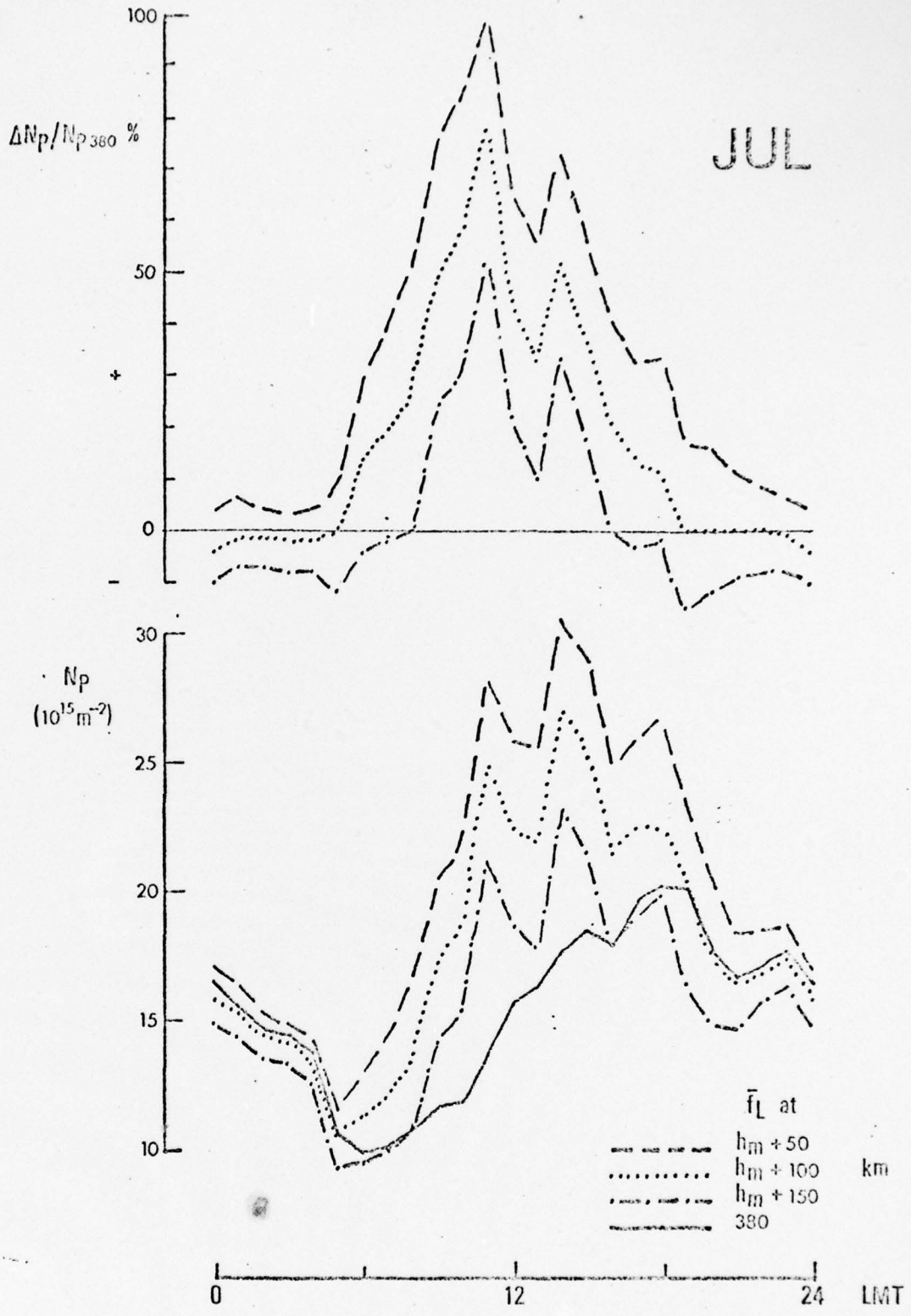

Fig.38. Effect of variable $\bar{f}_L$, evaluated for three height increments to h_m, on diurnal variation of N_p for Boulder for July 1974. The fluctuations around noon arise from the unrealistically large E-layer corrections applied in the estimation of h_m. Resulting values of N_p for a few hours about midday are almost certainly too large and must be treated with caution.

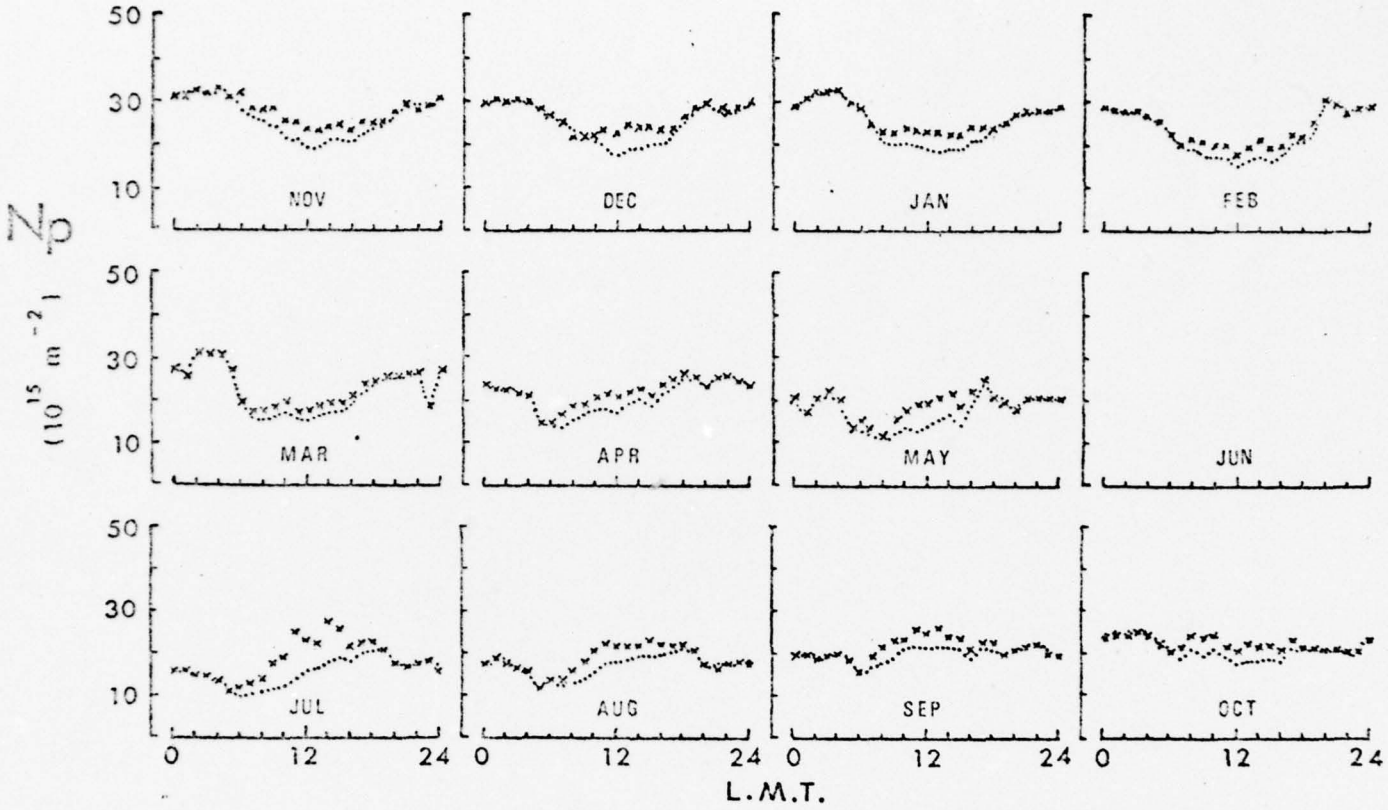

Fig.39. Comparison of monthly median hourly values of N_p for Boulder with $\bar{f}_L$ constant (dotted) with those for variable f_L evaluated at h_m + 100 km (crosses).

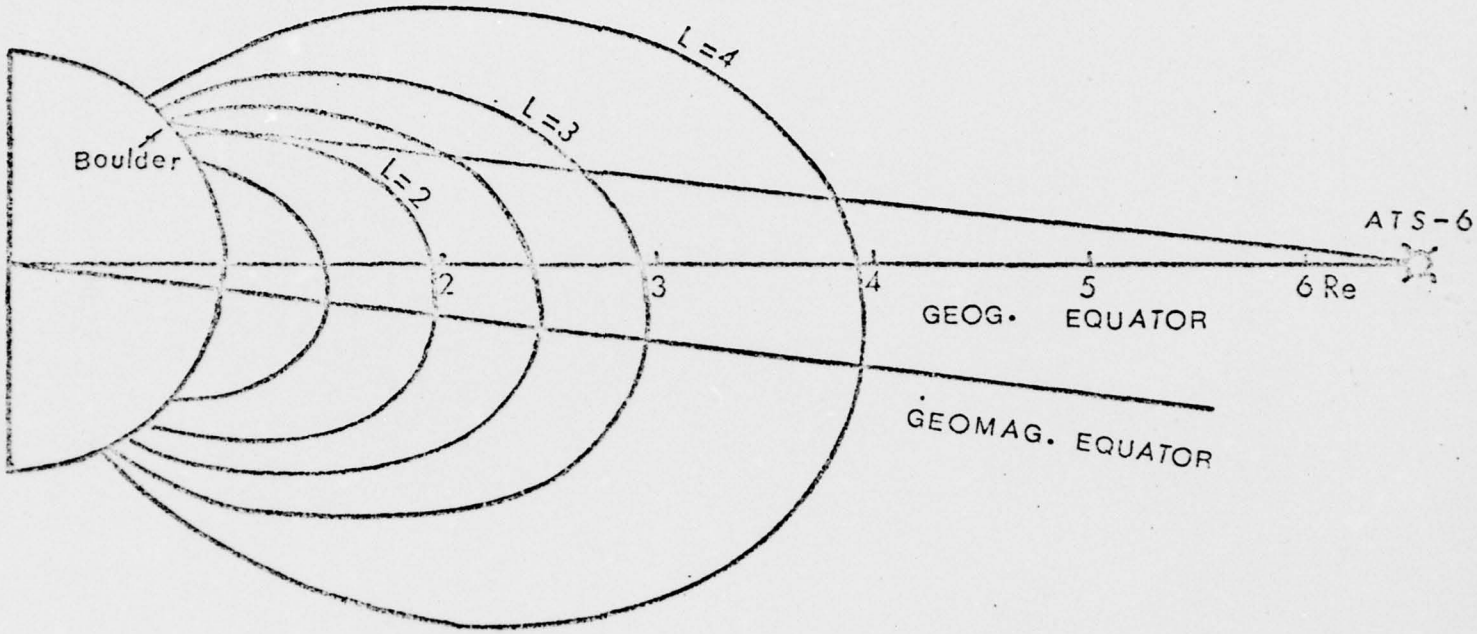

Fig.40. Geomagnetic field line configuration for ATS-6 to Boulder ray path.

contrast to the lower conjugate latitude for Aberystwyth. Thus, remembering the anomalous behaviour of the Antarctic ionosphere (BELLCHAMBERS and PIGGOTT, 1960), it seems possible that the explanation invoked to account for the Aberystwyth results, involving ionospheric/protonospheric interaction at both ends of a field line, may provide some qualitative interpretation of, not only the very low N_p values in summer but also, the inverted diurnal variation in the Boulder data for winter.

To examine this further, the monthly median f_oF2 data for Boulder mentioned earlier have been plotted in Fig.41 together with data from a similar period from Argentine Island (65°S, 64°W), this station being the ionosonde closest to the location (57°S, 127°W) conjugate at 300 km to the Boulder sub-ionospheric point. The latter data have been time shifted to correspond to the local mean time at Boulder.

As an additional aid to interpretation, the integrated fluxes (dN_p/dt) have been computed for Boulder using 3-hour running mean smoothed N_p data corrected by use of a variable $\overline{f}_L$ evaluated for h_m + 100 km. These are plotted in Fig. 42.

Considering first July, upwards fluxes are observed to commence some 2 to 3 hours after local sunrise when f_oF2 for Boulder rises from a minimum value about 3MHz to ∿ 5MHz before noon. The integrated fluxes are smaller than for Aberystwyth at this time and do not show quite the same rapid saturation because the average L- value of the intersecting tubes is greater. The small magnitude of the upwards fluxes and the low N_p values for July can be explained in terms of the long winter night of the

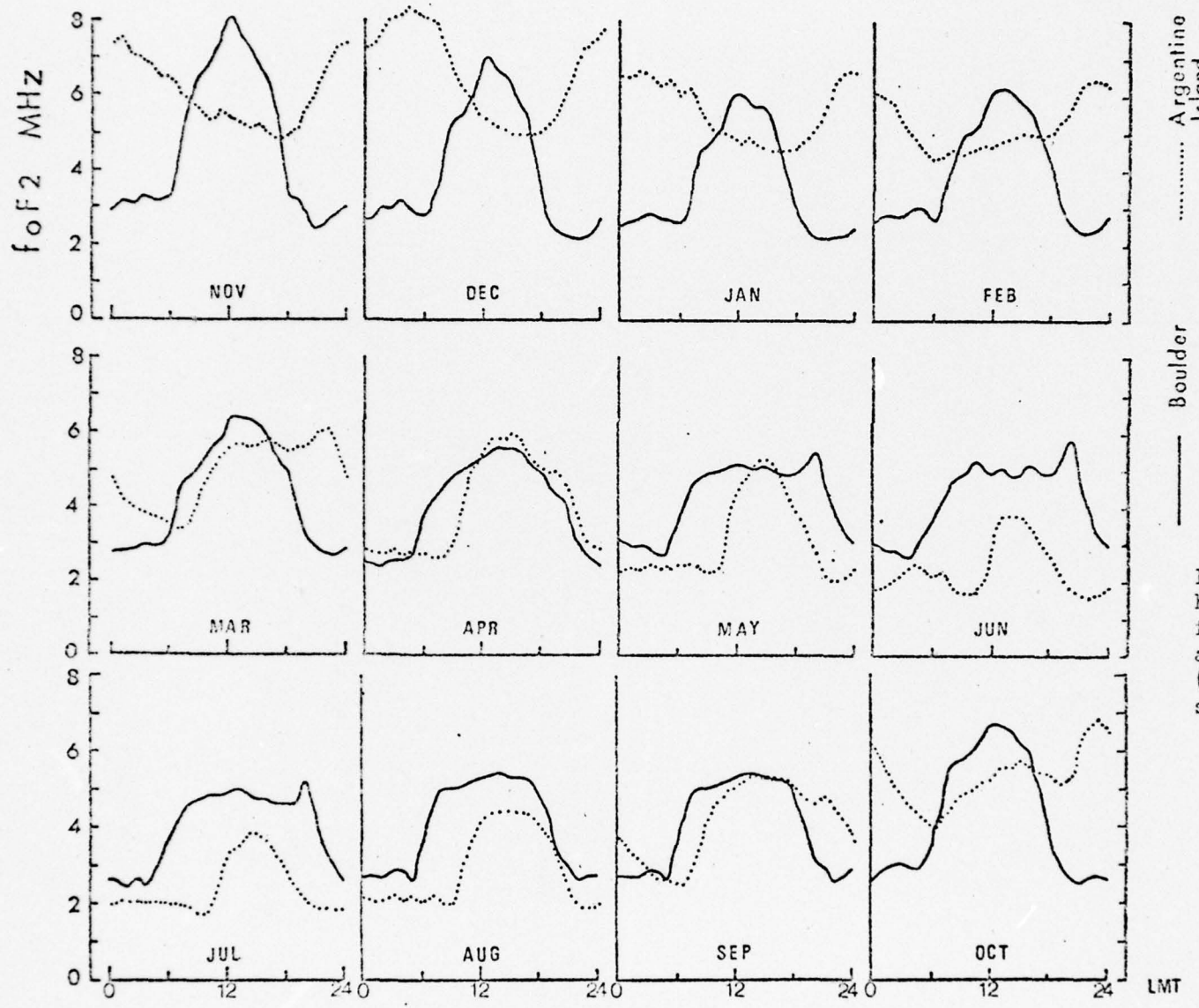

Fig.41. Monthly median hourly values of foF2 for Boulder (1963-64) and Argentine Island (1963-64), the latter shifted to LMT at Boulde

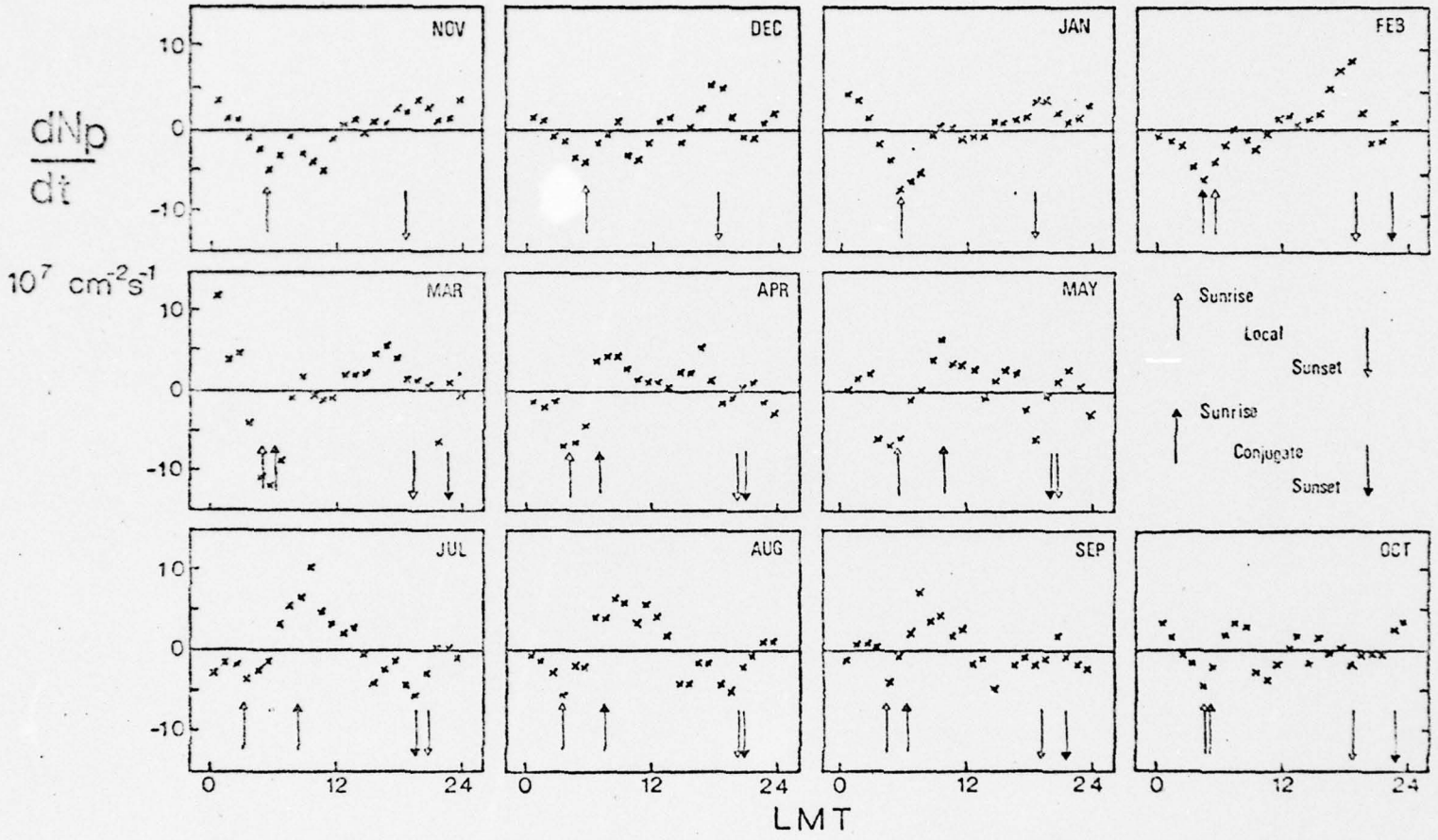

Fig.42. Diurnal variations of estimated integrated protonospheric flux (dN_p/dt) for Boulder by month from July 1974 to May 1975.

relatively high latitude conjugate ionosphere, with f_oF2 for Argentine Island < 2.5MHz, for some 20 hours. Thus in northern hemisphere summer there is a steady drain of plasma to the conjugate ionosphere for most of the day with little upwards compensation even during the short daylight hours. It is interesting to note that in July the f_oF2 diurnal variations for Slough and Boulder are very similar in form and magnitude but the markedly different N_p data for the two stations can be accounted for, at least qualitatively, by the differences in conjugate ionospheric behaviour and path/flux tube geometry.

For December, the noteworthy feature is the anomalous behaviour of f_oF2 for Argentine Island in response to the 300 km ionosphere being sunlit 24 hours a day. In fact, it should be noted that even at the Boulder conjugate latitude (57^oS) there is no ionospheric sunset from November to January. The resulting f_oF2 values minimise at $\sim$ 5 MHz in early afternoon, under the influence of the polewards neutral wind, (KOHL and KING, 1967), but by night the F2 critical frequencies become $\sim$ 8MHz. The Boulder f_oF2 values range from $\sim$ 3 MHz at night to $\sim$ 7 MHz at the single peak maximum in the middle of the winter day. The much higher N_p values for December compared to July can be attributed to the generally higher electron densities, particularly in the conjugate ionosphere. In addition, the daytime minimum in N_p reflects the anomalous behaviour of the conjugate ionosphere whose influence is dominant in northern hemisphere winter daytime. It can be noted with caution that use of h_m + 150 km in the correction of the N_p data raises the winter midday values further removing the minimum, a situation which may take account more closely of the behaviour of the local ionosphere.

It is possible to consider each month in detail and interpret features of both the N_p data and the integrated net fluxes in terms of ionospheric behaviour in the two hemispheres. However, we shall discuss only March since for this month the conjugate ionosonde data shows a dramatic change to a daytime peak with the arrival of ionospheric darkness in March, but the N_p data after correction have a dawn minimum and a nighttime peak which at first sight at least appears spurious. Some 2 to 3 hours after sunrise small positive fluxes are found which persist (apart from one possibly anomalous point although even this may be interpreted by a more complete model of the actual physical situation) to well after local and even conjugate sunrise. The post midnight strong upwards fluxes and the early morning peak in N_p may represent a protonospheric filling from the late evening peak in the conjugate hemisphere, delayed by several hours because of the relatively long flux tubes.

While it is recognised that there are limitations to this fairly simple qualitative approach to the interpretation of the protonospheric data, nevertheless the results obtained for Aberystwyth, together with some confirmation from the contrasting Boulder situation, would appear to justify further model studies of a quantitative nature. These should take account of both local and conjugate ionospheres and use multiple flux tube geometry with appropriate time constants which would more closely approximate to the actual experimental conditions.

10. CASE STUDIES

a. Introduction

This report has been concerned so far with monthly median values of various parameters determined by the ATS-6 radio beacon experiment. While these have provided us with information on the average behaviour of ionosphere and protonosphere they give little indication of the response to individual events, in particular to changing levels of geomagnetic activity. The response of ionospheric electron content to geomagnetic storms is reasonably well documented (e.g. MENDILLO and KLOBUCHAR, 1974) so attention has been concentrated here on the day to day behaviour of protonospheric content. As a short conclusion to this preliminary study of ATS-6 data two periods have been selected for discussion, both cover times of major storm activity but one also takes in a two week quiet days during which K_p rarely exceeds 3.

b. 13 November - 4 December, 1975

Hourly values of N_p available throughout this period are plotted in Fig. 43. Also shown for comparison, recurring for each day, is a plot of the average N_p for a 30 day period centred on 22 November 1976. Values of the 3-hour K_p index are presented above the corresponding N_p data.

The period starts with four days when K_p never exceeds 3 and the N_p values are seen to rise gradually. Enhanced geomagnetic activity, maximising on 17 November causes a drop in N_p around 1800 LMT on that day and values remain low during the moderate activity period to 20 November. Following $K_p = 5_-$ early on 21 November, N_p maximises around midday and relatively high values are maintained on 22 November. A sudden commencement at 2306 UT

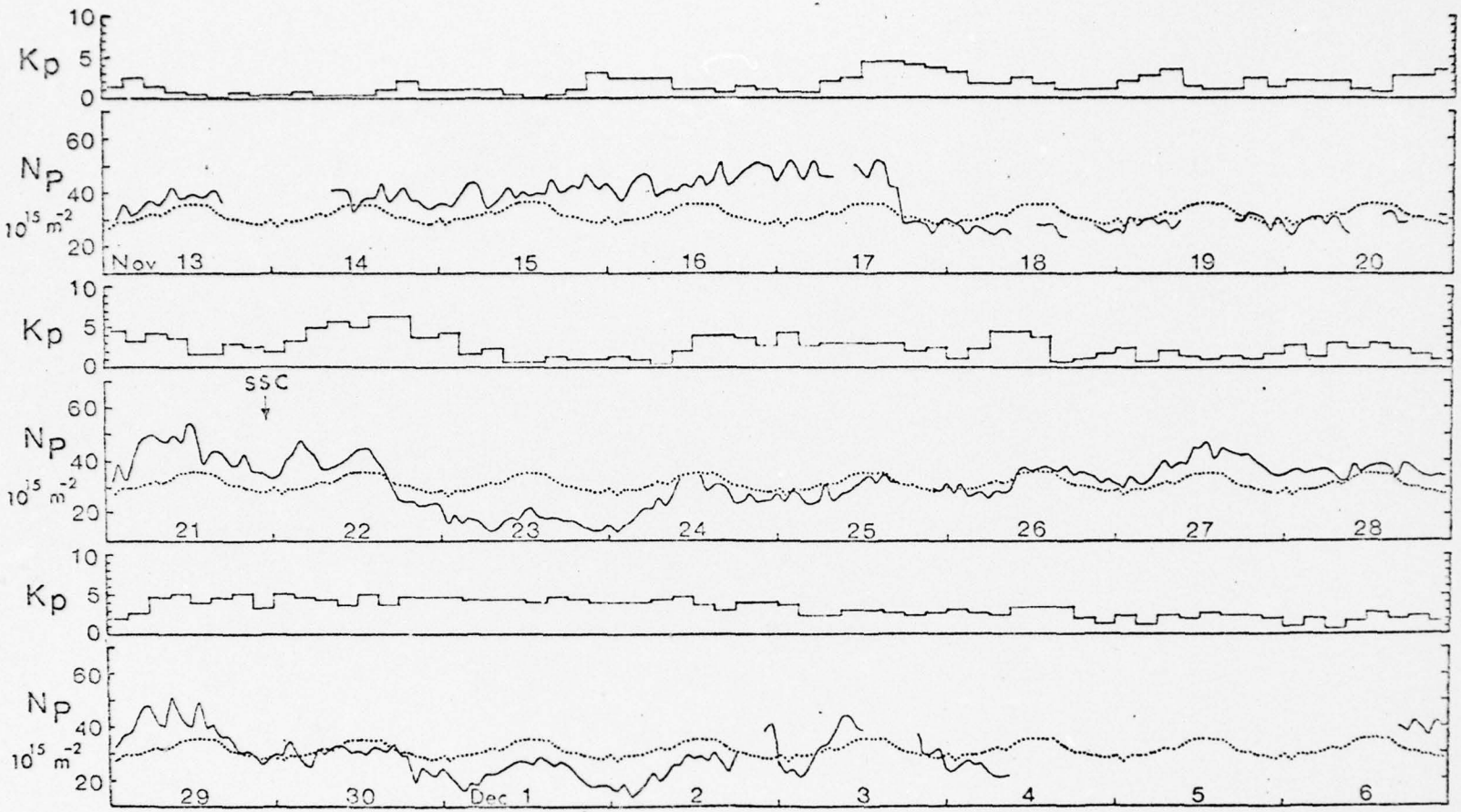

Fig.43. Variation of N_P and K_p from 13 November 1975 to 6 December 1975. Shown dotted are the average values for a 30-day period centred on 22 November 1975.

on 21 November, with $K_p = 6_+$ on the afternoon of the next day, is followed by a sharp drop in N_p around 1800 UT on 22 November. A steady refilling of the protonosphere is found till the 29 November with a clear diurnal pattern to be seen in N_p. Enhanced values of K_p, reaching 5 on 29 November are accompanied by high N_p on that day followed by a gradual depletion superposed on the regular diurnal variation till the morning of 2 December while K_p remains in the main > 4. The protonospheric content shows signs of subsequent recovery on 3 December as geomagnetic activity lessens.

c. 28 April - 21 May, 1976

The period (Fig. 44) starts with four days in which the geomagnetic activity reaches $K_p = 4_+$ late on 29 April and N_p shows a fluctuating pattern, particularly on 30 April and 1 May when the diurnal variation is almost masked by the apparently random variations. A major storm with sudden commencement at 1828 UT on 2 May and K_p reaching 8_+ is preceded by a sharp increase in N_p around midday to be followed by a depletion with N_p reaching very low values on the morning of 3 May and even lower magnitudes around midnight of that day. In fact this value 1.3×10^{16} m^{-2} was the lowest N_p found during the entire observing period. Three days follow with substantial breaks in the N_p data, but the values plotted show the trend of a replenishing protonospheric content which is continued until about 16 May, during a time of quiet geomagnetic activity. Superposed on this trend is a regular diurnal variation with increasing amplitude as the quiet period continues. From 16 to 19 May geomagnetic activity is very small and N_p is consistently above average with a continuing clear

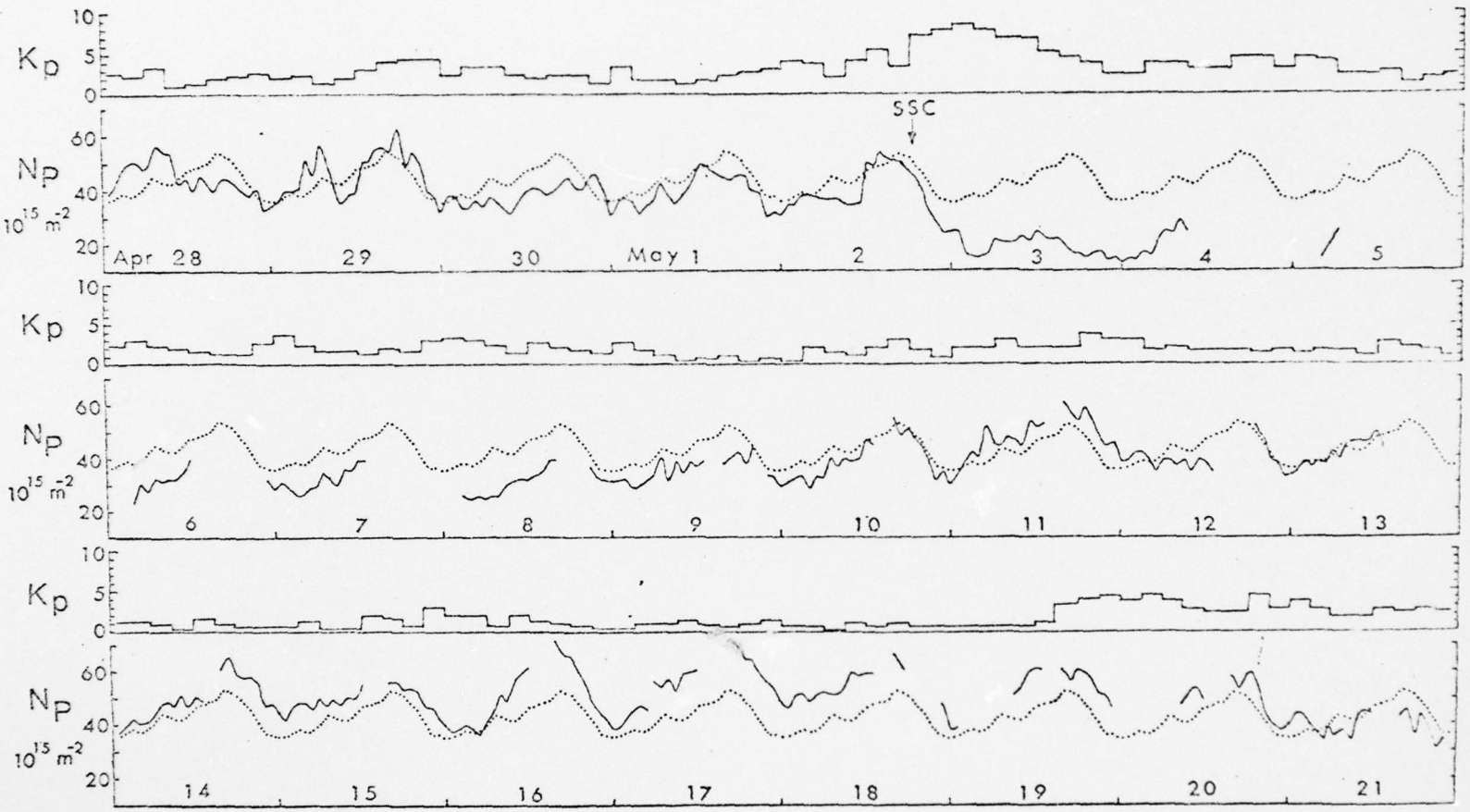

Fig.44. Variation of N_p and K_p from 28 April 1976 to 21 May 1976. Shown dotted are the mean values for May 1976.

large diurnal variation. It would thus appear that the depleted protonosphere of 3 May requires some 14 days of quiet conditions with steady diurnal partial filling and draining to reach a quasi-equilibrium situation about 16 May. Thus from 16 to 18 May the protonospheric content for ATS-6 to Aberystwyth geometry presents its equilibrium pattern for quiet geomagnetic activity with values maximising around 7×10^{16} m^{-2} during daytime filling and depleting to about 4×10^{16} m^{-2} at night.

This pattern is confirmed from the presentation of Fig. 45 where the maximum and minimum values of N_p for each day throughout this period are plotted and show that while both increase steadily from the storm depletion the daytime filling more than compensates the nighttime draining for some 12 to 14 days. Further confirmation is found in the increase in daytime N_p maximum/N_T% where in the equilibrium situation the daytime protonospheric content contributes some 20% to the total as opposed to only 11% on the day following the sudden commencement.

d. Discussion

The first point to note from this study of N_p changes during two extended periods is that the regular diurnal variation, with early morning minimum and afternoon maximum, is essentially a quiet time phenomenon. When K_p values exceeding 3 are found over a period of several days the diurnal pattern of N_p becomes irregular with noiselike quasi-random fluctuations which tend to mask the diurnal component of the variation.

Enhanced geomagnetic activity accompanying a sudden commencement is associated with an increase in the daytime protonospheric content. This result is consistent with that reported by POLETTI-LIUZZI et al. (1976) and agrees with the

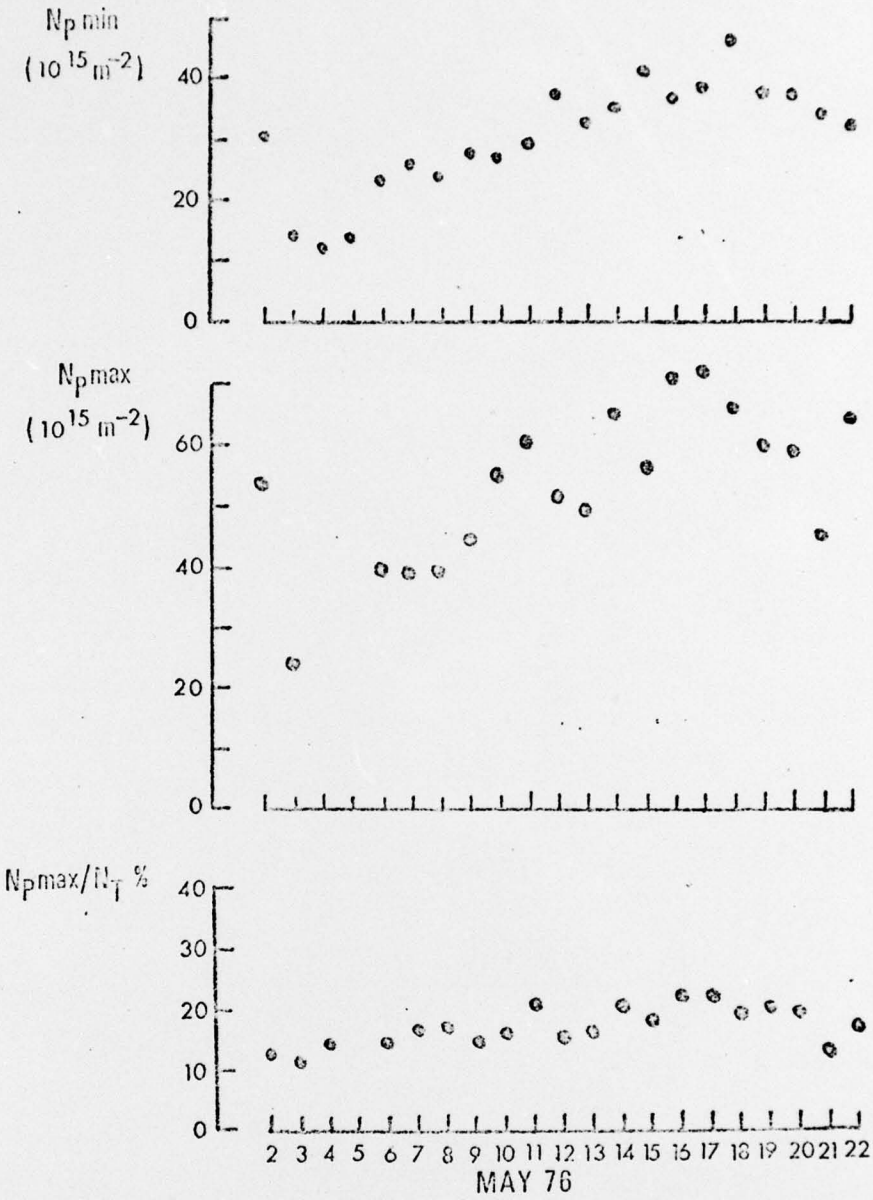

Fig.45. Daily values of minimum N_p, maximum N_p and the latter expressed as a percentage of N_T for 2 to 22 May 1976.

measurements of H^+ density above 400 km discussed by MARUBASHI et al. (1976) who report an upwards flow of light ions at high latitudes associated with the storm sudden commencement. It is well known that ionospheric electron content can show a significant positive effect during daytime following a sudden commencement (KERSLEY and DAS GUPTA, 1976). This daytime increase is associated with a raising of the ionisation under the influence of the magnetospheric electric field penetrating to the mid-latitude ionosphere and also neutral winds, possibly reversed in direction and blowing equatorwards in response to enhanced temperatures in the auroral zone. It is thus to be expected that the increase in ionospheric plasma will be reflected in enhanced protonospheric content. An additional factor which may cause some enhancement in slant N_p is the expansion of the plasmasphere in the afternoon sector in response to increased magnetospheric convection.

The rapid depletion in N_p as the line of sight moves into the nightside is consistent with the corresponding drop in ionospheric electron content and peak density reported by many workers. The main cause of this decrease is almost certainly linked to changes in thermospheric circulation reflected in an increased N_2/O ratio (PROLSS and VON ZAHN, 1974), but the enhanced magnetospheric electric field probably plays a role in depressing the nighttime ionisation and thus reducing the ionospheric electron content (KERSLEY and DAS GUPTA, 1976) and hence protonospheric content. An additional factor which will contribute to the depression of nighttime N_p during the main phase of the storm is the contraction of the plasmapause radius caused by the convection electric field. For example, PARK (1974)

found that the plasmapause moved in to L = 2.4 several hours after local midnight during a storm in which K_p reached 7.

The slow refilling of the protonosphere after the storm depletion was found to take ∿ 14 days to reach saturation during the quiet conditions in May. The results of the whistler studies reported by PARK (1974) indicate time constants to reach equilibrium ranging from ∿ 1 day at L = 2.5 to ∿ 8 days at L = 4. The storm of 2 May 1976 with K_p maximising at 8_+ was more intense than that discussed by PARK so that the protonospheric depletion may have been more complete in our observations where the lowest N_p value ever found occurred, however in terms of season and solar minimum epoch the data are comparable. It is interesting to note that PARK's observations were interrupted by substorm activity after 8 days so that he was unable to study possible saturation beyond L = 4. However, in the present observations the period of quiet extends to ∿ 17 days allowing complete equilibrium along the slant path to be reached after ∿ 14 days when the plasmapause radius had extended to its furthest possible quiet time position. An additional point of interest is that after ∿ 7 - 8 days the N_p magnitudes and their diurnal variation become comparable to the 30- day average values suggesting that the median protonospheric content and flux data discussed earlier in this report represent the integration over flux tubes up to L ∿ 4. This observation can be linked to PARK's comment that the plasmasphere usually consists of two distinct regions; an 'inner' plasmasphere, which is in equilibrium with the underlying protonosphere over a 24- hour period, and an 'outer' plasmasphere where L > 4.5, which is still recovering from the previous disturbance.

The average daytime upwards integrated protonospheric flux for 16 May, when equilibrium conditions had been reached, was $\sim 8 \times 10^{7}$ cm^{-2} s^{-1} which can be compared to a filling flux $\sim 3 \times 10^{8}$ cm^{-2} s^{-1} at 1000 km for L > 4 reported by PARK (1970). It should be noted that PARK has interpreted his data in terms of interaction with the ionosphere at one end of the flux tube while the present work suggests that the conjugate hemisphere must also be taken into consideration. Thus the present integrated value, only some 25% of PARK's would appear to give added confirmation to the suggestion made earlier in this report that saturation of the short inner tubes with L < 2 occurs after only a few hours filling almost every day.

11. CONCLUSIONS

The work reported here represents a first stage analysis of the ATS-6 radio beacon data for Aberystwyth. Attention has been concentrated in the main on hourly values of various parameters treated as monthly medians.

A consideration of the overall accuracy of the modulation phase and Faraday rotation measurements has indicated that in general the observational errors result in absolute protonospheric content data accurate to about ± 15%. The short term relative errors are usually much smaller so that a reliable picture of dynamic protonospheric changes can be obtained from ATS-6 observations. It has been shown that for geometry applicable to the Aberystwyth measurements the longitudinal gyrofrequency used in Faraday content evaluation is relatively insensitive to height, so that the error in N_p resulting from neglect of the

diurnal variation in F2-height is in general less than 6%. This was found to be much more favourable than for a station in the American sector where the corresponding error could be as large as 50%. Thus correction for layer height changes is of critical importance in the analysis and interpretation of N_p data for the American stations observing during Phase I ATS-6 operations but much less so for measurements made in Europe during Phase II.

The dynamic interchange of ionisation between ionosphere and protonosphere has been studied by estimating hourly values of average integrated fluxes from the temporal gradient of protonospheric content. The protonospheric flux shows a complex behaviour both diurnally and seasonally, but some considerable progress has been made in the interpretation of the results on a qualitative basis by considering diffusive interaction between ionosphere and protonosphere in both local and conjugate hemispheres. This interpretation has been given added confirmation by application to totally contrasting protonospheric data from an American station which nevertheless can be related to ionospheric behaviour in the two hemispheres.

The Aberystwyth observations indicate that the inner flux tubes intersected by the slant path are filled in a matter of hours almost every day and that the average behaviour of N_p reflects a diurnal partial draining but complete refilling of tubes for which $L < 4$. Following a geomagnetic storm depletion some 7 days are required to saturate these tubes, but approximately 14 quiet days are necessary to reach an absolute dynamic saturation along the slant path.

ACKNOWLEDGEMENTS

The ATS-6 observations at Aberystwyth have been financially supported by U.K. Science Research Council. Additional sponsorship for the analysis of the data has been received from Air Force Geophysical Laboratory, Bedford, U.S.A.

The ATS-6 observations were part of a collaborative programme with Apple[illegible] and the University of Lancaster. Thanks are due to [illegible]r Granville Beynon, F.R.S. for his interest and assistance in the planning of this joint venture. The authors are also grateful to Dr. E.N. Bramley and Dr. R. Browning, Appleton Laboratory and Dr. J.K. Hargreaves and Dr. S.Ganguly, University of Lancaster for many invaluable discussions in the preparation and execution of this project. The expertise of Mr. L.J. Martin, Appleton Laboratory in the supervision of the construction of the receiver and other aspects of experimental design and operation is gratefully acknowledged, as is the help of Mr. R.W.Smith of World Data Centre CI, Slough, U.K. in the provision of ionosonde data.

The American sector ATS-6 data have been obtained from a report published by World Data Center A, Boulder, U.S.A.

Thanks are due to Mrs. P.E. Pryce for typing the manuscript.

This report forms part of a thesis to be submitted to University of Wales by one of us (HHH).

REFERENCES

ALMEIDA, O.G., GARRIOTT, O.K. and DA ROSA, A.V.

1970 Planet. Space Sci., 18, 159-170.

ALMEIDA, O.G.

1973 J.Atmos.Terr.Phys., 35, 1657-1675.

ALMEIDA, O.G.

1974 J.Atmos.Terr.Phys., 36, 305.

BANKS, P.M. and DOUPNIK, J.R.

1974 Planet. Space Sci., 22, 79-94.

BELLCHAMBERS, W.H. and PIGGOTT, W.R.

1960 Proc.Roy.Soc.A., 256, 200-218.

BRADLEY, P.A. and DUDENEY, J.R.

1973 J.Atmos.Terr.Phys. 35, 2131-2146.

CAIN, J.C. and SWEENEY, R.E.

1970 J.Geophys.Res., 75, 4360-4362.

CARPENTER, D.L.

1966 J.Geophys.Res. 71, 693-709.

CARPENTER, D.L. and PARK, C.G.

1973 Rev.Geophys. and Space Phys. 11, 133-154.

CCIR 1967 Atlas of ionospheric characteristics, Rept.No.340, Union International des Telecommunications, Geneva.

CHAPPELL, C.R., HARRIS, K.K. and SHARP, G.W.

1971 J.Geophys.Res., 76, 7632-7647.

CHEN, A.J., GREBOWSKY, J.M. and MARUBASHI, K.

1976 Planet. Space Sic., 24, 765-769

COLIN, L. and MYERS, M.A.

1966 NASA TMX - 1233.

DAVIES, K.

1975 Informal circulated note, SEL, NOAA Boulder, USA.

DAVIES, K., FRITZ, R.B. and GRUBB, R.N.

1972 J. Environ. Sci., 15, 31-35.

DAVIES, K., FRITZ, R.B., GRUBB, R.N. and JONES, J.E.

1975a Radio Sci., 10, 785-799.

DAVIES, K., FRITZ, R.B., GRUBB, R.N., and JONES, J.E.

1975b IEEE Trans., AES-11, 1103-1109.

DAVIES, K., FRITZ, R.B. and GRAY, T.B.

1976 J.Geophys.Res., 81, 2825-2834.

EHRENSPECK, H.W. and STROM, J.A.

1971 AFCRL - 71 - 0234.

EVANS, J.

1972 J.Atmos.Terr.Phys., 34, 75-209.

EVANS, J.

1975a Planet. Space Sci., 23, 1461-1482.

EVANS, J.

1975b Planet. Space Sci., 23, 1611-1619.

FRITZ, R.B.

1976 Rept. UAG-58, World Data Center A, Boulder, USA.

GRUBB, R.N.

1972 Proc.Symp. on Future Applications of Satellite Beacon Measurements, Graz, Austria, 103-115.

GRUBB, R.N.

1975 Group delay calibration of S.B.F. Antennas, Informal circulated note, SEL, NOAA, Boulder, USA.

GRUBB, R.N., JONES, J.E. and ORSWELL, P.L.

1972 A modular receiving system for the ATS-F and other beacon satellite observations, Space Environment Laboratory, NOAA, Boulder, USA.

HANSON, W.B. and ORTENBURGER, I.B.,

1961 J.Geophys.Res., 66, 1425-1435.

HARGREAVES, J.K.

1970 Proc.Symp. on Future Applications of Satellite Beacon Experiments, Lindau, W.Germany, pp 16-1-16-9.

HARGREAVES, J.K. and HOLMAN, B.K.

1972 Proc.Symp. on Future Application of Satellite Beacon Measurements, Graz, Austria, pp129-138.

HARTMANN, G.H., DECENHARDT, W. and LEITINGER, R.

1976 Proc. COSPAR Satellite Beacon Symp., Boston, USA., pp219-230.

HARTMANN, G.H. and ENGELHARDT, W.

1974 Joint Satellite Studies Group Report 5 addendum, Lannion France, pp223-251.

HARTMANN, G.H. and ENGELHARDT, W.

1975 IEEE Trans., AP-23, 289.

HESS, W.N.

1968 "The Radiation Belts and Magnetosphere", Blaisdell Publishing Company, USA.

HO, M.C. and MOORCROFT, D.R.

1975 Planet. Space Sci., 23, 315-322.

KANE, R.P.

1975 J.Geophys.Res., 80, 3091-3099.

KERSLEY, L. and DAS GUPTA, A.

1976 Proc. COSPAR Satellite Beacon Symp., Boston, USA, 360-369.

KERSLEY, L. and SAMBROOK, D.J.

1971 Joint Satellite Studies Group Report, 4, Florence, Italy, 57-65.

KERSLEY, L. and TAYLOR, G.N.

1974 J.Atmos.Terr.Phys., 36, 93-102.

KLOBUCHAR, J.A. and KIDD, W.C.

1972 Proc.Symp. on Future Application of Satellite Beacon Measurements, Graz, Austria, pp79-86.

KOHL, H.

1966 Electron density profiles in ionosphere and exosphere, ed. J. Frihagen, Elvesier, Amsterdam, Netherlands, 231-238.

KOHL, H. and KING, J.W.

1967 J.Atmos.Terr.Phys., 29, 1045-1062.

MARUBASHI, K., REBER, C.A. and TAYLOR, H.A.

1976 Planet. Space Sci., 24, 1031-1041.

MAYR, H.G., FONTHEIM, E.G., BRACE, L.H., BRINTON, H.C., and TAYLOR JR., H.A.

1972 J.Atmos.Terr.Phys., 34, 1659-1680.

MENDILLO, M., KLOBUCHAR, J.A. and HAJEB-HOSSEINIEH, H.

1974 Planet. Space Sci., 22, 223-236.

MENDILLO, M. and KLOBUCHAR, J.A.

1974 AFCRL -74 - 0065.

PAPAGIANNIS, M.D., HAJEB-HOSSEINIEH, H. and MENDILLO, M.

1975 Planet. Space Sci., 23, 107-113.

PARK, C.G.

1970 J.Geophys.Res., 75, 4249-4260.

PARK, C.G.

1974 J.Geophys. Res., 78, 672-683.

POLLETTI-LIUZZI, D.A., YEH, K.C. and LIU, C.H.

1976 Proc. COSPAR Satellite Beacon Symp., Boston, USA, pp197-218.

PROLSS, G.W. and VON ZAHN, U.

1974 J.Geophys.Res. 79, 2535.

REES, P.R., KERSLEY, L. and EDWARDS, K.J.

1977 J.Atmos.Terr.Phys., In press.

RISHBETH, H. and KOHL, H.

1976 J.Atmos.Terr.Phys., 38, 775-780.

SAMBROOK, D.J.

1974 Ph.D. Thesis, University of Wales.

SHIMAZAKI, T.

1955 J.Radio Res.Labs., Japan, 2, 85.

SMITH, D.H.

1970 J.Geophys.Res., 75, 823-828.

SOICHER, H.

1975 Nature, Lond. 253, 252-254.

SOICHER, H.

1976a Nature, Lond., 259, 33-35.

SOICHER, H.

1976b Nature, Lond., 264, 46-48.

SOICHER, H.

1976c Proc.COSPAR Satellite Beacon Symp., Boston, USA, pp231-243.

TITHERIDGE, J.E.

1972 Planet. Space Sci., 20, 353-369.

YOUNG, D.M.L., YUEN, P.C. and ROELOFS, T.H.

1970 Planet. Space Sci., 18, 1163-1179.